Proinflammatory CD20^{+} T cells:

Their origin and therapeutic depletion

in CNS-directed autoimmunity

Dissertation for the award of the degree
"Doctor rerum naturalium"
of the Georg-August-Universität Göttingen

within the doctoral program molecular medicine
of the Georg-August University School of Science (GAUSS)

submitted by

Jasmin Ochs

Born in Ansbach

Göttingen, December 2020

Thesis Committee

Prof. Dr. Martin Weber
Department of Neuropathology
University Medical Center, Georg-August-University Göttingen

Prof. Dr. Jürgen Wienands
Institute for Cellular and Molecular Immunology
University Medical Center, Georg-August-University Göttingen

Prof. Dr. Alexander Flügel
Institute for Neuroimmunology and Multiple Sclerosis Research
University Medical Center, Georg-August-University Göttingen

Members of the Examination Board

Referee: Prof. Dr. Martin Weber

2nd Referee: Prof. Dr. Jürgen Wienands

Further members of the Examination Board
Prof. Dr. Alexander Flügel
Institute for Neuroimmunology and Multiple Sclerosis Research
University Medical Center, Georg-August-University Göttingen

Prof. Dr. Holger Reichardt,
Abtl. Zelluläre und Molekulare Immunologie,
University Medical Center, Georg-August-University Göttingen

Prof. Dr. Dr. Hannelore Ehrenreich
Klinische Neurowissenschaften
Max-Planck-Institut für Experimentelle Medizin

Prof. Dr. med. Jutta Gärtner
Klinik für Kinderheilkunde und Jugendmedizin
University Medical Center, Georg-August-University Göttingen

Date of oral examination: 02.03.2021

AFFIDAVIT

Here I declare that my doctoral thesis entitled “Proinflammatory $CD20^+$ T cells: their origin and therapeutic depletion in CNS-directed autoimmunity” has been written independently with no other sources and aids than quoted.

_____

Göttingen, December 2020

Für all die Menschen, die meinen Weg geprägt haben

Table of Contents

List of figures:

List of tables:

Abbreviations

Ab	Antibody
AF	Alexa Fluor
Ag	Antigen
ANOVA	Analysis of variance
APC	Allophycocyanin
APC	Antigen-presenting cell
BCR	B cell receptor
BV	Brilliant violet
CD	Cluster of differentiation
CFA	Complete Freud's adjuvant
CFSE	Carboxyfluorescein succinimidyl ester
CIS	Clinical isolated syndrome
CNS	Central nervous system
CSF	Cerebrospinal fluid
Ctrl	control
DAB	3,3'-Diaminobenzidine
DAPI	4',6-diamidino-2-phenylindole
DDSA	2-Dodecenylsuccinic Acid Anhydride
dH_2O	Distilled water
ddH_2O	Bidistilled water
DMSO	Dimethyl sulfoxide
DNA	Deoxyribonucleic acid
EAE	Experimental autoimmune encephalomyelitis
e.c.	Extracellular
EDSS	Expanded disability status scale
EDTA	Ethylenediamine Tetraacetic Acid Disodiumsalt Dihydrate
e.g.	Exempli gratia
FACS	Fluorescence activated cell sorting

FCS	Fetal calf serum
FITC	Fluorescein isothiocyanate
G	Gramm
GM-CSF	Granulocyte-macrophage colony-stimulating factor
h	Hour(s)
H&E	Haematoxilin and eosin
H_2O_2	Hydrogen peroxide
i.c.	intracellular
IFN	Interferon
IL	Interleukin
i.p.	Intraperitoneal
i.v.	Intravenously
KO	Knock-out
l	Liter
mAb	Monoclonal antibody
MACS	Magnetic activated cell sorting
MBP	Myelin basic protein
MFI	Mean fluorescence intensity
MHC	Major histocompatibility complex
µl	Microliter
µm	Micrometer
µM	Micromolar
mg	Milligram
ml	Milliliter
mm	Millimeter
mM	Millimolar
min	Minute(s)
MOG	Myelin oligodendrocyte glycoprotein
MS	Multiple Sclerosis

OVA	Ovalbumin
PB	Pacific Blue
PBMC	Peripheral blood mononuclear cell
PBS	Phosphate buffered saline
PCR	Polymerase chain reaction
PE	Phycoerithrin
PFA	Paraformaldehyde
p.i.	Post immunization
PMA	Phorbol 12-Myristate 13-Acetate
PPMS	Primary progressive multiple sclerosis
PTX	Pertussis Toxin
q	Quantitative
RA	Rheumatoid arthritis
rMOG	Recombinant Myelin oligodendrocyte glycoprotein
RNA	Ribonucleic acid
RPMI-1640	Roswell Park Memorial Institute-1640
RRMS	Relapsing-remitting multiple sclerosis
s	Second(s)
SD	Standard deviation
SEM	Standard error
SPMS	Secondary progressive multiple sclerosis
Tc	Cytotoxic T cells
TCR	T cell receptor
Th	T helper cells
TNF	Tumor necrosis factor
Tris	Tris(Hydroxymethyl)Aminomethane
ZTE	Zentrale Tierexperimentelle Einrichtung

Abstract

Anti-CD20 antibody (ab) treatment exhibits an unprecedented therapeutic benefit in multiple sclerosis (MS). The very fact that B cell depletion is effective in a disease that was generally considered T cell-driven was astonishing. In addition to the extensive analysis of B cells, it also led to the discovery and the consideration of $CD20^+$ T cells in MS pathology. $CD20^+$ T cells are described as a small population of T cells that is increased in autoimmune diseases such as MS, but little else is known. Therefore, we wanted to understand which role $CD20^+$ T cells play in MS and dissect whether their depletion by anti-CD20 abs partakes in the positive therapeutic effect. We also wanted to analyze the origin of $CD20^+$ T cells in MS and in experimental autoimmune encephalomyelitis (EAE) as our model system.

In this context, we discovered and described $CD20^+$ T cells in mice. Since we were unable to expand the $CD20^+$ T cell population *in vitro* without B cell-dependent T cell activation, we ascertained that murine $CD20^+$ T cells cannot endogenously express CD20. As a result, we examined the hypothesis of a trogocytotic transfer of CD20 from CD20-highly expressing B cells to T cells during antigen-dependent T cell-B cell interaction. We could demonstrate in various *in vitro* and *in vivo* experiments that trogocytosis is indeed the actual origin of $CD20^+$ T cells in mice. These results suggest that CD20 on T cells could serve as a marker for T cell activation by B cells.

In EAE mice, but also in MS patients, we could determine $CD20^+$ T cells to be predominantly proinflammatory cells, which strongly express pathogenic attributes, promoting their potential relevance in MS development and progression. The expansion of $CD20^+$ T cells in EAE mice and MS patients and their depletion with anti-CD20 antibodies in both species furthers the hypothesis of their pertinence in the disease.

Ultimately, adoptive transfer experiments and the characterization of $CD20^+$ T cells in greater detail strongly indicate their pathogenicity in EAE, respectively MS.

1. Introduction

1.1.Multiple Sclerosis

MS is a chronic inflammatory demyelinating disease of the central nervous system (CNS) concerning approximately 2.8 million people worldwide[1, 2]. Its incidence is higher in women than in men with an average onset age of 30 years[2, 3, 4]. In 1996, the US National Multiple Sclerosis Advisory Committee on Trials in MS provided standardized definitions for four main MS clinical courses: relapsing-remitting (RR), which gradually transitions into a secondary progressive (SP) disease course in 80 % of the patients one to two decades after RRMS diagnosis, primary progressive (PP), and progressive relapsing (PR)[5].

In 2014, Lublin et al. reviewed these definitions and softened them into two main clinical courses: primarily progressive and primarily relapsing disease courses. Additionally, the primarily relapsing course is divided into active and not active, while the primarily progressive course is divided into active with progression, active without progression, not active with progression, and not active without progression. Activity is defined by magnetic resonance imaging (MRI) activity and/or clinical relapses[6].

About 85 % of MS cases show a primarily relapsing clinical course with an initial episode of neurological dysfunctions followed by a remission period with clinical recovery. In the aftermath, recurring bouts of relapses and remissions define this clinical course. Relapses coincide with inflammation and demyelination of the CNS that are discernible in MRI as MRI lesions[4]. Over time, the improvement after relapses, occurring in the remission phase can diminish and the patient gradually transitions into a more progressive disease course (SP) with proceeding disability[6]. At this stage, inflammatory lesions are no longer characteristic, and a progressive neurological decline is additionally accompanied by CNS atrophy. CNS atrophy is defined by decreased brain volume and increased axonal loss[4].

About 10 % of MS patients show a primarily progressive clinical course. This is generally diagnosed in older patients and considered more aggressive, with a faster decline, progression, and an relative absence of the RR stages characteristic for the primarily relapsing disease course[7].

Clinical symptoms of MS vary from fatigue, motor impairments, sensory and visual disturbances to pain and cognitive impairments. The specific symptoms in each patient are derived from the location of the MS lesion in the brain and/or spinal cord[1]. Lesions are caused by immune cells crossing the blood-brain barrier, accumulating and attacking the CNS. Therefore, lesions are considered a hallmark of MS and are widely used as diagnostic criterion[4].

CNS-infiltrating cells are predominantly T cells, but also B cells and other antigen-presenting cells migrate into the CNS **(Fig.1)**. This causes CNS-inflammation, demyelination, gliosis, and neuroaxonal degeneration, which leads to demyelinated areas in the white and grey matter of the brain and spinal cord through the loss of myelin sheaths and oligodendrocytes, resulting in the disruption of neuronal signaling[8].

The exact cause of MS remains unknown. Two models of MS development are taken into consideration. One is the inside-out, CNS-intrinsic model, where events in the CNS might lead to the release of CNS antigens into the periphery. Such antigens could already be observed in the cervical lymph nodes of MS patients[9] and might trigger disease development via priming lymphocytes for CNS antigen[4, 10, 11].

The outside-in, CNS extrinsic (peripheral) model on the other hand suggests the activation of T cells in the periphery[12, 13, 14]. Those activated, autoreactive T cells then migrate to the CNS along with activated B cells and monocytes[15]. The outside-in model is consistent with EAE, a MS model in animals[4].

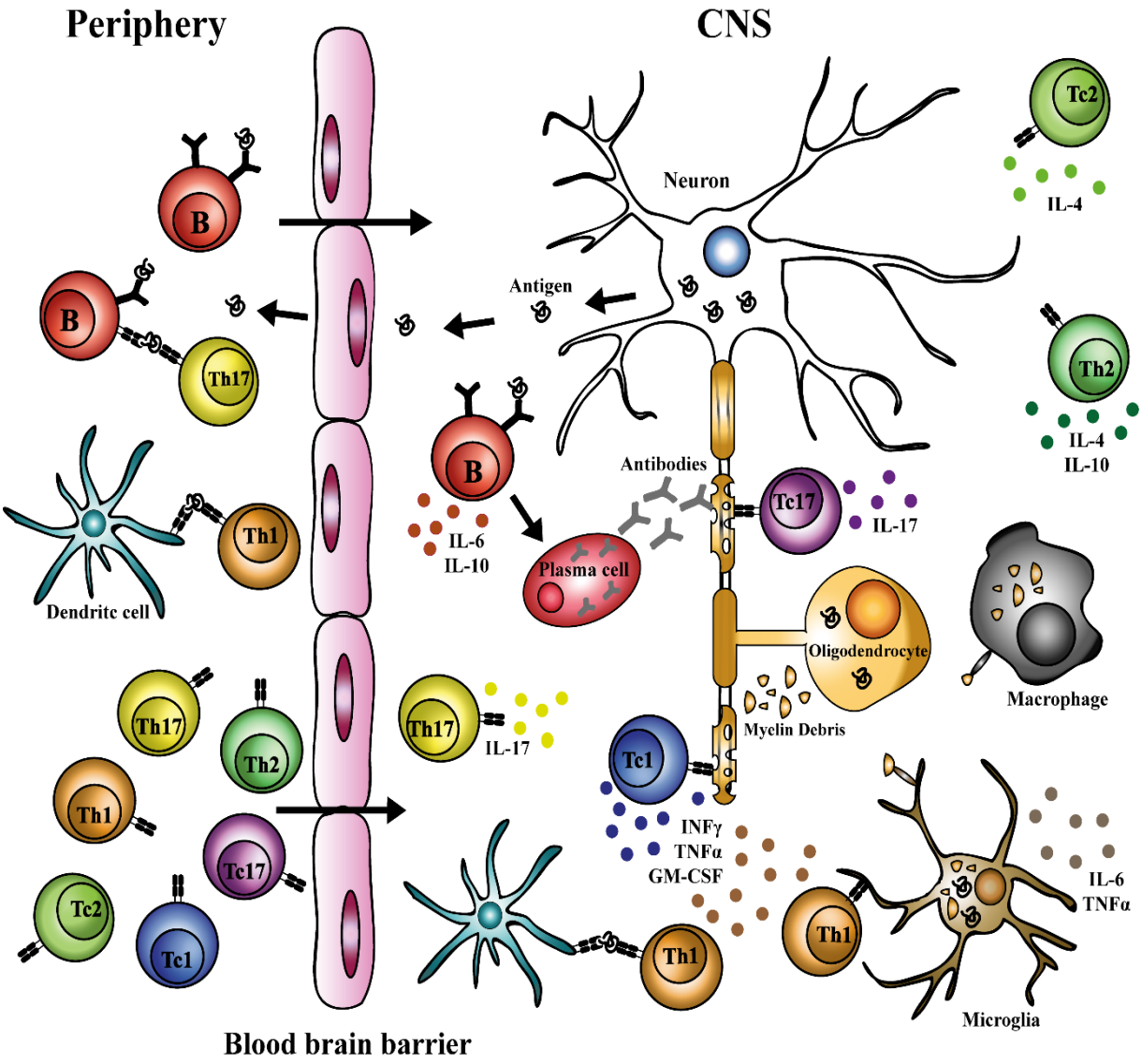

Fig.1: Model of autoimmune processes in multiple sclerosis[16, 17]
This model illustrates the inside-out model. Here, CNS antigens are released into the periphery, where it is presented to T cells by various antigen-presenting cells like B cells and dendritic cells. The activated, auto-aggressive T cells then travel through the blood-brain barrier into the CNS, where they are reactivated by CNS-inherent or -infiltrated antigen-presenting cells and attack and destroy the myelin sheath. Additionally, auto-aggressive T cells release proinflammatory cytokines to further inflammation. CNS-antigen activated B cells also migrate through the blood-brain barrier into the CNS, where they can release proinflammatory cytokines, reactivate T cells or differentiate into plasma cells and release CNS-directed antibodies. CNS-infiltrating macrophages and CNS-inherent microglia phagocyte myelin debris, resulting from autoimmune demyelination. However, anti-inflammatory B and T cells also migrate into the CNS, where they release anti-inflammatory cytokines. Th = Thelper; Tc = cytotoxic T cells; IL = Interleukin; IFNγ = Interferon-γ; TNFα = tumor necrosis factor α; GM-CSF = granulocyte-macrophage colony-stimulating factor.

1.2. Experimental autoimmune encephalomyelitis

EAE is the most commonly used animal model in MS research[18, 19]. EAE is an inflammatory disease of the CNS, induced via an immune response against CNS-specific antigens[20]. It can be induced in various species, e.g. in guinea pigs, monkeys, mice and rats[21]. Here, the focus lies on EAE in mice. Generally, EAE can be induced in three different ways, which lead to either an acute monophasic, a relapsing-remitting or a chronic progressive disease course. EAE induction can be divided into spontaneous EAE, an active EAE induction, and passive EAE[19].

In spontaneous EAE, mice are genetically modified to spontaneously develop EAE at a certain age. One example for such a genetic modification is the expression of B cell- and T cell-receptors against myelin peptides such as myelin oligodendrocyte glycoprotein (MOG_{35-55})[22].

In active EAE induction **(Fig.2)**, a $CD4^+$ T cell-mediated inflammation is evoked by subcutaneous injection of CNS-specific antigens emulsified in complete Freud's adjuvant (CFA), which contains immune stimulants. This results in the generation of pathogenic $CD4^+$ Th1 and Th17 cells in the immunization draining lymph nodes and secondary lymphatic organs. The generated proinflammatory T cells, along with activated B cells and other antigen-presenting cells such as dendritic cells, enter the circulation and migrate through the blood-brain barrier to cause inflammation within the CNS, leading to demyelination and axonal loss[23].

In addition, Pertussis toxin (PTX) is injected to induce high frequencies of activated immune cells, e.g. peptide-specific Th1 cells[24]. This form of EAE provides a powerful model to study the pathogenesis and immune regulation of Th1/Th17-mediated myelin damage, which is considered a relevant model for the autoimmune aspects of MS[25, 26, 27].

The primarily utilized CNS-specific antigens to induce EAE are MOG, myelin basic protein (MBP) and proteolipid protein (PLP). In SJL/J mice, immunization with the immunodominant epitope of PLP, $PLP_{139-151}$, induces a relapsing-remitting EAE course[28]. Immunization of young C57BL/6 mice with the immunodominant epitope of MOG, MOG_{35-55} peptide, or the recombinant MOG_{1-117} protein leads to an acute, monophasic EAE course. However, in middle-aged male C57BL/6 mice immunized with the MOG_{35-55} peptide, develop a severe chronic EAE[21]. While all models generate auto-inflammatory $CD4^+$ T cells, the MOG_{1-117} protein model also generates a population of antigen-activated B cells, which promote the development of antibodies against MOG protein[29]. Therefore, this model is considered a B cell-mediated EAE model, while immunization with MOG_{35-55} peptide is a mainly T cell-driven model[29].

To induce passive EAE, myelin antigen-activated and recombinant IL-12 and anti-IFNγ stimulated T cells are adoptively transferred to naïve mice, which leads to a relatively rapid onset of EAE[30, 31].

The clinical manifestation of EAE in C57BL/6 mice immunized with MOG_{35-55} peptide or MOG_{1-117} protein is an ascending paralysis, starting at the tip of the tail and progressing from complete tail paralysis to complete hindlimb paralysis. In more severe EAE cases, hindlimb paralysis is followed by forelimb paralysis and subsequently death **(Fig.2)**[32].

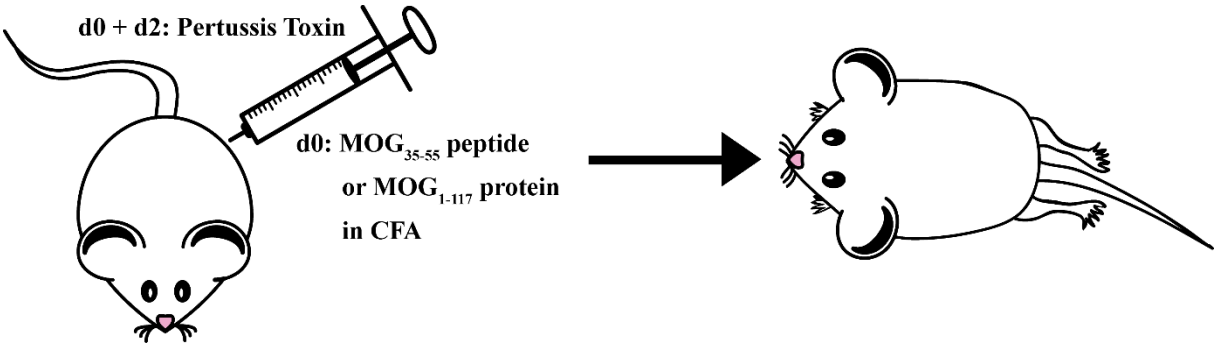

Fig.2: Model of EAE induction in the mouse
Healthy mice are immunized via a subcutaneous injection with an emulsion composed of CFA and a CNS antigen (here MOG_{35-55} peptide or MOG_{1-117} protein) on d0. Additionally, PTX is injected intraperitoneally at d0 and d2. At d10-14 post immunization, mice develop ascending paralysis beginning at the tip of the tail and progressing to complete hind limb paralysis.

1.3.T cells in MS, respectively EAE

Pathogenic T cells are considered important effector cells of MS, respectively EAE[23, 33]. Accordingly, T cells are frequently examined for their impact on disease development and progression. T cells can be divided in two main subgroups: $CD4^+$ and $CD8^+$ T cells. There are four main subsets of $CD4^+$ T cells **(Fig.3)**[34]:

- Th1 cells are defined by their expression of the chemokine receptor CXCR3[35], the transcription factor Tbet, and their signature cytokine IFNγ[27, 36];
- Th2 cells are characterized by their expression of the transcription factor GATA3, the chemokine receptor CCR4[35] and the production of the anti-inflammatory cytokines IL-4 and IL-10[36];
- Th17 cells can be distinguished by their expression of the transcription factor RORγt and production of the proinflammatory cytokine IL-17[37];
- Treg cells are characterized by their expression of the activation marker CD25, the transcription factor Foxp3 and the production of anti-inflammatory cytokines such as IL-10 and TGF-β[38].

Originally, Th1 cells were thought to be the main pathogenic T cells in MS and EAE[39]. This hypothesis was assumed since IFNγ, a proinflammatory cytokine mainly expressed by Th1 cells, worsened disease in MS patients. Direct injection of IFNγ into the CNS caused an inflammatory pathology resembling EAE[40, 41, 42]. Furthermore, IFNγ disrupts tight junctions and induces adhesion molecule expression on the blood-brain barrier endothelial cells. This allows the transendothelial migration of $CD4^+$ T cells into the parenchyma[43]. Within the CNS, astrocytic chemokine production is also triggered by IFNγ, which leads to the enhanced recruitment and activation of myeloid cells[44]. In MS, IFNγ was found to be increased in the blood, cerebrospinal fluid (CSF), and brain lesions of MS patients[45, 46] and IFNγ levels are positively correlated with disease activity[47]. Additionally, mice unable to express IL-12p40, a component of IL-12, which is required for Th1 T cell differentiation, were resistant to EAE induction[48]. However, it was discovered that mice lacking Th1 cells and therefore IFNγ, develop a more severe EAE[49].

This paradox was resolved by discovering that IL-12 shares the subunit p40 with the cytokine IL-23[50]. Mice that were deficient in the IL-23-specific subunit p19 were completely resistant to active EAE[51], while mice deficient in the IL-12-specific subunit p35 developed a more severe EAE[52, 53], just as mice deficient in IFNγ. IL-23 promotes encephalitogenic Th17 cells[26] that furthers inflammation due to their IL-17 secretion[54]. IL-17 also increases blood-brain barrier permeability *in vitro*[55] and induces chemokine production by CNS-resident cells[56, 57]. In MS, higher frequencies of IL-17-producing Th17 cells could be observed in the CSF of RRMS patients during relapse compared to in remission[58]. However, blocking of the p40 subunit showed no clinical benefit in MS[59]. Similar to IFNγ, IL-17 was shown to be dispensable for EAE, since EAE could be actively induced in IL-$17A^{-/-}$ mice by adoptive transfer of IL-$17^{-/-}$ $CD4^+$ T cells[60].

Due to the fact that neither IFNγ nor IL-17 are essential for EAE induction, but both Th1 and Th17 cells can independently induce EAE[25, 61], GM-CSF, another cytokine that is produced by both T cell subsets was analyzed[62, 63]. In mice deficient in GM-CSF or its receptor, a strong resistance to EAE induction could be observed[64]. Additionally, the adoptive transfer of GM-CSF-deficient Th1- and Th17-polarized cells strongly reduced EAE manifestation and completely prevented EAE induction in some mice[63, 65, 66]. GM-CSF-producing T cells are also increased in the blood and CSF of MS patients and have been identified in active MS lesions[67].

Another cytokine produced by Th1 and Th17 cells is TNFα[26]. The overexpression of TNFα in the CNS resulted in demyelination[68, 69], whereas blocking of TNFα before disease onset extenuates EAE[70, 71]. Mice deficient in TNFR1, one of the two distinct TNFα receptors, are

completely resistant to EAE or develop a milder case[72, 73]. TNFR1 signaling supports the migration of leukocytes into the parenchyma by promoting chemokine and adhesion molecule expression of CNS-resident cells in EAE[74] and triggers oligodendrocyte death[69]. TNFα levels in the blood and CSF have also been shown to correlate with MS disease activity[75, 76].

In contrast to the proinflammatory, disease-promoting effect of Th1 and Th17 cells, Th2 and Treg cells exhibit an anti-inflammatory, autoimmune-mediating effect. In Tregs, expression of CD25 contributes to maintaining self-tolerance via the down-regulation of immune responses to self and non-self antigens[77]. In addition, the expression of Foxp3 in Tregs is essential for immune-regulatory functions[78, 79]. Moreover, transfer of Tregs in MOG-induced EAE ameliorated disease severity[80]. It could be shown that the positive effects of Treg cells is due to their secretion of anti-inflammatory cytokines such as IL-10, since IL-10$^{-/-}$ Tregs failed to influence EAE[81]. Furthermore, their production of TGF-β can suppress MOG-specific Th17 responses and protect against EAE[82].

Th2 cells can also function as EAE regulators, mainly through their secretion of the anti-inflammatory cytokines IL-4 and IL-10[83]. Especially IL-10 seems to be effective since IL-10 transgenic mice were observed to be highly resistant to EAE induction while IL-10$^{-/-}$ mice were highly susceptible[84].

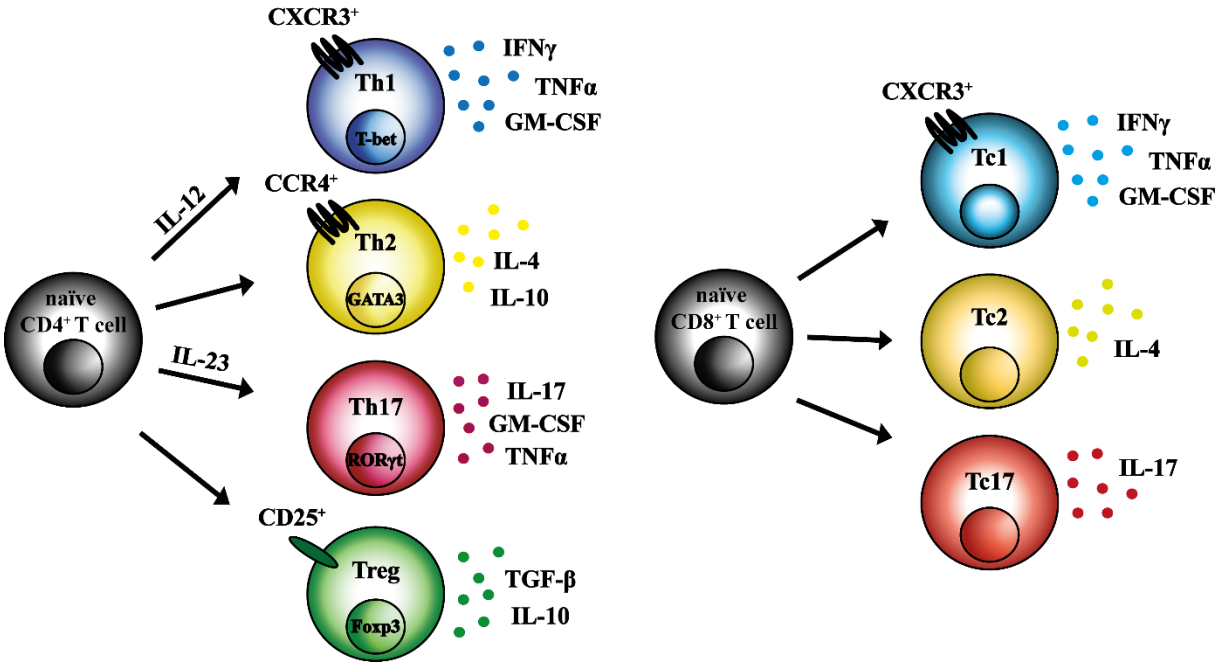

Fig.3: T cell subtypes

Naïve CD4$^+$ T cells can differentiate into various T helper cells: proinflammatory IFNγ-, TNFα- and GM-CSF-cytokine expressing CXCR3$^+$Tbet$^+$ Th1, anti-inflammatory IL-4 and IL-10-expressing CCR4$^+$GATA3$^+$ Th2, proinflammatory IL-17-expressing RORγt$^+$ Th17 or anti-inflammatory TGF-β and IL-10-expressing CD25$^+$Foxp3$^+$ Treg cells. Naïve CD8$^+$ T cell can differentiate into various cytotoxic T cells: proinflammatory CXCR3$^+$ IFNγ-, TNFα- and GM-CSF-expressing Tc1, proinflammatory IL-17-expressing Tc17 or anti-inflammatory IL-4-expressing Tc2 cells.

$CD8^+$ T cells, the other main T cell subgroup, can also be divided in three main subsets **(Fig.3)**:

- Tc1 are characterized by the expression of the chemokine receptor CXCR3 and their secretion of IFNγ and TNFα[85, 86, 87];
- Tc2 cells are characterized by their secretion of IL-4[87];
- Tc17 cells are defined by their production of IL-17[88, 89].

$CD8^+$ T cells occur at a higher frequency in MS lesions than $CD4^+$ T cells. They show oligoclonal expansion in the blood, CSF and plaques[90], indicating their pathogenicity in MS. Myelin-specific $CD8^+$ T cells could also be detected in MS[91]. In addition, the cytokines secreted by $CD8^+$ T cells take similar effects as the same cytokines produced by $CD4^+$ T cells. Therefore, $CD8^+$ T cell cytokine expression can have proinflammatory (IFNγ, GM-CSF, TNFα, IL-17) as well as anti-inflammatory (IL-4) effects in MS, respectively EAE[17].

To further analyze T cells in this study, various other surface molecules and cytokines were measured:

- IL-2, also known as T cell growth factor, functions as a potent mitogen and growth regulator of T cells *in vitro* and expressed by all T cell subsets[92, 93].
- CD25 and CD69 are T cell activation markers, in which CD69 is a marker for early activation[94] and CD25 mainly marks late activation[95].
- Lymphocyte function-associated antigen 1 (LFA-1 or CD11a) and α4 integrin (VLA-α4 or CD49d) are T cell adhesion molecules, required for T cells to migrate through the endothelial cells of the blood-brain barrier into the CNS[96, 97].

Additionally, T cell maturation was tracked via the expression of various surface molecules. In this study, T cells are divided in the maturation stages of **(Fig.4)**[38]:

- $CCR7^+CD45RO^-$ naïve (T_N) or stem cell-like T memory cells (T_{SCM}),
- $CCR7^+CD45RO^+$ central memory T cells (T_{CM}),
- $CCR7^-CD45RO^+$ effector memory T cells (T_{EM}),
- $CCR7^-CD45RO^-$ terminally differentiated T cells (T_{EMRA}).

Due to e.g. stimulation by an antigen-presenting cell, T_N cells maturate from T_{CM} to T_{EM} to T_{EMRA} cells. Thereby, they lose their stem cell-like potential and proliferation capacity and gain effector function and increased peripheral homing[38].

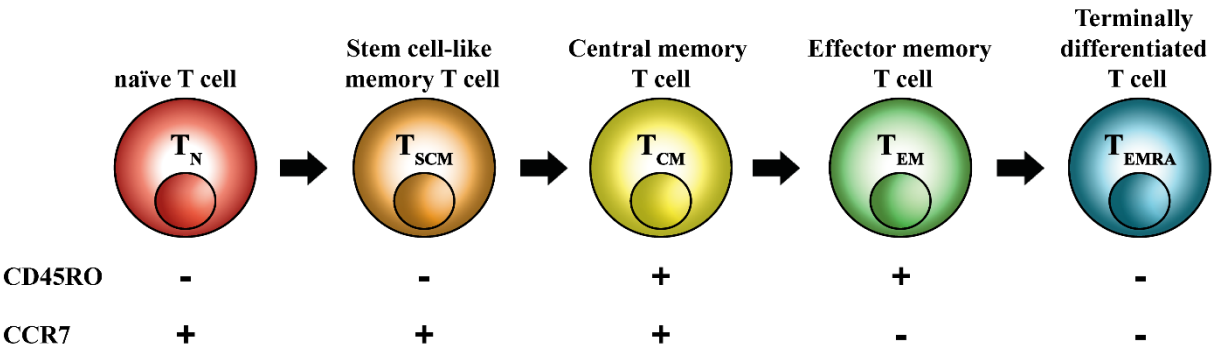

Fig.4: T cell developmental stages[38]
T cells occur in the periphery in a naïve state, before they are activated by antigen-presenting cells. Then, they develop from naïve cells (T_N) to stem cell-like memory (T_{SCM}) to central memory (T_{CM}) to effector memory (T_{EM}) and finally to terminally differentiated T cells (T_{EMRA}). Stem cell like potential and proliferation capacity decrease with maturation, while effector function and peripheral homing increase.

1.4. Anti-CD20 antibody therapy

The development of anti-CD20 monoclonal antibodies (abs) started in 1980, when CD20, a transmembrane protein expressed on B cells, was identified[98]. CD20 can be detected on B cells from the pre-B cells stage up until the plasma cell stage during B cell maturation[98]. Despite various approaches, the role of CD20 on B cells remains unclear and no ligand has been identified so far. The effect of anti-CD20 abs is due to their binding to CD20 on the surface of B cells. This binding induces significant complement-dependent cytotoxicity, antibody-dependent cellular cytotoxicity, and antibody-dependent phagocytosis, leading to the depletion of CD20-expressing B cells[99]. Using CD20 as target molecule is advantageous since CD20 is expressed on B cells in the maturation stages, in which B cells actively participate in inflammatory processes such as T cell activation[98]. However, longterm immunities acquired by previous infections or via vaccinations are not abolished, since plasmablasts and plasma cells responsible for longterm immunity do no more express CD20[100]. Admittedly, it has to also be considered that a depletion of mature B cells also leads to a stop in the replenishment of plasmablasts and plasma cells. Since those cells do not have an infinite lifespan, permanent B cell depletion also results in the gradual loss of plasma cells and plasmablasts. This loss leads to the reduction of IgM and IgG antibodies in the serum of anti-CD20 ab treated MS patients and a potentially increased risk for the contraction of infectious diseases[101].

Treatment with anti-CD20 abs led to an impressive activity in patients with B cell malignancies[102]. In 1997, the US Food and Drug Administration (FDA) approved the first anti-

CD20 ab rituximab for the treatment of relapsed or refractory non-Hodgkin lymphoma[103]. Rituximab is a humanized chimeric monoclonal anti-CD20 antibody[104]. In 2004, rituximab therapy was tested and used for the treatment of inflammatory, autoimmune diseases, starting with rheumatoid arthritis (RA)[105]. Here, the hypothesis was that the removal of autoantibody producing and/or T cell-activating B cells might lead to a clinical improvement. And indeed, anti-CD20 ab treatment exhibited an indisputable clinical benefit in RA treatment[106]. Therefore, treatment with anti-CD20 abs was examined in other autoimmune diseases including systemic lupus erythematosus (SLE) and MS[107]. In RRMS, a single course of rituximab treatment reduced inflammatory brain lesions and clinical relapses for 48 weeks[108]. An observational study in RRMS and PPMS for rituximab therapy revealed its safety and effectiveness in the treatment of RRMS. Additionally, some PPMS patients could also benefit from rituximab therapy[109]. Over time, several potentially improved anti-CD20 antibodies were developed. One of those newly developed antibodies was Ocrelizumab, a humanized anti-CD20 monoclonal antibody with the same CD20 binding site as rituximab **(Fig.5)[110]**. Another was Ofatumumab a fully humanized monoclonal anti-CD20 antibody with a binding site different from rituximab/ocrelizumab[111].

The observed clinical benefit of anti-CD20 therapy in MS was surprising, since MS was considered a mainly T cell-driven disease[23]. Therefore, $CD20^+$ T cells, which were discovered in the blood of healthy donors in 1993[112], must also be considered in this context.

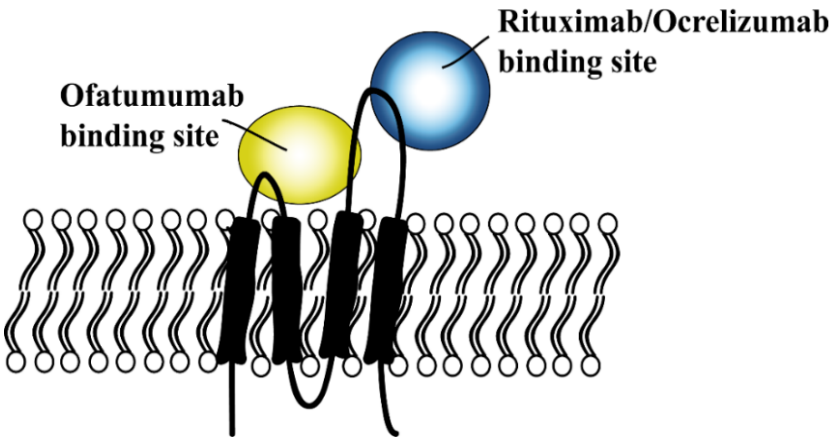

Fig.5: Binding sites of anti-CD20 antibodies
Model of the transmembrane protein CD20 and the binding sites of the three main anti-CD20 abs.

1.5. CD20$^+$ T cells

CD20$^+$ T cells **(Fig.6)** were first described by Hultin et al. in 1993[112] in the blood of healthy donors, where they accounted for 2.4±1.5 % of all peripheral blood lymphocytes. Before that, CD20 was considered a marker exclusively expressed on B cells. After the discovery of CD20$^+$ T cells was published, it was debated, if the dim CD20 signal on this small T cell population occurs as flow cytometry artefact due to the unintentional analysis of B cell-T cell doublets[113]. This controversy was mainly founded on the fact, that the group of Henry et al. was unable to isolate the CD20$^+$ T cell population and expand them by direct T cell stimulation[113]. Ensuing studies could establish CD20$^+$ T cells as a subpopulation of T cells in the human blood and various other compartments[114, 115]. An increase of CD20$^+$ T cells could be detected in autoimmune diseases such as rheumatoid arthritis, where they accumulate in the synovial fluid of inflamed joints[116]. Additionally, CD20$^+$ T cells were detected in higher frequencies in the blood of MS patients compared to healthy controls[115, 117]. Furthermore, an accumulation of CD20$^+$ T cells could be observed in the CSF of MS patients[115].

CD20$^+$ T cells were observed to have a primarily proinflammatory phenotype, due to their high production of proinflammatory cytokines such as IL-17, IFNγ and TNFα[114]. In ascites of patients with ovarian cancer, CD20$^+$ T cells were expanded and exhibited a predominantly Tc1 effector memory phenotype[118]. In primary Sjögren's syndrome, a considerably large percentage of IL-17-producing Th17 cells co-expressed CD20[119]. Since IL-17[55, 120, 121], as well as IFNγ[41, 48] and TNFα[17, 122], are known to play a considerable role in the development and progression of these autoimmune diseases, CD20$^+$ T cells are considered as an important part in autoimmune disease development and progression.

Since anti-CD20 ab treatment was shown to have a substantial therapeutic effect in rheumatoid arthritis and especially in MS[105, 108, 110, 123, 124]. Anti-CD20 abs could also be determined to deplete CD20$^+$ T cells[116, 117, 125], particularly activated, myelin-specific CD20$^+$ T cells[91]. These findings raised the question, if the depletion of CD20$^+$ T cells plays a considerable role in the positive treatment effect of anti-CD20 ab therapy[126].

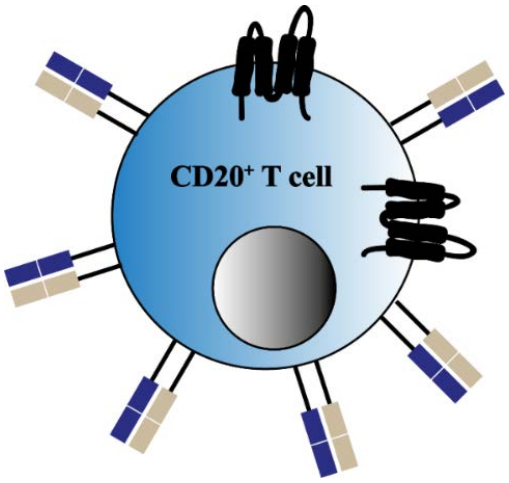

Fig.6: CD20$^+$ T cell
CD20$^+$ T cells are a population of approximately 3-5 % of all T cells that show a dim expression of the B cell marker CD20[114].

1.6.Aim of the study

Anti-CD20 ab treatment leads to a positive treatment effect in MS patients[108]. CD20$^+$ T cells, a small subset of T cells that was published to exhibit a proinflammatory phenotype[114], are also depleted by this therapy[117, 125]. The aim of the study was to determine if CD20$^+$ T cells play a role in MS pathology and if their depletion is at least partially responsible for the positive treatment effect of anti-CD20 antibody therapies. In addition, we examined the origin of CD20$^+$ T cells and if they might represent a distinct T cell subset.

First, we determined, if CD20$^+$ T cells can be found in wild type mice, which represent our main model organism. We were especially interested where CD20$^+$ T cells originate from and if they are a uniform population or if CD20 is some kind of activation marker that can occur in pro- as well as in anti-inflammatory T cells.

Secondly, we analyzed the potential pathogenicity of CD20$^+$ T cells via activation markers, adhesion molecules and cytokine secretion in the mouse. We also investigated CD20$^+$ T cells in the context of EAE, the murine model of MS.

Thirdly, we analyzed CD20$^+$ T cells in MS patients for their potential pathogenicity and their depletion by anti-CD20 ab therapy. Since we found that CD20$^+$ B cells reoccur more differentiated and activated in MS patients after anti-CD20 ab treatment stop[127], we examined CD20$^+$ T cells before depletion and at reoccurrence to check for similar events.

2. Material and Methods

2.1.Material

2.1.1. Reagents

Table 1: Reagents

Reagent	Supplier
Acetic acid	Merck, Millipore, Darmstadt Germany
Anti-CD20 or isotype-control	Genentech, South San Francisco, USA
Agarose	Starlab Gmbh, Hamburg, Germany
β-Mercaptoethanol	Sigma Aldrich, USA
BD FACS Clean™	BD Biosciences, Franklin Lakes, NJ, USA
BD FACS Flow™	BD Biosciences, Franklin Lakes, NJ, USA
BD FACS Rinse™	BD Biosciences, Franklin Lakes, NJ, USA
BD FACS™ Lysing Solution, 10x	BD Biosciences, Franklin Lakes, NJ, USA
BD Pharm Lyse™, 10x	BD Biosciences, Franklin Lakes, NJ, USA
CFSE	BioLegend, San Diego, CA, USA
Cytofix/Cytoperm™	BD Biosciences, Franklin Lakes, NJ, USA
Cytofix™	BD Biosciences, Franklin Lakes, NJ, USA
Chloral Hydrate	Merck Millipore, Darmstadt, Germany
Citric acid	Merck Millipore, Darmstadt, Germany
DAB	Sigma-Aldrich Chemie Gmbh, Steinheim, Germany
DAPI	Sigma-Aldrich Chemie Gmbh, Steinheim, Germany
DEPEX	Vwr International, Darmstadt, Germany
DMSO	Sigma Aldrich, St. Louis, Mo, USA
EDTA	Carl Roth, Karlsruhe, Germany
Ethanol, 100 %	Merck Millipore, Darmstadt, Germany
FCS	Sigma Aldrich, St. Louis, Mo, USA
FoxP3 Fix/Perm Concentrate	eBioscience, San Diego, Ca, USA
FoxP3 Fix/Perm Diluent	eBioscience, San Diego, Ca, USA
FoxP3 Perm Buffer, 10x	eBioscience, San Diego, Ca, USA
GelRed	Biotium, Inc., Fremont, CA, USA
Go-Taq® Dna Polymerase Buffer, 5x	Promega, USA
Golgi Plug	BD Biosciences, Franklin Lakes, NJ, USA
HCl	Merck Millipore, Germany
H_2O_2, 30 %	Merck Millipore, Germany
HyperLadder™ 50 bp	Meridian Bioscience, BioCat GmbH, Germany

Ionomycin	Sigma Aldrich, USA
Isopropyl alcohol	Th. Geyer GmbH & Co. KG, Germany
L-Glutamine, 200 mM	Sigma Aldrich, USA
LIVE/DEAD™ Fixable NIR Dead Cell Stain Kit	Thermo Fisher Scientific, Waltham, USA
Mayer's Hemalum	Merck Millipore, Germany
MemBrite™ Fix 488/515	Biotium, Inc., Fremont, CA, USA
MemBrite™ Fix 405/430	Biotium, Inc., Fremont, CA, USA
MOG_{35-55} peptide	Auspep, Parkville, Australia
MOG_{1-117} protein	GenScript Biotech, Leiden, Netherlands
NaCl, 0.9 % solution, sterile	B. Braun Melsungen Ag, Germany
$NaCO_3$	Merck Millipore, Germany
$NaHCO_3$	Merck Millipore, Germany
Paraffin Oil	Carl Roth, Germany
PBS, sterile	Sigma Aldrich, USA
Penicillin, 10 000 Units	Sigma Aldrich, USA
Perm/Wash™ Buffer, 10x	BD Biosciences, Franklin Lakes, NJ, USA
POX (Peroxidase conjugated Avidin)	Sigma Aldrich, USA
PFA, powder	Merck Millipore, Germany
PMA	Sigma Aldrich, USA
PTX	Sigma Aldrich, USA
RPMI-1640	Sigma Aldrich, USA
Sodium Pyruvate, 100 mM	Sigma Aldrich, USA
qPCRBIO SyGreen	Nippon Genetics Europe GmbH, Dueren, Germany
TMB	Moss Inc., Maryland, USA
Tris	Carl Roth, Germany
Trypan Blue	Sigma Aldrich, USA
Tween	Merck Millipore, Germany
Xylol	Th. Geyer GmbH & Co. KG, Germany

2.1.2. Solutions and buffers

Table 2: Solutions and buffers

Solution/buffer	Composition
Blocking buffer for immunohistochemistry	• PBS • 10 % FCS
CFA	• Paraffin oil • 15 % mannide monooleate • 6.7 mg/ml Mycobacterium tuberculosis H37RA
Chloral hydrate, 14 %	• distilled water • 14 % chloral hydrate
Citric acid buffer, 10 Mm	• 2.1 g citric acid • 1 l distilled water • NaOH, adjust to pH 6
Coating buffer	• 8.4 g NaHCO3 • 3.5 g NaCO3 • 1 l distilled water • Stir filter, adjust to pH 9.5
Cryo medium	• 60 % RPMI complete • 20 % DMSO • 20 % FCS
3,3'-Diaminobenzidine tetrachloride (Dab) working solution	• PBS • 0.5 mg/ml DAB • add 20 µl 30 % hydrogen peroxidase per 50 ml DAB solution before use
ELISA wash buffer	• 1 ml Tween • 1.8 l distilled water • 200 ml 10x PBS
ELISA stop solution	• 1 N H_2SO_4 solution
1 % Eosin	• 70 % isopropyl alcohol • 1 % eosin G • stir filter, before use add 0.5 % acetic acid
Fluorescence-activated cell sorting (FACS) buffer	• PBS, sterile • 2 % FCS
1 % HCl	• 1 % HCl absolute

	• 70 % ethanol
Magnetic Activated Cell Sorting (MACS) buffer	• PBS, sterile • 0.5 % FCS • 2 mM EDTA • pH 7.2
10x PBS	• 95.5 g PBS • 1 l distilled water
RD1 buffer (ELISA block buffer)	• 200 ml 10x PBS • 20 g BSA • 1.8 l distilled water
RPMI complete	• RPMI-1640 • 10 % FCS • 1 mM sodium pyruvate • 50 µM β-Mercaptoethanol • 100 units penicillin • 2 mM L-glutamine
TAE (Tris, acetic acid, EDTA) buffer	• 40 mM Tris • 20 mM acetic acid • 1 mM EDTA • 1 l distilled water (adjusted to pH 8)

2.1.3. Consumables

Table 3: Consumables

Reagent	Supplier
96-well round bottom plate	Sarstedt, Germany
96-well flat bottom plate	Greiner bio-one, Austria
96-well Transwell plate 0.4 µm	Sigma-Aldrich Chemie Gmbh, Germany
Cell strainer (70 µm)	Greiner bio-one, Austria
FACS Tube, 5 ml	Sarstedt, Germany
LS columns	Miltenyi Biotec, Germany
Needles	BD Biosciences, USA
Pre-Separation filters, 30 µm	Miltenyi Biotec, Germany
Syringes	BD Biosciences, USA
Tubes (50 ml, 15 ml, 10 ml, 2 ml, 1.5 ml, 0.5 ml)	Sarstedt, Germany

2.2. Patients

Peripheral blood mononuclear cells (PBMCs) were obtained after informed consent. The protocol was approved by the Ethics committee of the University Medicine of Göttingen, approval number 3/4/14. For longitudinal analysis, only patients without cortisone-obligatory relapse within the last three months before sample collection were included.

Table 4: Characteristics of the patient cohort

Number of patients (samples before/ depletion/ early repletion/ late repletion)	**14 (11/13/10/10)**
Sex (w/m)	**8/6**
EDSS score at start of the study (median, IQR/range)	3 ± 2.5
Age at start of study (years; mean ± standard deviation (SD))	40.36 ± 9.09
Time since multiple sclerosis diagnosis (years; mean ± SD)	11 ± 6.54
Observation time after anti-CD20 treatment start (years; mean ± SD)	4.07 ± 0.83
Last treatment before rituximab (cases):	
Dimethyl fumarate	3
Fingolimod	4
Azathioprine	1
Natalizumab	1
Glatiramer acetate	1
Methylprednisolone	3
None (i.e. treatment naïve)	1
Wash-out periods (weeks; mean ± SD)	8.15 ± 4.85

2.3. Animals

Table 5: Mouse lines

Mouse strain	**Specifications**
C57BL/6J	6-8 week old mice were purchased either from Charles River laboratories, Germany or directly from the ZTE, the animal facility of the University medical center Göttingen. 1 day-, 1 week-, 2 week- and 3 week-old mice were purchased from the ZTE Göttingen.
Balb/c	6-8 week old mice were purchased from Charles River laboratories, Germany.
2D2	MOG_{35-55} TCR transgenic 2D2 mice were kindly provided by Dr. Kuchroo (Boston, USA) and bred at the ZTE, the central animal facility of the University medical center Göttingen. We used hemizygous mice, which exhibit $CD4^+$ T cells expressing the transgenic MOG_{35-55} specific TCR (defined by Valpha3.2 and Vbeta11 expression) responsive to whole myelin oligodendrocyte glycoprotein and to MOG_{35-55} peptide.

CD20KO	CD20 knockout (KO) mice were generated by Genentech and bred at the animal facility of the European neuroscience institute Göttingen. CD20KO mice are genetically modified to not express the CD20 protein on any cell.
OT II	Ovalbumin 323-339 ($OVA_{329-337}$) TCR transgenic OT II mice were purchased from Jackson Laboratory (Sacramento, California, USA; stock No: 004194) and bred at the ZTE, the central animal facility of the University medical center Göttingen. These mice express the mouse alpha-chain and beta-chain T cell receptor that pairs with the CD4 co-receptor and is specific for chicken $OVA_{329-337}$ peptide in the context of $I\text{-}A^b$. This results in $CD4^+$ T cells that primarily recognize OVA peptide residues 323-339 when presented by the MHC class II molecule.
MHC IIKO	MHC IIKO mice were purchased from Jackson Laboratory (Sacramento, California, USA; stock No: 003584). This strain lacks MHC class II genes *H2-Ab1*, *H2-Aa*, *H2-Eb1*, *H2-Eb2*, *H2-Ea*, serving as an appropriate background for developing xenogenic class II MHC transgenic strains.
µMT	µMT mice were purchased from Jackson Laboratory (Sacramento, California, USA; stock No: 002288) and bred at the ZTE, the central animal facility of the University medical center Göttingen. These mice lack mature B cells, due to a mutation in one of the membrane exons of the gene encoding the µ-chain constant region. Therefore, B cell development is arrested at the pre-B cell stage in these mice.[128]
Mb1-cre	Mb1-cre mice were purchased from Jackson Laboratory (Sacramento, California, USA; stock No: 020505) and bred at the ZTE, the central animal facility of the University medical center Göttingen. These mice lack mature B cells, since they carry an allele in which exons 2 and 3 of the *Cd79a* gene have been replaced with a codon optimized Cre recombinase gene and the ATG codon of exon 1 is deleted; both abolishing endogenous *Cd79a* gene function and placing *cre* expression under the control of the endogenous *Cd79a* promoter/enhancer elements. Cre recombinase expression is directed at the earliest stages and throughout B-lymphocyte development and differentiation.

All animal experiments and breeding were carried out in accordance with the guidelines of the Central Department for Animal Experiments, University Medical Center, Göttingen and approved by the Office for Consumer Protection and Food Safety of the State of Lower Saxony (protocol number 33.9-42502-04-15/1804 and 33.9-42502-04-16/2267).

2.4. Methods

2.4.1. EAE induction and scoring

Female C57BL/6J mice were immunized by subcutaneous injection with either 100 µg MOG_{35-55} peptide (Auspep, Parkville, Australia) or 75 µg MOG_{1-117} protein (GenScript Biotech) emulsified in CFA, containing 250 µg killed *Mycobacterium tuberculosis* H37 Ra. This was followed by intraperitoneal injections of 200 ng of *Bordetella pertussis* toxin (Sigma-Aldrich) at the day of immunization and 2 days after. Adoptive transfer EAE was induced by immunizing donor mice with 200 µg MOG_{35-55} peptide. Spleens and inguinal lymph nodes were extracted at d12 after immunization and single cell solutions thereof were stimulated with MOG_{35-55} peptide, recombinant IL-12 and anti-IFNγ antibodies for 3 days. Thereafter, B cells were removed via MACS separation and $1.44x10^6$ lymph nodes cells or $20x10^6$ splenocytes without B cells were i.v. injected into CD20KO mice. To deplete $CD20^+$ T cells, mice received weekly intraperitoneal injections of 200 µg of murine anti-CD20 ab or isotype-control (provided by Genentech). The EAE score, the measure of disease severity, was evaluated daily and illustrated in a scale from 0 to 5: 0 = no clinical signs; 1.0 = tail paralysis; 2.0 = hindlimb paresis; 3.0 = severe hindlimb paresis; 4.0 = paralysis of both hindlimbs; 4.5 = hindlimb paralysis and beginning forelimb paresis 5.0 = moribund / death.

2.4.2. Anti-CD20 treatment

For depletion of $CD20^+$ T and B cells, C57BL/6J mice received weekly intraperitoneal injections with either 200 µg of murine anti-CD20 or isotype-control (provided by Genentech, South San Francisco, USA) for 3 weeks before further experiments.

2.4.3. Histology and immunohistochemistry

Mice were euthanized with CO_2 and transcardially perfused with PBS followed by 4 % paraformaldehyde (PFA). CNS, spleen and liver were processed and embedded in paraffin. 1 µm-thick slices were stained with hematoxylin and eosin (H&E). T cells and B cells were detected by immunohistochemistry with an avidin-biotin technique using antibodies specific for CD3 (SP7; DCS Innovative Diagnostik-Systeme) and CD45R/B220 (RA3-6B2; BD Biosciences) and their respective secondary antibodies **(Table 6).** Histological sections were captured using a digital camera (DP71; Olympus Europa GmbH, Hamburg, Germany) mounted on a light microscope (BX51; Olympus Europa GmbH). Inflammatory cells were quantified at 400x magnification using an ocular counting grid and are shown as cells/mm². At least 6 spinal

cord cross sections were taken for each analysis. Slices of spleens from µMT and wild type mice were pretreated with citrate buffer and stained with the primary antibodies anti-B220 (RA3-6B2; BD Biosciences) and anti-CD3 (SP7; DCS Innovative Diagnostik-Systeme), followed by staining with the respective secondary antibodies anti-rat AF488 (Dianova), anti-rabbit Cy3 (Jackson ImmunoResearch) and DAPI (dilactate; Invitrogen).

Table 6: Antibodies for immunohistochemical staining

Reactivity	Antigen	Species	Clone	Antigen retrieval/ fixation	Dilution	Supplier
Anti-mouse	CD3	rabbit	CD3-12	microwave, citrate buffer	1:200	DCS Innovative Diagnostik-Systeme, Germany
	B220	rat	RA3-6B2	microwave, citrate buffer	1:200	BD Biosciences, USA
Secondary antibodies	Anti-rabbit Cy3	goat	-	-	1:200	Jackson Immuno Research, USA
	Anti-rat AF488	goat	-	-	1:200	Dianova, Germany
	Anti-rabbit	goat	-	-	1:100	Jackson Immuno Research, USA
	Anti-rat	goat	-	-	1:500	DCS Innovative Diagnostik-Systeme, Germany

2.4.4. Isolation of human and murine leukocytes

Human PBMCs from healthy donors and MS patients were isolated with ficoll gradient centrifugation (Biochrom GmbH, Berlin, Germany). Single cell suspensions of murine spleens and inguinal lymph nodes were generated by gentle dissection and passing through a 70 µm cell strainer (Greiner bio-one, Kremsmuenster, Austria). CNS mononuclear cells were isolated by either:

- digestion of perfused CNS tissue using the multi tissue dissociation kit 1 (Miltenyi, Bergisch Gladbach, Germany) and a gentleMACS™ Octo Dissociator (Miltenyi, Bergisch Gladbach, Germany), passing digested tissue through a 70 µm cell strainer (Greiner bio-one) followed by debris and red blood cell removal
- digestion of perfused CNS tissue using Collagenase D and DNAse I, passing digested tissue through a 70 µm cell strainer (Greiner bio-one), followed by a percoll gradient
- passing through a 70 µm cell strainer (Greiner bio-one) for untreated cells
- passing through a 70 µm cell strainer (Greiner bio-one), followed by a percoll gradient

- passing through a 70 µm cell strainer (Greiner bio-one), followed by a ficoll gradient (Biochrom GmbH, Berlin, Germany)
- passing through a 70 µm cell strainer (Greiner bio-one), followed by MACS separation using myelin removal beads (Miltenyi, Bergisch Gladbach, Germany)

Murine blood was collected in PBS containing 1 mM EDTA and erythrocytes were lysed using BD Pharm Lysing Buffer. Murine splenic B cells were purified or removed by MACS separation using a mouse CD19 beads kit (BioLegend or Miltenyi). Murine T cells were isolated by negative MACS separation using a mouse pan T cell isolation kit II (Miltenyi, Bergisch Gladbach, Germany).

2.4.5. Adoptive B cell transfer

To introduce B cells into B cell-deficient mice, weekly intravenous (i.v.) injections of $10x10^6$ MACS isolated B cells were performed for 3-4 weeks. Afterwards, B cells were allowed to migrate and accumulate in the spleen for 10 weeks for *ex vivo* analysis and 8 weeks before MOG_{1-117} protein immunization without PTX injections. *Ex vivo* analysis of immunized mice was performed at d14 after immunization.

2.4.6. Adoptive transfer of fluorescence-sorted T cells

To analyze the pathogenicity of $CD20^+$ T cells, $CD20^+$ or $CD20^-$ T cells were transferred into EAE induced mice at the inflammatory stage of EAE before symptom development. Donor mice were immunized with 100 µg MOG_{35-55} peptide and spleens were harvested at d10 post immunization. Whole spleens were stained and FACS-sorted for $CD20^+$ and $CD20^-$ T cells. 200 000 $CD20^+$ or $CD20^-$ T cells were i.v. injected at d5 and d8 after MOG_{35-55} peptide EAE induction of acceptor mice (50 µg MOG_{35-55} peptide at d0 + 2x 100 ng PTX at d0 and d2).

2.4.7. T cell-B cell coculture assays

For B cell–T cell coculture assays, B cells from wild type or CD20KO mice and T cells from $MOGp_{35-55}$ TCR transgenic 2D2 mice were MACS-separated from splenocytes. Following separation, B cells and T cells were evaluated for purity (>99 %) by flow cytometric staining for CD19 and CD3. 400 000 B cells and 50 000 T cells were plated for culture and after 24-48 h, cells were evaluated by flow cytometry. As control for effects independent of cell-cell contact, coculture was performed in transwell plates, where B cells and T cells were separated by a cell-impenetrable 0.4 µm membrane. To display trogocytotic membrane transfer,

B cells and T cells were stained with membrane stain (B cells: MemBrite™ Fix 488/515, green; T cells: MemBrite™ Fix 405/430, blue) according to the manufacturer´s instructions.

2.4.8. α-CD3/α-CD28 T cell stimulation

To analyze T cell proliferation, T cells were stained with CFSE (BioLegend). For differentiation analysis, T cells remained unstained. T cells were incubated in leaf™ purified anti-mouse CD3 (clone 145-2C11 for murine T cells) / leaf™ purified anti-mouse CD28 (clone 37.51 for murine T cells) (BioLegend) pre-coated wells for 48-72 h.

2.4.9. Flow cytometry

Composition of murine and human immune cells were analyzed using the following antibodies:

Table 7: Monoclonal antibodies for flow cytometry

Reactivity	Application	Antigen	Fluorochrome	Clone	Dilution	Supplier
Anti-mouse	**Lineage marker**	**CD3e**	PE	145-2C11	1:200	BioLegend
	Lineage marker	**CD4**	BV510	GK1.5	1:100	BioLegend
	Lineage marker	**CD4**	PE	RM4-5	1:100	BioLegend
	Lineage marker	**CD8a**	FITC	53-6.7	1:100	BioLegend
	Lineage marker	**CD8a**	BV421	53-6.7	1:100	BioLegend
	Lineage marker	**CD8a**	PE/Dazzle594	53-6.7	1:100	BioLegend
	Adhesion	**CD11a**	FITC	M14/4	1:100	BioLegend
	Lineage marker	**CD11b**	BV510	M1/70	1:100	BioLegend
	Fc-Block	**CD16/32, TruStainfcX**	-	-	1:200	BioLegend
	Lineage marker	**CD19**	PerCP-Cy5.5	1D3	1:100	BioLegend
	Lineage marker	**CD20**	AF647	SA275A11	1:1000	BioLegend
	Activation	**CD25**	PE	PC61.5	1:100	eBioscience
	Lineage marker	**CD45**	FITC	30-F11	1:100	BioLegend
	Adhesion	**CD49d**	PE	9C10	1:100	BioLegend
	Activation	**CD69**	PE/CY7	H1.2F3	1:100	BioLegend
	Activation	**MHC II**	PB	AF6-120.1	1:100	BioLegend
	Lineage marker	**FoxP3**	PE	FJK-16s	1:100	eBioscience
	Proinflammatory cytokine	**IL-17a**	PE	TC11-18H10	1:100	BD
	Proinflammatory cytokine	**GM-CSF**	PE/Cy7	MP1-22E9	1:100	BioLegend

	Proinflammatory cytokine	**IFNγ**	FITC	XMG1.2	1:100	BioLegend
Anti-human	**Lineage marker**	**CD3**	BV510	UCHT1	1:100	BioLegend
	Lineage marker	**CD4**	PE/Cy7	RPA-T4	1:100	BD
	Lineage marker	**CD8a**	FITC	RPA-T8	1:100	BioLegend
	Lineage marker	**CD14**	PerCP-Cy5.5	M5E2	1:100	BioLegend
	Lineage marker	**CD19**	PerCP-Cy5.5		1:100	BioLegend
	Lineage marker	**CD20**	PE	REA780	1:200 /500	Miltenyi Biotec
	Differentiation	**CD45RO**	AF700	UCHL1	1:100	BD
	Adhesion	**CD49d**	BV421	9F10	1:100	BioLegend
	Activation	**CD69**	BV785	FN50	1:100	BioLegend
	Th2 marker	**CCR4**	BV510	1G1	1:100	BD
	Differentiation	**CCR7**	PE-CF594	G043H7	1:100	BioLegend
	Th1 marker	**CXCR3**	PE/Cy5	1C6	1:100	BD
	Proinflammatory cytokine	**GM-CSF**	APC	BVD2-21C11	1:50	BioLegend
	Proinflammatory cytokine	**IL-17a**	PE-Dazzle	BL168	1:50	BioLegend
	Proinflammatory cytokine	**TNFα**	AF700	Mab11	1:50	BD
	Proinflammatory cytokine	**IFNγ**	BV421	B27	1:50	BioLegend
	Staining ctrl	**Mouse IgG1, k Isotype ctrl**	BV510	X40	1:100	BD
	Staining ctrl	**Mouse IgG1, κ Isotype ctrl**	BV605	X40	1:100	BD
	Staining ctrl	**Mouse IgG2a, κ Isotype ctrl**	PE-CF594	G155-178	1:100	BD
	Staining ctrl	**Mouse IgG1, κ Isotype ctrl**	BV421	MOPC-21	1:200 /50	BioLegend
	Staining ctrl	**Mouse IgG1, κ Isotype ctrl**	BV785	MOPC-21	1:100	BioLegend
	Staining ctrl	**REA Ctrl (S)**	PE	REA293	1:200 /500	Miltenyi Biotec
	Staining ctrl	**Mouse IgG1 κ Isotype ctrl**	PE/Cy5	MOPC-21	1:100	BD

	Staining ctrl	**Mouse IgG1, κ Isotype ctrl**	PE/Dazzle 594	MOPC-21	1:200	BioLegend
	Staining ctrl	**Mouse IgG1, κ Isotype ctrl**	AF700	MOPC-21	1:50	BD

Fc receptors were blocked using monoclonal antibodies specific for CD16/CD32. Necrotic cells were stained with LIVE/DEAD™ Fixable NIR Dead Cell Stain Kit (Thermo Fisher Scientific, Waltham, USA). Treg cell differentiation was analyzed by intracellular FoxP3 staining after fixation and permeabilization with the fixation / permeabilization kit (eBioscience). For Th1 and Th17 cell differentiation, cell suspensions were stimulated with 50 ng/ml phorbol 12-myristate 13-acetate (PMA; Sigma-Aldrich) and 0.5 µg/ml ionomycin (Sigma-Aldrich) for 3 h, followed by 2 h in the presence of 1 µl/200 µl brefeldin A (BD Bioscience) and stained for IFNγ, IL-17a and GM-CSF after fixation and permeabilization (BD Bioscience).

For human T cell cytokine production, PBMCs were stimulated with 10 ng/ml PMA (Sigma-Aldrich) and 0.5 µg/ml ionomycin (Sigma-Aldrich) first for 1 h, followed by 12 h in the presence of 1 µl/200 µl brefeldin A (BD Bioscience) and staining for IL-17a, IFNγ, GM-CSF and TNFα after fixation and permeabilization (BD Bioscience). Isotype control antibodies were applied as negative staining control.

For $CD20^+$ T cells analysis, pre-gates were utilized to control for B cell contamination. T cells were pre-gated for single cells, cell size (to exclude apoptotic and early apoptotic cells), living cells (live/dead stain), $CD19^-CD3^+$ or $CD19^-CD4^+$ or $CD19^-CD8^+$ cells and gated for CD20 on CD20KO T cells or a fluorescence minus one as negative gating control **(Fig.7).**

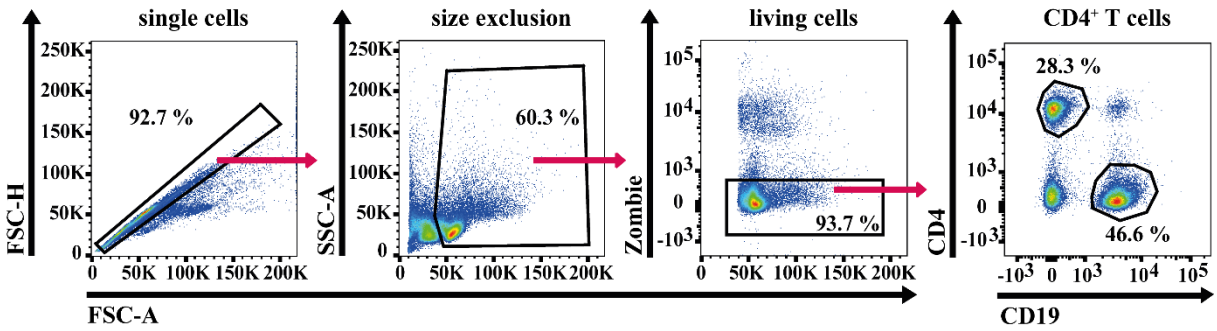

Fig.7: Pregating strategy
Pregating of flow cytometrically analyzed cells to exclude doublets, necrotic and apoptotic cells, and B cells from the T cell population.

Samples were acquired on a BD LSR Fortessa (BD Bioscience). All data evaluation was performed using FlowJo software (FlowJo LLC, Ashland, USA).

2.4.10. Analysis of cytokine content via enzyme-linked immunosorbent assay (ELISA)

The production of IFNγ, IL-17, IL-4, TNFα and GM-CSF of murine FACS-sorted T cells was measured by ELISA MAX Standard Set kits (BioLegend). IL-2 and IL-10 production was quantified employing ELISA MAX Standard Set kits (R&D Systems). Absorbance was measured at 450 nm with subtraction of a 540 nm reference wavelength on the iMark microplate reader (Bio-Rad laboratories Inc., Hercules, USA).

2.4.11. Quantitative real-time polymerase chain reaction (PCR)

T cells and B cells were FACS-sorted from splenocytes. Total RNA was isolated using the RNeasy mini kit (Qiagen, Hilden, Germany) and transcribed into cDNA using the QuantiNova Reverse Transcription kit (Qiagen) according to the manufacturer´s instructions. Quantitative real-time PCR (qPCR) was performed using 500 nM per primer and qPCRBIO SyGreen (Nippon Genetics Europe GmbH, Dueren, Germany) in a total volume of 10 µl on a QuantStudio 7 (Applied Biosystems, Waltham, USA). Primer pairs were purchased from eurofins genomics:

Table 8: Oligonucleotide primer

Target gen	Primer sequence	Amplicon size (bp)	Melting temp. [°C]	Annealing temp. [°C]
CD3	**Forward:** ATG CGG TGG AAC ACT TTC TGG **Reverse:** GCA CGT CAA CTC TAC ACT GGT	126	84.64	67
CD19	**Forward:** GGA GGC AAT GTT GTG CTG C **Reverse:** ACA ATC ACT AGC AAG ATG CCC	164	87.25	67
CD20-1	**Forward:** GCT CCA AAA GTG AAC CTC AAA AG **Reverse:** CCC AGG GTA ATA TGG AAG AGG C	121	82.51	67
CD20-2	**Forward:** CAA ACT TCC AAG CCG TAT GTT G **Reverse:** CCG ACA GAA TGC CCA AGA AC	125	80	67
GAPDH	**Forward:** CAT GGC CTT CCG TGT TCC TA **Reverse:** TGT CAT CAT ACT TGG CAG GTT TCT	83	84.1	67
B2M	**Forward:** CGG CCT GTA TGC TAT CCA GA **Reverse:** GGG TGA ATT CAG TGT GAG CC	227	83.2	67

RT-PCR runs were performed at 95 °C denaturating and 67 °C annealing temperature. Elongation was performed for 30 s and 40 cycles with subsequent melt-curve analysis. Samples were analyzed in triplicates and considered valid when Ct<35 and SD Ct<0.5. Analyzed expression was normalized to beta-2-microglobulin (B2M) and Glycerinaldehyd-3-phosphat-Dehydrogenase (GAPDH) (house keeping genes) expression loading control (delta-Ct). Results were analyzed using QuantStudio™ Real-Time PCR Software v1.3.

2.4.12. Agarose gel electrophoresis

Generated RT-PCR products were analyzed for their size by gel electrophoresis in a 2 % agarose gel, containing GelRed (Biotium) to stain nucleic acids and UV-light illumination. HyperLadder™ 50 bp (BIOLINE) was used to gauge product sizes.

2.4.13. Statistical analysis

Statistics were calculated using the software GraphPad Prism 6. Murine immune cell frequencies, cytokine concentrations and T cell activation are shown as mean or mean ± SD and were analyzed by two-way analysis of variance (ANOVA) followed by Holm-Sidak multiple comparison test. Correlations of the mean fluorescence intensity (MFI) of CD20 and membrane stain or B cell and $CD20^+$ T cells frequency were calculated by Pearson's correlation analysis or nonparametric Spearman correlation depending on whether values were normally distributed. Clinical scores are depicted as mean ± standard error (SEM). $CD3^+$ T cell infiltration was shown as mean ± SD analyzed using unpaired t test with Welch's correction. Human immune cell frequencies, T cell activation and development were calculated using Wilcoxon matched-pairs signed rank test or ratio-paired t test depending on whether values were normally distributed. A value of $p \leq 0.05$ was considered significant and is shown by one asterisk. $P \leq 0.01$ = **, $p \leq 0.001$ = *** and $p \leq 0.0001$ = ****, respectively.

3. Results

In humans, CD20$^+$ T cells are by now established as a small T cell population (3-5 %), that can be found in numerous compartments, e.g. blood, bone marrow and cerebrospinal fluid[114]. These CD20$^+$ T cells occur in healthy subjects as well as in patients with various autoimmune diseases, such as MS, rheumatoid arthritis or psoriasis[114, 118, 129, 130]. CD20$^+$ T cells have been suggested to play a role in inflammatory processes, especially in MS[115]. Therefore, we plan to search for and analyze CD20$^+$ T cells in mice as our model organism. Here, we aim to examine the potential patogenicity of CD20$^+$ T cells in EAE, before we do the same in MS patients.

3.1. CD20$^+$ T cells exist in wild type mice

To date, little is known about CD20$^+$ T cells in any other species apart from humans. To ascertain that CD20$^+$ T cells are present in mice, we analyzed C57B6/J wild type mice for the expression of CD20 on T cells via flow cytometry **(Fig.8a**). To confirm the specificity of the utilized CD20 antibody, CD20 staining on mouse CD19$^+$ B cells, which are known to express CD20 at high levels[112], was compared to stained B cells from a CD20KO mouse strain of the same background. CD20 shows only a dim staining on human T cells. Therefore, it is difficult to differentiate between CD20-positive and -negative cells, and CD20KO T cells were used as a negative control. Additionally, pregating as described in **2.4.9** controled for doublets so as to not measure the CD20 signal of a B cell on an attached T cell. Under these conditions, we were able to detect the presence of CD20$^+$ T cells in B6J wild type mice **(Fig.8a)**. Analyzing new born mice in their development over the course of a few weeks, we found that CD20$^+$ T cells, as well as B cells, are present in the spleen already one week after birth **(Fig.8b-c)**. At 2 weeks of age, both B and CD20$^+$ T cells greatly expand and subsequently slightly decrease with age to reach a steady level in adult mice. Balb/c mice, as an other wild type mouse line, were also analyzed for the presence of CD20$^+$ T cells. They presented similar levels of CD20$^+$ T cells, as well as CD19$^+$ B cells and CD3$^+$ T cells compared to C57B6/J mice **(Fig.8d-g)**. Merely the amount of CD20 on B cells was slightly elevated in Balb/c mice in all compartments and the frequency of B cells was slightly reduced in the blood in favor of T cells. CD20$^+$ T cells in the spleens of Balb/c mice were also slightly elevated. Overall, we could prove the existence of CD20$^+$ T cells in mice.

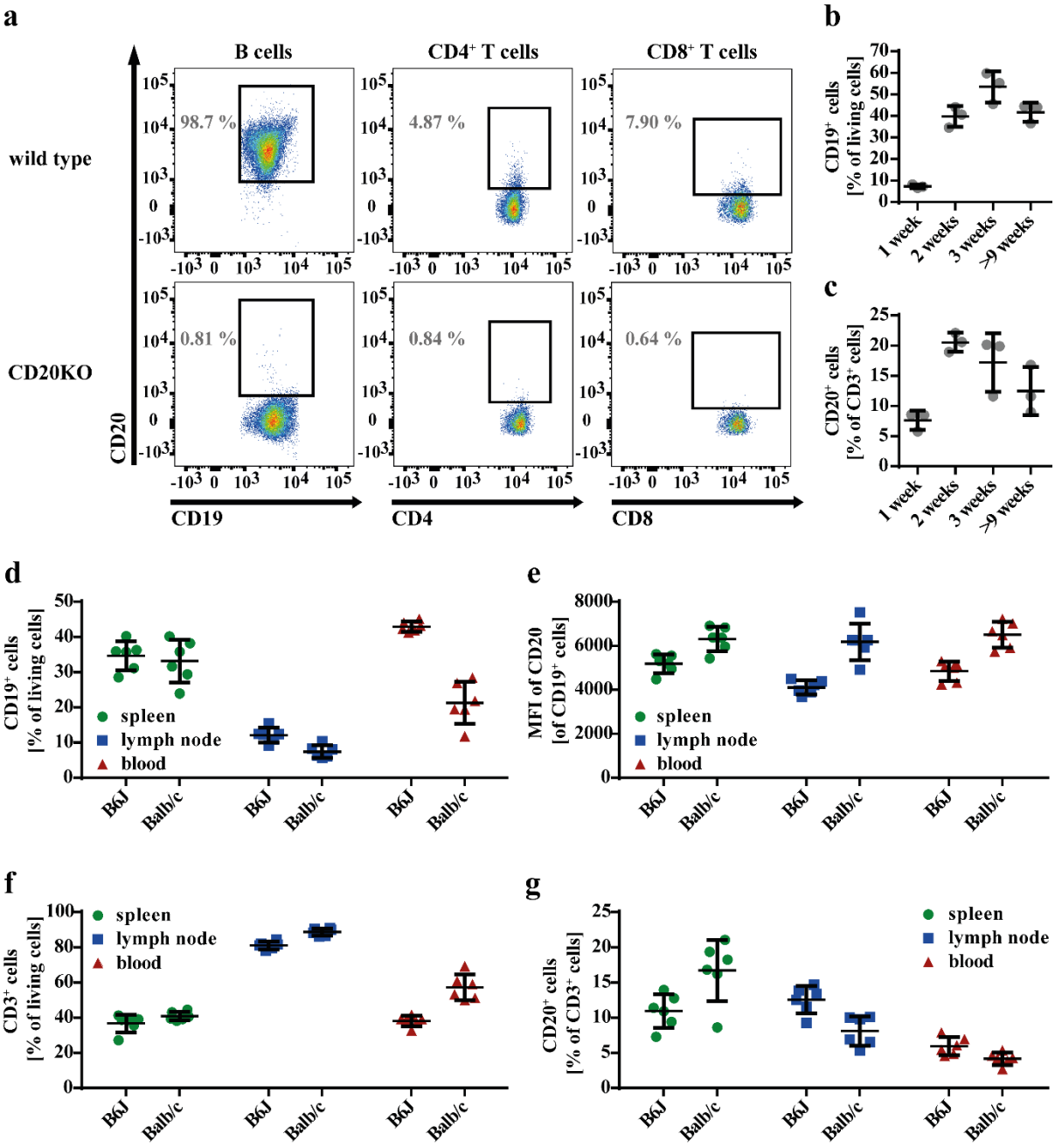

Fig.8: CD20⁺ T cells exist in wild type mouse strains.

a, Representative CD20 staining on CD19⁺ B cells, CD4⁺ T cells and CD8⁺ T cells isolated from wild type and CD20KO mice. Percentage of **b,** CD19⁺ B cells and **c**, CD3⁺CD20⁺ T cells in murine spleens during development (n=3 per group, representative of two independent experiments, displayed as mean ± SD). **d-g,** Flow cytometric analysis of spleen, lymph nodes and blood from C57B6/J and BALB/c mice for **d**, frequency of CD19⁺ B cells, **e**, MFI of CD20 on CD19⁺ B cells, **f**, frequency of CD3⁺ T cells and **g**, frequency of CD20⁺ T cells (n=6 mice per group).

3.2. T cells acquire CD20 via trogocytosis during B cell-T cell interaction

3.2.1. B cell-deficient mice do not contain CD20$^+$ T cells

Since we now know, that CD20$^+$ T cells exist in wild type mice, we analyzed two different B cell-deficient mouse lines (µMT and mb1-cre), which both lack mature B cells, for their frequency of CD20$^+$ T cells. In these mouse lines, without any B cells inherently in the system, we would be able to examine the sole effect of CD20$^+$ T cell depletion in EAE **(Fig.9)**. As expected, µMT and mb1-cre mice did not contain CD19$^+$ B cells in any of the analyzed compartments **(Fig.9a)**. Interestingly, no CD20$^+$ T cells could be detected in B cell-deficient mice either **(Fig.9b).** Unfortunately, this made it impossible for us to use them as a model to study the selective depletion of CD20$^+$ T cells.

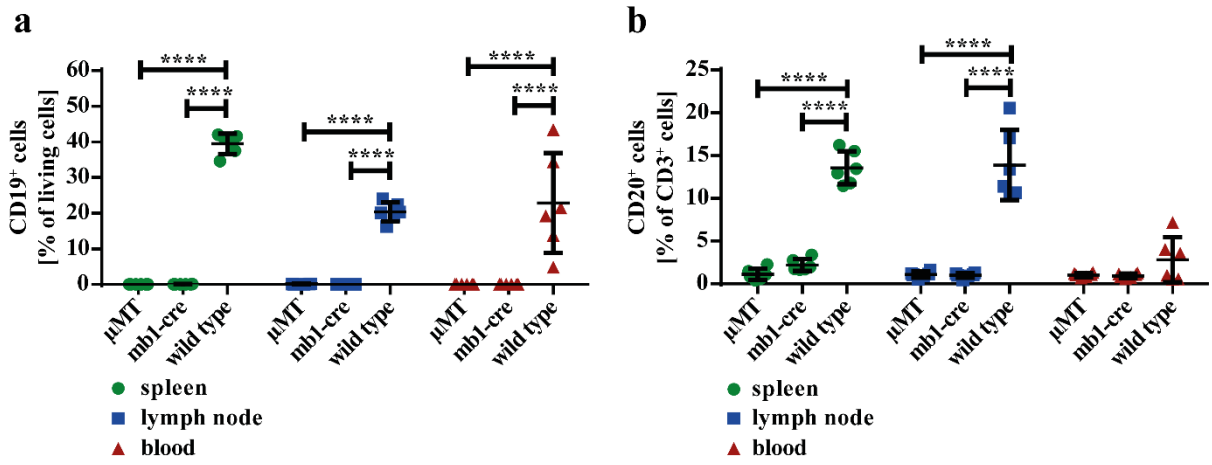

Fig.9: B cell-deficient mice do not contain any CD20$^+$ T cells.
Flow cytometric analysis of the percentage of **a,** CD19$^+$ B cells and **b,** CD3$^+$CD20$^+$ T cells in spleen, lymph nodes and blood from wild type or B cell-deficient mice (µMT and mb1-cre; n=6 per group; displayed as mean ± SD). p values were calculated via two-way ANOVA with Holm-Sidak's post hoc; ****=$p \leq 0.0001$.

3.2.2. CD20$^+$ T cells do not expand in direct T cell stimulation

At the same time, we attempted to expand the realtively small CD20$^+$ T cell population *in vitro* by direct T cell stimulation via α-CD3/α-CD28 for further analysis **(Fig.10)**. As expected, T cells proliferated in a concentration dependent manner **(Fig.10a,b)**. However, the frequency of CD20$^+$ T cells did not change **(Fig.10c)**.

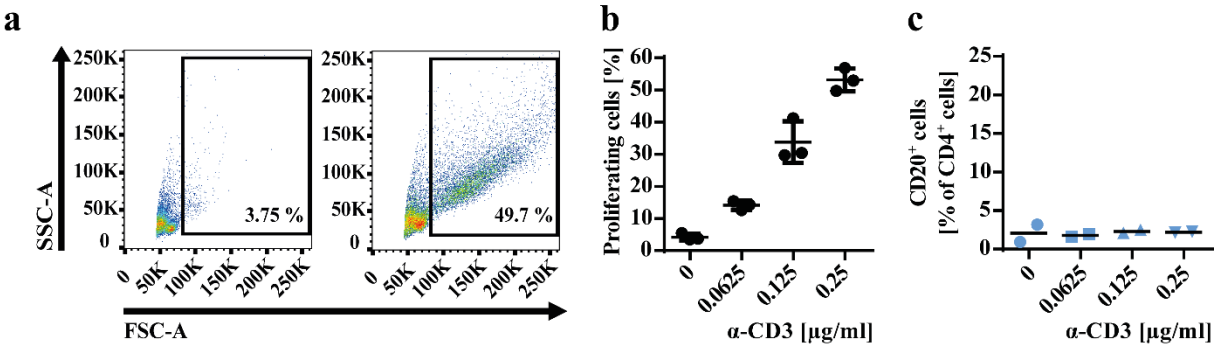

Fig.10: T cells proliferate under direct stimulation, but CD20$^+$ T cells do not expand.
a-c, Flow cytometric analysis of MOG$_{35-55}$ TCR transgenic 2D2 mouse splenocyte cultures stimulated with anti-CD3/anti-CD28 antibodies for 48 h. **a,b**, Proliferation measured by cell size (**a**, exemplary flow cytometry blots for proliferation measurement). **c**, Percentage of CD20$^+$ cells of CD4$^+$ cells. All figures representative of at least two independent experiments.

3.2.3. CD20$^+$ T cells cannot endogenously express CD20

As seen in **3.2.1** and **3.2.2**, CD20 expression on T cells was not triggered by direct T cell activation and B cell-deficient mice do not contain any CD20$^+$ T cells. Therefore, the question arose, if CD20$^+$ T cells might be unable to endogenously express CD20. To answer this question, FACS-sorted CD20$^+$ T cells were analyzed via real-time quantitative PCR for their expression of CD20 with two different primer pairs **(Fig.11**). The primer specificity was confirmed by size analysis of the PCR products by agarose gel electrophoresis. B cells and whole T cells were similarly FACS-sorted and utilized as positive and respectively negative controls for cell type and purity of the sorted cells, function and specificity of primer pairs. While their respective lineage markers CD19 and CD3 were present in B and T cells, CD20 expression was only detectable in B cells but not in whole T cells or sorted CD20$^+$ T cells **(Fig.11)**. In conclusion, in our system murine CD20$^+$ T cells seem to be unable to endogenously express CD20.

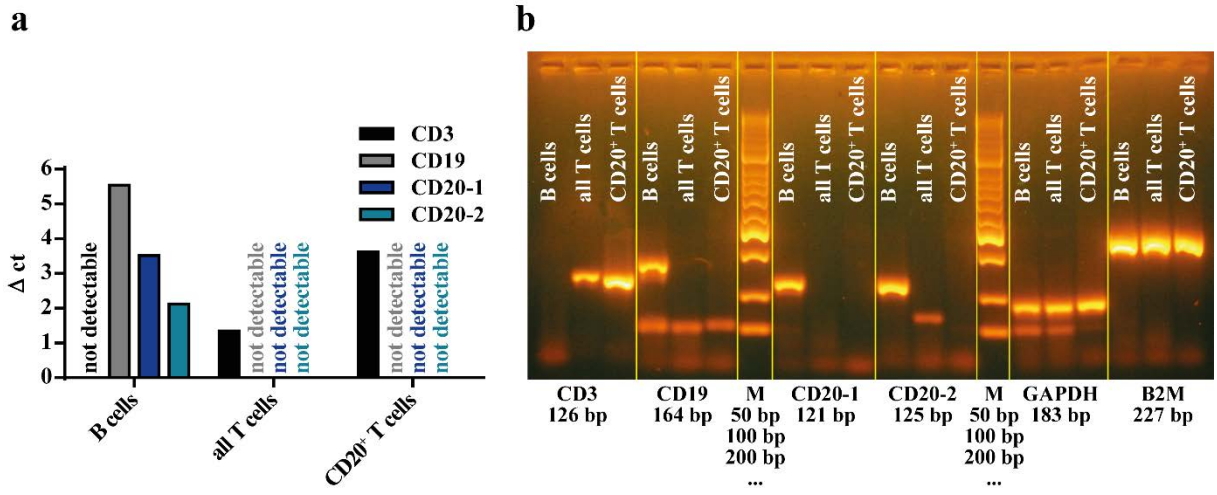

Fig.11: CD20$^+$ T cells cannot endogenously express CD20.
a, Reverse transcription polymerase chain reaction (RT-PCR) of FACS-sorted CD19$^+$ B cells, CD3$^+$ T cells and CD3$^+$CD20$^+$ T cells with primer pairs for CD3, CD19 or CD20 (CD20-1, CD20-2); shown are Δct normalized target gene expression levels (housekeeping genes: GAPDH and B2M). **b**, Agarose gel with products from RT-PCR reaction. All figures representative of at least two independent experiments.

3.2.4. CD20$^+$ T cells expand exclusively in B cell-containing cultures

Due to the fact that CD20$^+$ T cells seem incapable to endogenously express CD20 **(as shown in 3.2.3)**, the possibility of a trogocytotic transfer of CD20 from CD20-expressing B cells during B cell-T cell interaction was investigated. Therefore, splenocyte cultures from MOG_{35-55} TCR transgenic 2D2 mice were stimulated with MOG_{35-55} peptide and analyzed for T cell proliferation and the frequency of CD20$^+$ T cells **(Fig.12a-c)**. Stimulation of T cells via their interaction with antigen presenting cells (APCs) led to an antigen concentration-dependent proliferation and expansion of CD20$^+$ T cells. The amount of CD20 on the T cell surface remained relatively stable throughout several divisions **(Fig.12c)**. However, in splenocyte cultures, lacking B cells, no change in the frequency of CD20$^+$ T cells could be observed **(Fig.12d)**, even though the T cells proliferated **(Fig.12e)**, were activated **(Fig.12f,g)** and expressed proinflammatory cytokines **(Fig.12h,i)** at similar levels as B cell-containing splenocyte cultures. Therefore, the interaction with B cells seems to be a requirement to generate CD20$^+$ T cells. These results make trogocytosis the most likely origin of CD20$^+$ T cells.

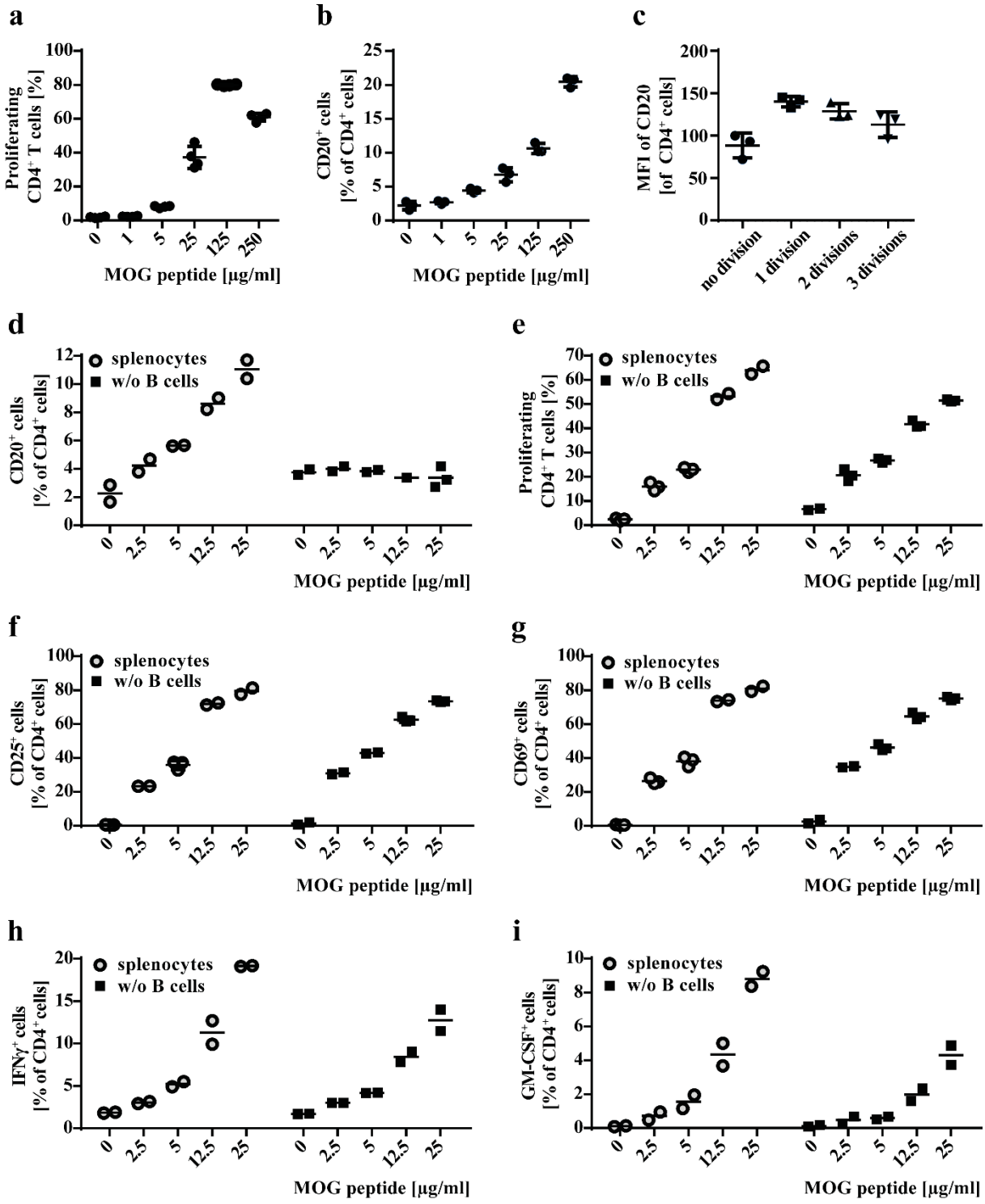

Fig.12: CD20$^+$ T cells only expand in B cell containing cultures.
a-i, Flow cytometric analysis of MOG_{35-55} TCR transgenic 2D2 mouse **a-c**, splenocyte cultures and **d-i,** splenocyte cultures with and without B cells stimulated with MOG_{35-55} peptide for 48 h. Cultures were analyzed for **a**,**e,** CD4$^+$ T cell proliferation (measured by cell size), **b,d,** percentage of CD20$^+$CD4$^+$ T cells, **c**, percentage of CD20$^+$ T cells during T cell proliferation, examined via CFSE staining to categorize the undergone divisions, activation (**f**, CD25 and **g**, CD69) and cytokine production (**h**, IFNγ and **i**, GM-CSF). All figures representative of at least two independent experiments.

3.2.5. CD20 transfer from B cells to T cells is not antigen-specific

We further wanted to exclude the possibility that the expansion of $CD20^+$ T cells in B cell-containing splenocyte cultures is antigen-specific, splenocyte cultures from $OVA_{329-337}$ TCR transgenic OTII mice were stimulated with $OVA_{329-337}$ peptide. $OVA_{329\ 337}$ TCR transgenic OTII mouse splenocyte cultures and splenocyte cultures without B cells showed similar results as splenocyte cultures with MOG_{35-55} TCR transgenic 2D2 mice **(Fig.12, Fig.13)**. The frequency of $CD20^+$ T cells expanded only in B cell-containing splenocyte cultures **(Fig.13a)**, despite similar T cell proliferation **(Fig.13b)** and activation (CD25/CD69) **(Fig.13c,d)** in B cell-removed cultures. The expansion of $CD20^+$ T cells in B cell-containing splenocyte cultures was therefore not antigen-specific.

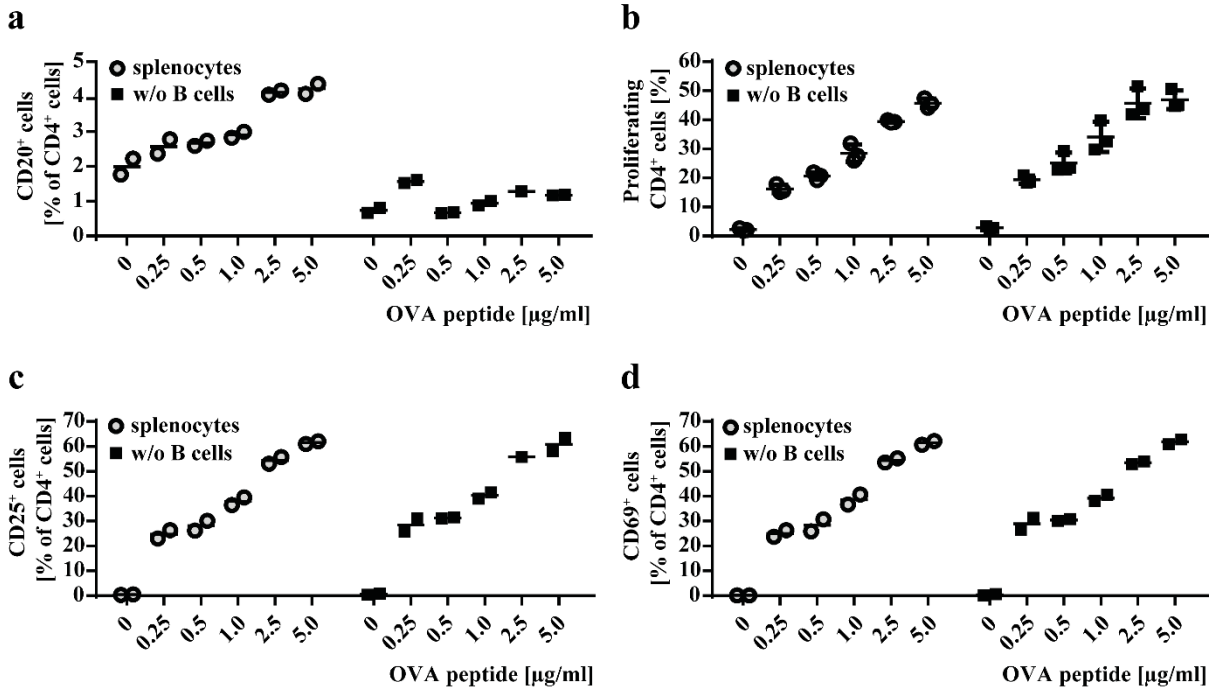

Fig.13: B cell-driven expansion of $CD20^+$ T cells is not antigen-specific.
a-d, Flow cytometric analysis of $OVA_{329-337}$ TCR transgenic OTII mouse whole splenocyte cultures and splenocyte cultures without B cells stimulated with $OVA_{329-337}$ peptide. Percentages of **a**, $CD20^+$ of $CD4^+$ cells, **b**, proliferating $CD4^+$ T cells **c**, $CD25^+$, and **d**, $CD69^+$ cells of $CD4^+$ T cells. All figures representative of at least two independent experiments.

3.2.6. $CD20^+$ T cells only expand in direct interaction with $CD20^+$ B cells

Next, we wanted to exclude the possibility that T cells gain CD20 from interactions with splenocytes other than B cells and to confirm that stimulation by B cells leads to the presence of CD20 on T cells, B cell-T cell cocultures were performed. MOG_{35-55} TCR transgenic 2D2 mouse T cells were cocultured with either CD20-expressing or CD20KO B cells and stimulated with MOG_{35-55} peptide or MOG_{1-117} protein **(Fig.14a-f)**. Noticeably, only cocultures containing CD20-expressing B cells exhibited an antigen-dependent increase in their $CD20^+$ T cell frequency, while cocultures containing CD20KO B cells did not **(Fig.14a,b)**. Meanwhile, both cocultures showed similar T cell activation **(**CD25, CD69) **(Fig.14c-f).** To examine if only the existence of $CD20^+$ B cells in the culture leads to an increase in the frequency of $CD20^+$ T cells or if direct interaction with B cells is required, cocultures with MHC IIKO B cells were performed **(Fig.14g-i)**. MHC II is necessary for B cells to interact with and subsequently activate $CD4^+$ T cells, which are almost the exclusive T cell subtype in MOG_{35-55} TCR transgenic 2D2 mice. In cocultures, containing MHC IIKO B cells, no increase in the frequency of $CD20^+$ T cells could be detected **(Fig.14g)**. Additionally, as expected, T cells were not activated in MHC IIKO B cell containing cocultures **(Fig.14h,i)**. To further confirm the need for direct B cell-T cell interaction, transwell cocultures, where B cells and T cells were separated by a semi-permeable 0.4 µm membrane, which cells cannot pass through, were conducted **(Fig.14j)**. When B cells and T cells could not directly interact, no T cell proliferation and expansion in the frequency of $CD20^+$ T cells could be measured. These results confirm the need for T cells to interact with CD20-expressing B cells to obtain CD20 on their surface.

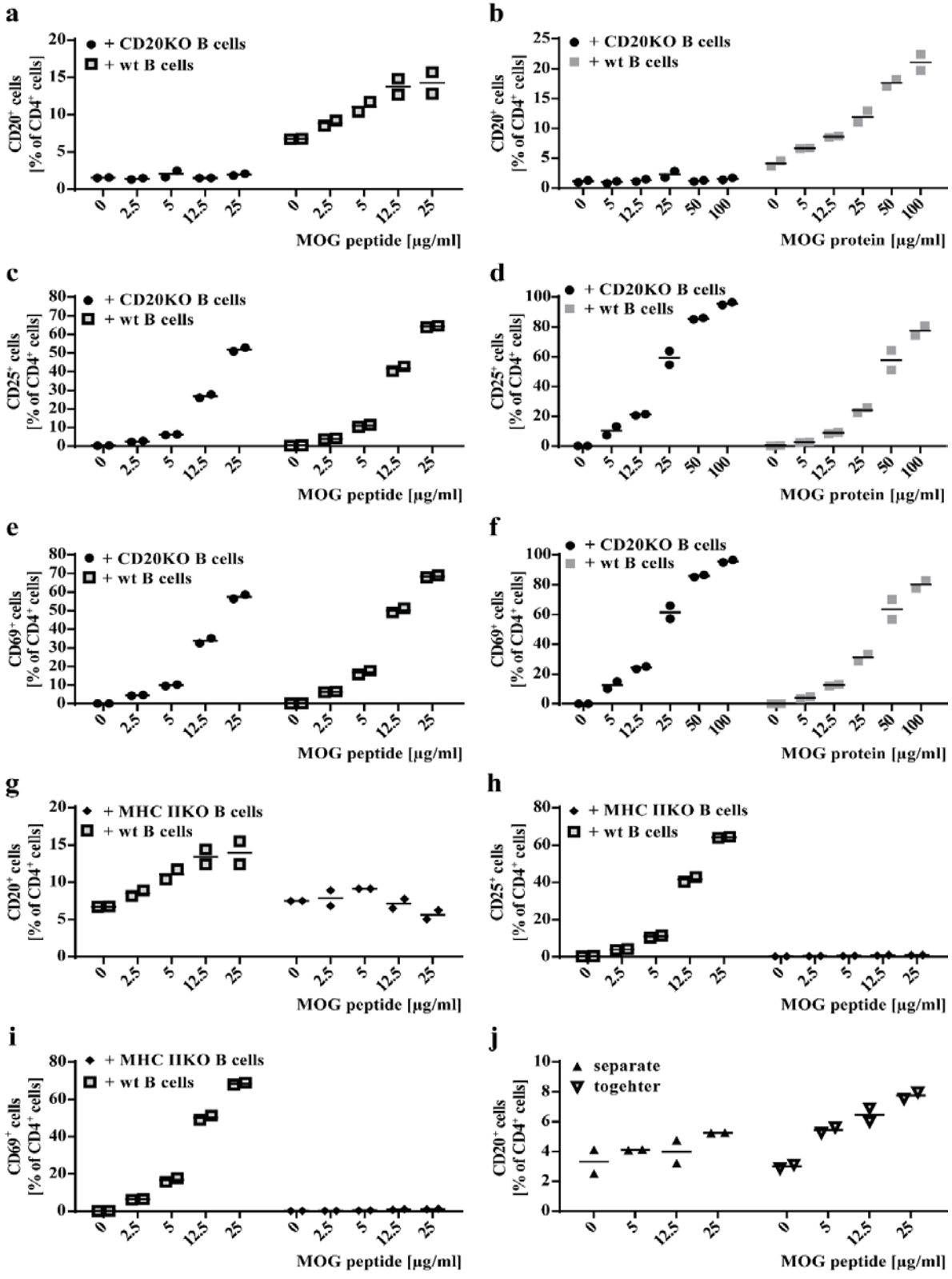

Fig.14: CD20$^+$ T cells only expand via direct interaction with CD20 expression B cells.

a-f, Purified B cell/T cell cocultures using wild type or CD20KO B cells and MOG_{35-55}-specific T cells stimulated with **a,c,e**, MOG_{35-55} peptide or **b,d,f**, MOG_{1-117} protein. Percentages of **a**,**b**, CD20$^+$ of CD4$^+$ cells, **c**,**d**, CD25$^+$, and **e,f**, CD69$^+$ cells of CD4$^+$ T cells. **g-i**, Purified B cell/T cell cocultures using wild type or MHC IIKO B cells and MOG_{35-55}-specific T cells stimulated with MOG_{35-55} peptide. Percentages of **g**, CD20$^+$ of CD4$^+$ cells, **h**, CD25$^+$, and **i**, CD69$^+$ cells of CD4$^+$ T cells. **j**, Transwell-coculture and non-separated coculture of wild type B cells and MOG_{35-55}-specific T cells stimulated with MOG_{35-55} peptide analysed for the percentage of CD20$^+$ of CD4$^+$ T cells. All figures are representative of at least two independent experiments.

3.2.7. T cells obtain CD20 via trogocytotic transfer in direct interaction with CD20$^+$ B cells

As we now know, to expand the CD20$^+$ T cell population, the interaction of T cells with CD20-expressing B cells seems to be required. Trogocytosis was suggested as the process in which T cells receive CD20 from B cells. In trogocytosis, pieces of membrane and membrane proteins can be transferred from one cell to another cell during cell-cell interaction. Therefore, cocultures of CD20$^+$ B cells, stained with MemBrite™ Fix membrane stain, a dye that stains membrane lipids and proteins, together with unstained T cells were performed to confirm that CD20 on CD20$^+$ T cells actually originates from CD20$^+$ B cells and is trogocytotically transferred during direct B cell-T cell interaction. If trogocytotic transfer from B cell to T cell takes place, T cells should develop a slight, positive staining for the B cell membrane stain. In cocultures containing membrane-stained B cells, T cells with a high membrane stain signal were excluded, since those approximately 3 % of the CD4$^+$ T cells can be assumed to be a result from the <1 % contamination of T cells in the MACS-sorted, membrane-stained B cells used for the cocultures **(Fig.15).** Therefore, only membrane stain^{low} CD4$^+$ T cells were measured as membrane stain-transferred T cells to analyze the trogocytotic membrane transfer form B cells to T cells.

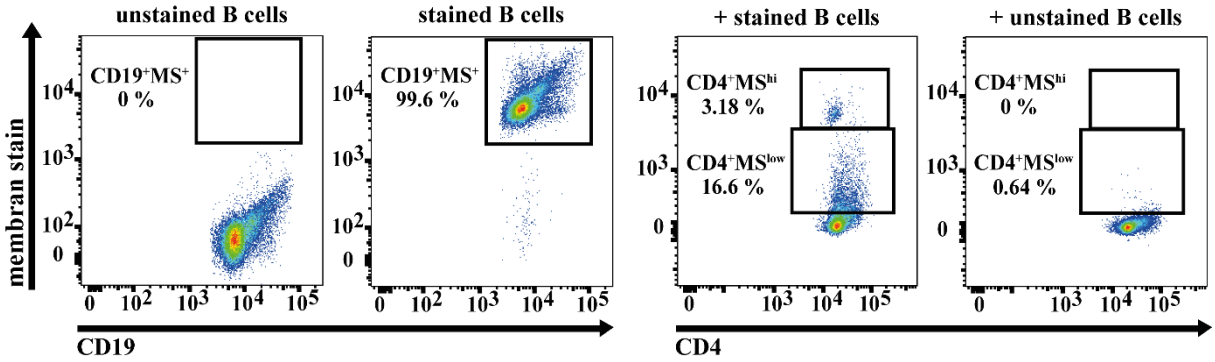

Fig.15: Gating for membrane stain-transferred T cells.
Representative flow cytometry blots for membrane-stained or unstained B cells, membrane stain-transferred MOG_{35-55}-specific T cells and membrane-stained wild type T cells from cocultures stimulated for 24 h with MOG_{35-55} peptide.

Membrane stain was transferred to T cells in an antigen concentration-dependent manner **(Fig.16a)**. This effect could be shown for cocultures with wild type $CD20^+$, as well as CD20KO B cells. To prove, that the membrane stain transfer takes place during B cell-T cell interaction and that the membrane stain did not simply "leak" from stained B cells to stain T cells, MHC IIKO B cell cocultures and transwell cocultures were performed **(Fig.16b,c)**. In cocultures containing membrane-stained MHC IIKO B cells no membrane stain-positive T cells developed. In transwell cocultures, where membrane-stained B cells were separated from T cells by a semipermeable membrane, no membrane stain-positive T cells could be detected either. These results indicate that a direct, antigen-dependent B cell-T cell interaction is required for trogocytosis symbolized by membrane stain-transfer. Interestingly, $CD20^+$ T cells also showed a higher membrane stain signal compared to $CD20^-$ T cells **(Fig.16d).** To visualize trogocytotic CD20-transfer to T cells, fluorescence microscopic analysis of membrane-stained B and T cells, which were also stained with fluorescence-labeled antibodies, revealed a "patchy" B cell-membrane stain and CD20 signal in the same spot on the surface of a $CD3^+$, membrane-stained T cell **(Fig.16e)**. Coculture experiments also revealed a significant positive correlation between the amounts of transferred membrane stain and CD20 on T cells **(Fig.16f)**. Cocultures containing membrane-stained CD20KO B cells served as negative control and showed no CD20-membran stain correlation on T cells **(Fig.16g)**. These results strongly indicate that *in vitro*, CD20 is transferred from B cells to T cells via trogocytosis.

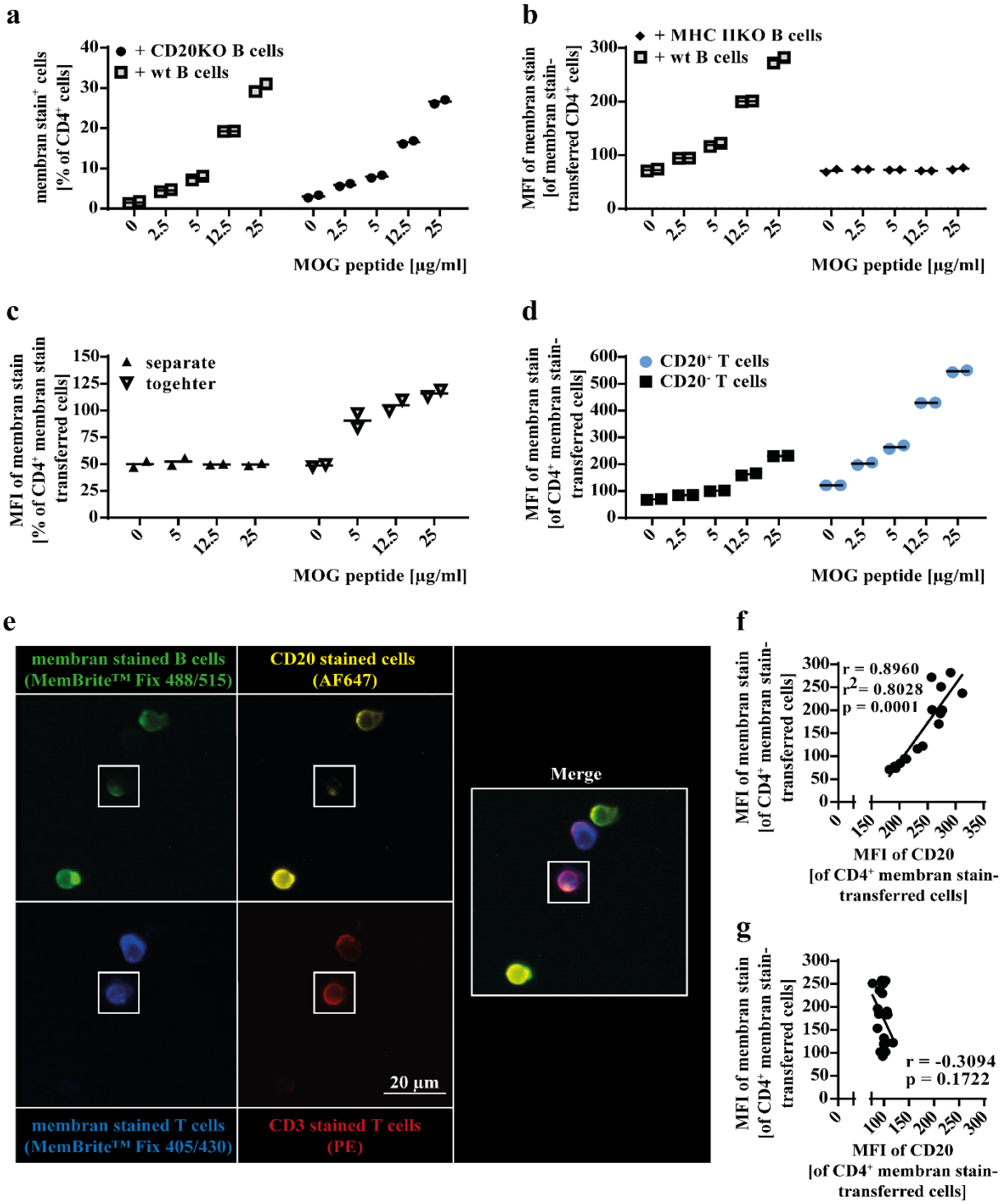

Fig.16: CD20$^+$ T cells develop via trogocytotic transfer in direct interaction with CD20$^+$ B cells.
Cocultures with membrane-stained **a**, wild type or **b**, MHC IIKO B cells and unstained MOG_{35-55}-specific T cells stimulated for 24 h with MOG_{35-55} peptide. **a**, Percentage and **b**, MFI of membrane stain-positive CD4$^+$ T cells. **c**, Transwell-coculture and non-separated coculture of membrane-stained wild type B cells and unstained MOG_{35-55}-specific T cells stimulated with MOG_{35-55} peptide. **d**, MFI for membrane stain of CD20$^+$- and CD20$^-$ CD4$^+$ T cells. **e,** Fluorescence microscopic examination of cocultures using membrane-stained B cells (MemBrite™ Fix 488/515, green) and membrane-stained T cells (MemBrite™ Fix 405/430, blue) stained for CD3 (PE, red) and CD20 (AF647, yellow). **f,g**, Correlation of the MFI for CD20 with the MFI of the membrane stain on CD4$^+$ T cells for **f**, wild type and **g**, CD20KO B cells cultures; calculated via Pearson's correlation. All figures representative of at least two independent experiments.

3.2.8. Adoptive CD20$^+$ B cell transfer generates CD20$^+$ T cells *in vivo*

To confirm our *in vitro* results regarding the trogocytotic transfer of CD20 in an *in vivo* model, B cell-deficient mice lacking both CD20$^+$ B and T cells were used as model organism. Here, it was concluded that B cell-deficient mice lack CD20$^+$ T cells because there are no CD20$^+$ B cells to obtain CD20 from. Therefore, CD20$^+$ B cells were adoptively transferred into B cell-deficient mice to potentially generate CD20$^+$ T cells. After B cells were able to accumulate in B cell-deficient mice **(Fig.17a,b)**, their spleens and inguinal lymph nodes were analyzed for the potential development of CD20$^+$ T cells. Here, CD20KO B cells were transferred into B cell-deficient mice and then used as negative control. Remarkably, only the transfer of CD20-expressing B cells showed a highly significant generation of CD20$^+$ T cells in their spleens **(Fig.17c)**. In inguinal lymph nodes of recipient mice, where none of the transferred CD20$^+$ B cells accumulated, no CD20$^+$ T cells could be detected. Additionally, the frequency of the developed CD20$^+$ T cells in the spleen positively correlates with the frequency of transferred CD20$^+$ B cells, highlighting their connection **(Fig.17d)**. To further increase B cell-T cell interactions in our model, B cell-transferred mice were MOG_{1-117} protein immunized, after B cell accumulation. In immunized mice, CD20$^+$ B cells could be detected in the spleens and in immunization draining lymph nodes, where they were recruited to **(Fig.17e)**. Following the hypothesis, that CD20$^+$ T cells are generated during B cell-T cell interaction, CD20$^+$ T cells developed at a similar frequency in immunized and naïve mice. However, in immunized mice, CD20$^+$ T cells also developed in the immunization draining lymph nodes **(Fig.17f)**. Additionally, the transfer of CD20KO B cells, while showing a similar B cell accumulation, did not lead to the development of CD20$^+$ T cells. Furthermore, fluorescence immunohistochemistry analysis of B cell-transferred mice shows that B cells are organized into follicular structures and are in close proximity to T cells in the spleen, enabling B cell-T cell interactions in this compartment **(Fig.17g)**. In conclusion, we could demonstrate the trogocytotic transfer of CD20 from B cells to T cells *in vitro* as well as *in vivo*.

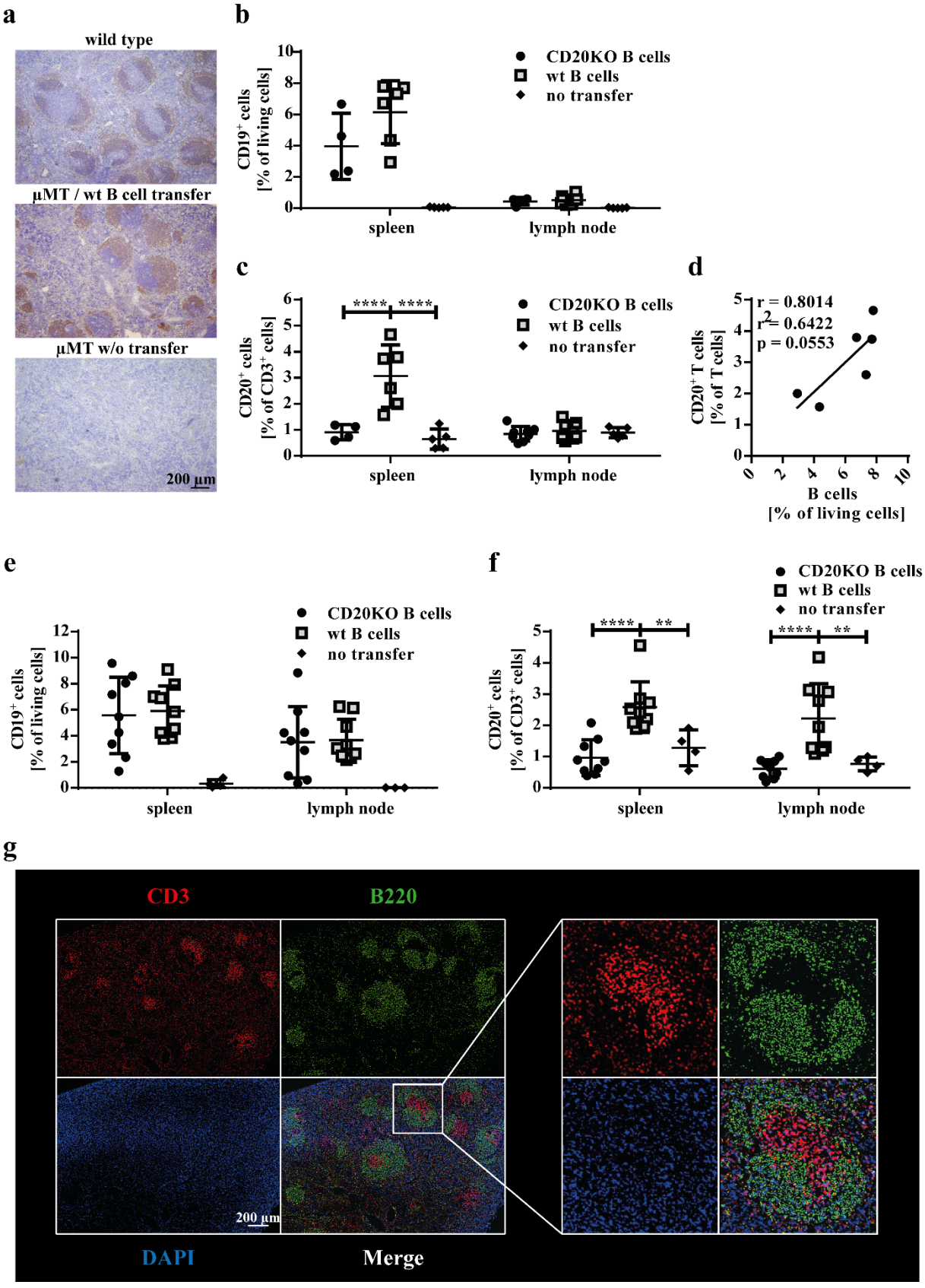

Fig.17: Adoptive B cell-transfer restores the ability of B cell-deficient mice to generate CD20⁺ T cells.
a, Representative histological staining of B220 of wild type, control µMT and B cell-transferred µMT mouse spleens. **b-d**, Flow cytometric analysis of **b,** $CD19^+$ B cells and **c,** $CD20^+$ T cells from spleen and lymph nodes of B cell-deficient µMT mice adoptively transferred with CD20KO B cells or wild type B cells and non-transferred

B cell-deficient µMT mice (n=4-6 mice per group from 2 independent experiments). **d**, Pearson's correlation analysis of the percentage of transferred B cells and generated $CD20^+$ T cells in the spleen. **e,f,** Flow cytometric analysis of **e,** $CD19^+$ B cells and **f,** $CD20^+$ T cells from spleen and lymph nodes of MOG_{1-117} protein immunized B cell-deficient µMT mice adoptively transferred with CD20KO B cells or wild type B cells and non-transferred B cell-deficient µMT mice (n=4-10 mice per group, pooled from 2 independent experiments). **g**, Representative fluorescence histological staining of B220-FITC, CD3-PE and DAPI of wild type B cell-transferred µMT mouse spleens. P values were calculated using two-way ANOVA with Holm-Sidak's post hoc analysis. **=p≤0.01, ***=$p \leq 0.001$, ****=$p \leq 0.0001$.

3.3. $CD20^+$ T cells display pathogenic properties

In 3.2. we examined the origin of $CD20^+$ T cells, subsequently we were then interested in their potential pathogenicity in EAE, and respectively MS.

3.3.1. CD20 positivity is associated with earlier and stronger activation

Research of human $CD20^+$ T cells revealed, that they exhibit a more proinflammatory phenotype compared to $CD20^-$ T cells, due to the higher expression of proinflammatory cytokines such as IFNγ, IL-17 and TNFα[114]. Therefore, $CD20^+$ T cells generated in antigen-stimulated splenocyte cultures were compared to $CD20^-$ T cells for their activation state and cytokine expression. The data were normalized to be able to compare the relatively small $CD20^+$ T cell population with the remaining $CD20^-$ T cells. Here, $CD20^+$ T cells were more sensitive to stimulation and exhibited an earlier and stronger activation compared to $CD20^-$ T cells measured via the T cell activation markers CD25 and CD69 **(Fig.18a,b)**. Additionally, a higher frequency of proinflammatory cytokine IFNγ- and GM-CSF-producing cells could be found in the $CD20^+$ T cells population **(Fig.18c,d)**. Interestingly, $CD20^+$ T cells also contained a slightly higher frequency of Foxp3-expressing regulatory T cells **(Fig.18e)**. However, these experiments could only show the higher frequency of activated, proinflammatory-producing cells in the $CD20^+$ T cell population, but not state the amount of cytokines produced by each cell.

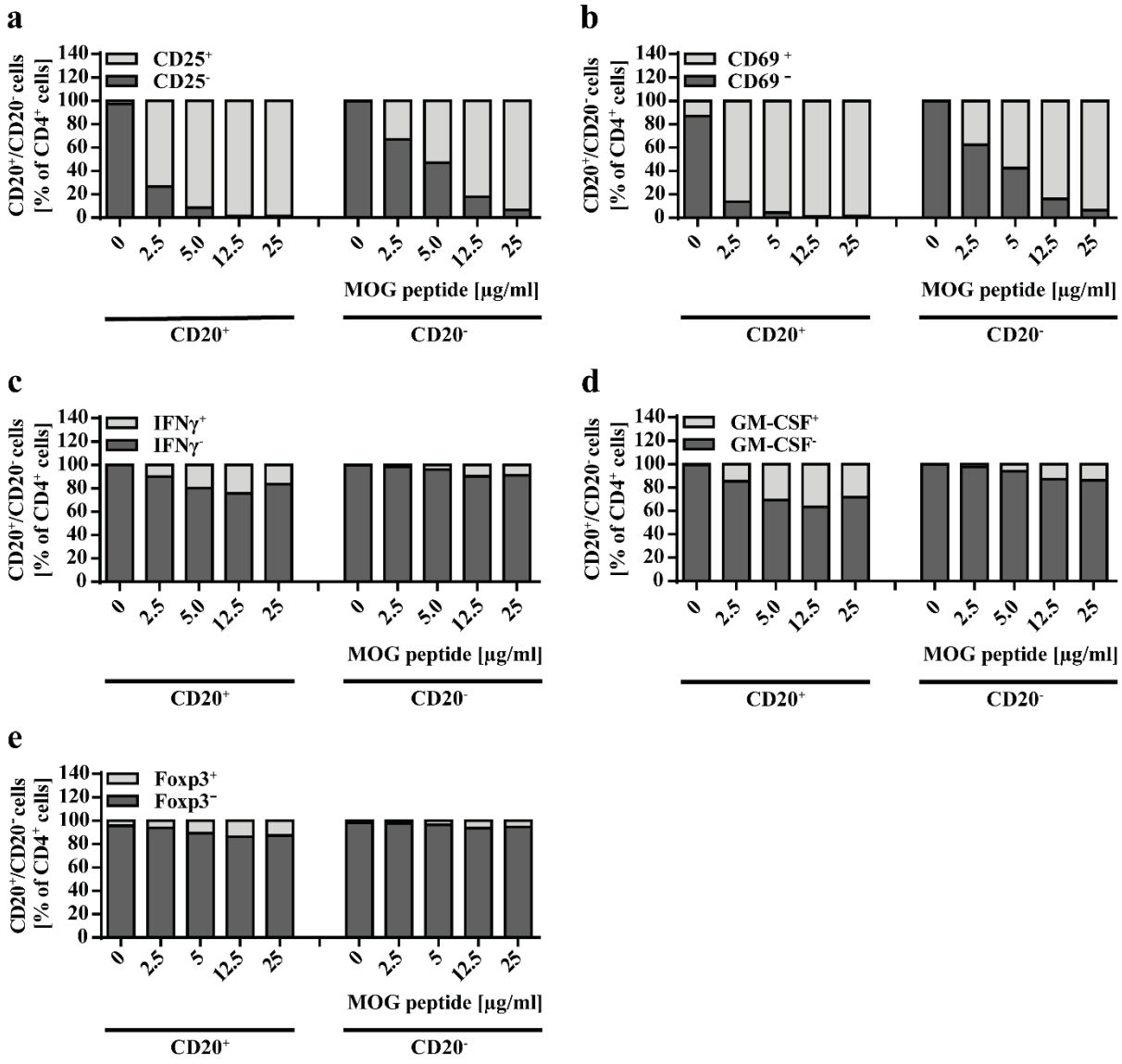

Fig.18: CD20 positivity is associated with stronger activation and enhanced cytokine production
a-e, Normalization of flow cytometric data of $CD4^+CD20^+$ and $CD4^+CD20^-$ T cells form splenocyte cultures from MOG_{35-55} TCR transgenic mice stimulated with MOG_{35-55} peptide for 48 h examined for **a**, CD25, **b**, CD69, **c**, IFNγ, **d**, GM-CSF and **e**, Foxp3. All figures are representative of at least two independent experiments.

3.3.2. CD20$^+$ T cells express high levels of proinflammatory cytokines

To more directly assess the cytokine production of CD20$^+$ T cells, CD20$^+$ T cells were FACS-sorted, directly stimulated with α-CD3/α-CD28 and the supernatants analyzed for cytokine production via ELISA. Here, CD20$^-$ T cells were used as comparison. Interestingly, the production of IL-2, also known as T cell growth factor, was significantly reduced in CD20$^+$ T cells from naïve mice and unchanged in CD20$^+$ T cells from MOG_{35-55} peptide immunized mice, compared to their respective CD20$^-$ T cell controls **(Fig.19a,f)**. IL-2 was measured to control for proliferation differences between the T cell groups and consequential differences in the cytokine expression. CD20$^+$ T cells from naïve mice expressed significantly higher levels of the proinflammatory cytokines IFNγ, GM-CSF, IL-17 and TNFα **(Fig.19b-e)** compared to CD20$^-$ T cells. This difference was further increased when the T cells originated from MOG_{35-55} peptide immunized mice **(Fig.19g-j)**. These results demonstrate the increased production of inflammatory cytokines in CD20$^+$ T cells.

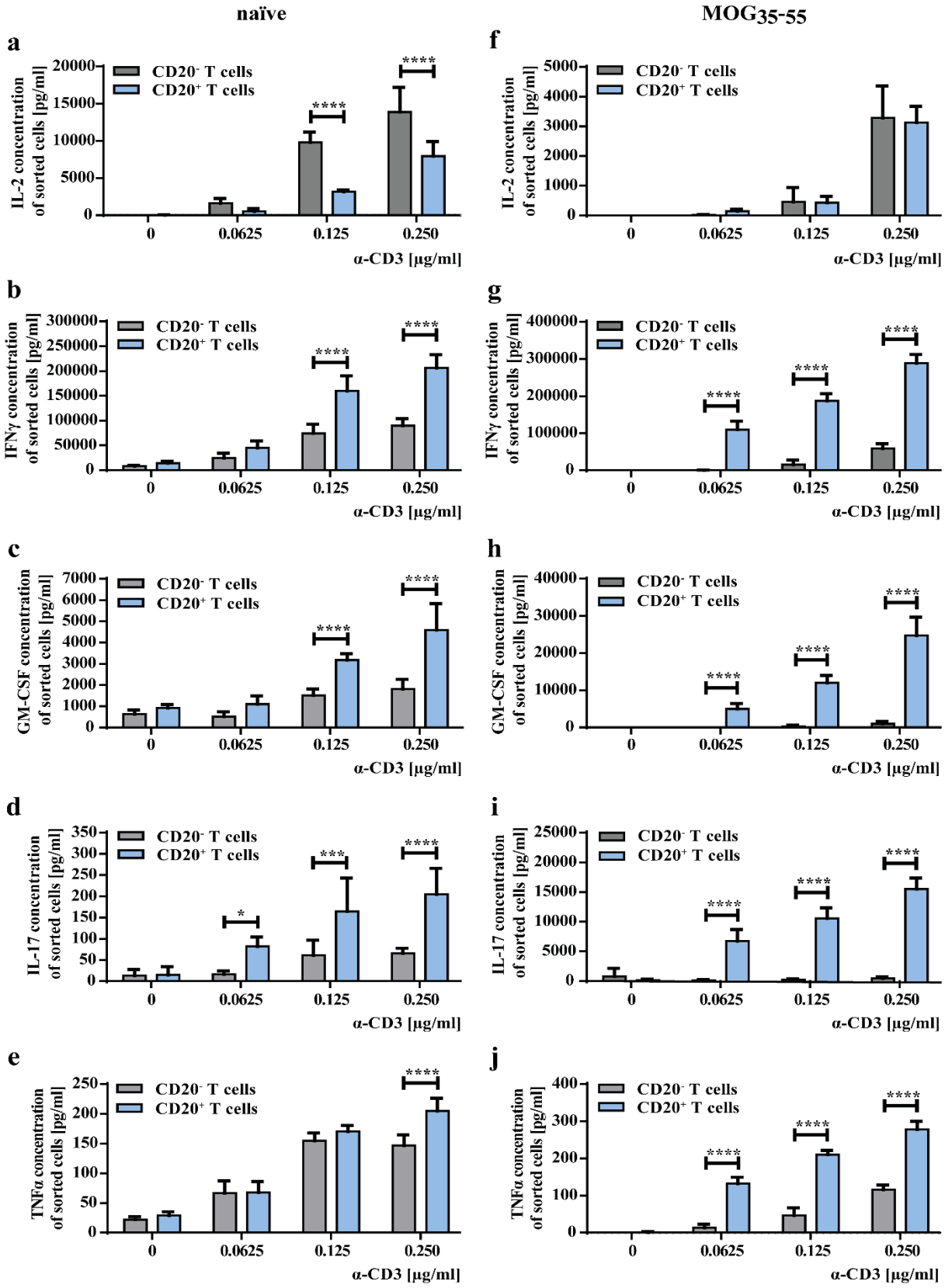

Fig.19: CD20 positivity of T cells is tightly associated with increased production of pro-inflammatory cytokines. a-j, ELISA-based cytokine analysis of the supernatant of FACS-sorted CD20$^+$ and CD20$^-$ T cells from spleens of **a-e** naïve or **f-j** MOG_{35-55} peptide immunized mice stimulated with α-CD3/α-CD28; (n=3-7 wells, representative of at least two independent experiments). P values were calculated using two-way ANOVA with Holm-Sidak's post hoc analysis. All figures representative of at least two independent experiments. *=p≤0.05, ***=p ≤ 0.001, ****=p ≤ 0.0001.

3.3.3. Anti-inflammatory cytokines are also produced by CD20$^+$ T cells

However, since CD20$^+$ T cells were also shown to be a part of the Foxp3$^+$ Treg cell population **(Fig.18e)**, anti-inflammatory cytokine production was also analyzed. Compared to CD20$^-$ T cells, CD20$^+$ T cells from naïve mice expressed significantly higher levels of the anti-inflammatory cytokines IL-10 **(Fig.20a,b)** and IL-4 **(Fig.20c)**. This effect could again be increased when the stimulated T cells originated from MOG_{35-55} peptide immunized mice. However, the overall amounts of anti-inflammatory cytokines were considerably lower compared to the expression of proinflammatory cytokines **(Fig.19)**.

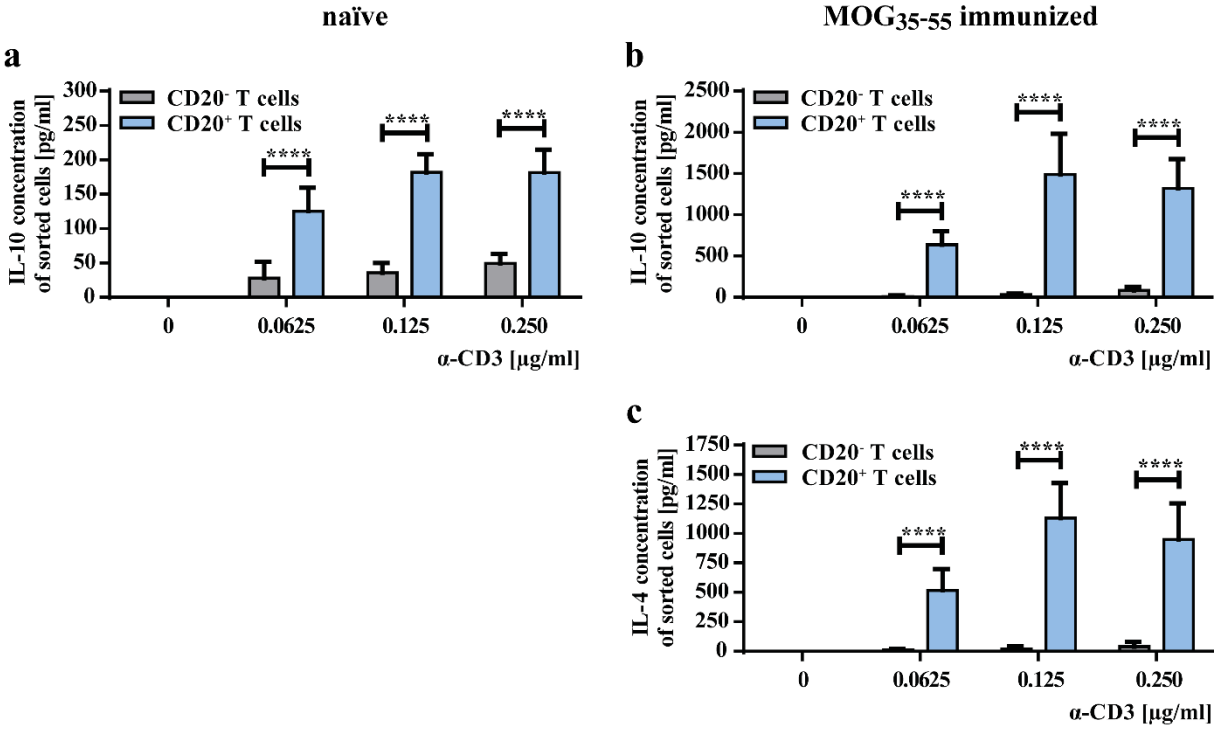

Fig.20: CD20 positivity of T cells is associated with production of anti-inflammatory cytokines.
a-c, ELISA-based cytokine analysis of the supernatant of FACS-sorted CD20$^+$ and CD20$^-$ T cells from spleens of **a** naïve or **b,c,** MOG_{35-55} peptide immunized mice stimulated with α-CD3/α-CD28; (n=3-7 wells, representative of at least two independent experiments). P values were calculated using two-way ANOVA with Holm-Sidak's post hoc analysis. All figures representative of at least two independent experiments. ****=$p \leq 0.0001$.

3.3.4. CD20$^+$ T cells are no NKT cells

We were also interested, if CD20$^+$ T cells belong to or are a part of the natural killer T (NKT) cell population. Flow cytometric analysis showed that CD20$^+$ T cells do not belong to the CD3$^+$NK1.1$^+$ NKT cell population **(Fig.21)**.

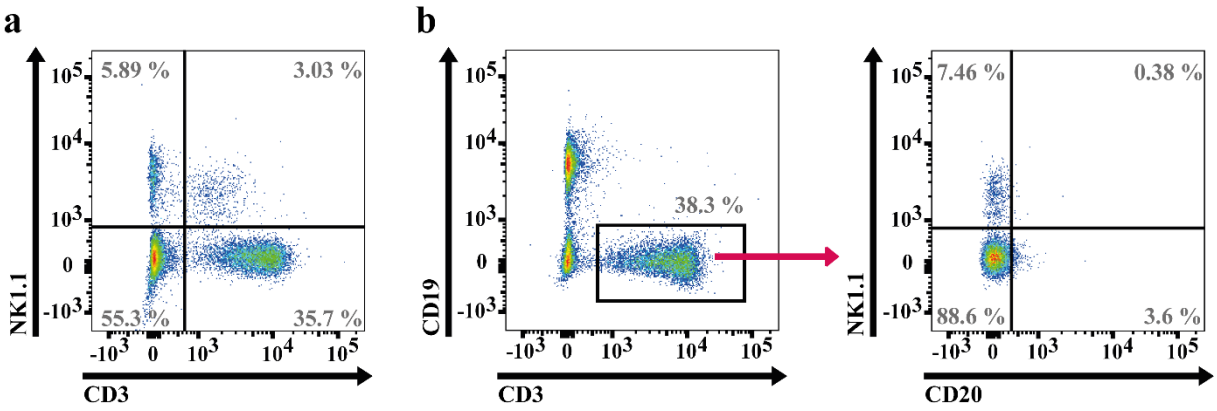

Fig.21: CD20$^+$ T cells are no NKT cells.
Representative staining of **a,** NK1.1 and CD3 on living splenocytes and **b**, CD20 and NK1.1 on CD3$^+$ T cells from wild type mice.

3.4. CD20$^+$ T cells are pathogenic *in vivo*

CD20$^+$ T cells could be determined to be a predominantly activated population of T cells that express proinflammatory cytokines at a high level in *in vitro* stimulation. Now, we were interested in the potential effects of CD20$^+$ T cells *in vivo* in the murine MS model EAE.

3.4.1. CD20$^+$ T cells expand upon MOG immunization

Previous studies reported that untreated MS patients contain CD20$^+$ T cells at a higher frequency in the blood compared to healthy controls[115, 117]. Additionally, it was discovered that CD20$^+$ T cells occur at a high frequency in the cerebrospinal fluid of MS patients[115]. These results indicate a potential role of CD20$^+$ T cells in MS pathogenicity. To dissect this notion, wild type mice were immunized with MOG_{35-55} peptide or MOG_{1-117} protein to analyze if the increase of CD20$^+$ T cells also occurs in the inflammatory context of the MS mouse model EAE. A significant increase in the percentage of CD4$^+$CD20$^+$ T cells could be detected in the immunization draining lymph nodes **(Fig.22a,c)**. CD8$^+$CD20$^+$ T cells were also increased in their frequency due to immunization, but their expansion was not significant **(Fig.22b,d)**. No

effect could be detected in the spleen. It was also observed, that $CD19^+$ B cells significantly decreased in the spleen and increased in the draining lymph nodes **(Fig.22e)**. This might hint towards their recruitment from the spleen to the side of inflammation. When comparing $CD4^+CD20^+$ to $CD4^+CD20^-$ T cells *ex vivo*, $CD20^+$ T cells showed a significantly higher frequency of the activation marker CD69 and a slight increase in the frequency of the activation marker CD25 **(Fig.22f,g)**. These results are in line with the findings of the *in vitro* cultures in **3.3.1 (Fig.18a,b).**

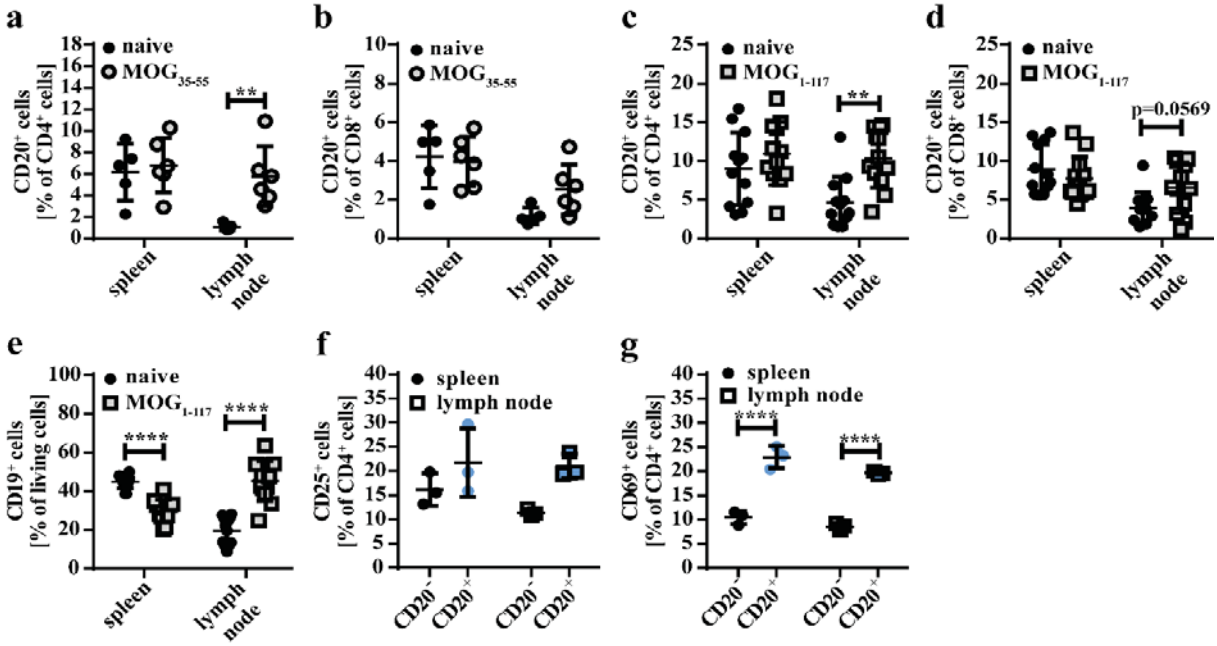

Fig.22: $CD20^+$ T cells expand and are increasingly activated during EAE induction in secondary lymphoid organs. Spleen and lymph nodes from naïve mice and mice immunized with **a,b**, MOG_{35-55} peptide or **c-e,** conformational MOG_{1-117} protein were analysed for the frequency of CD20 **a,c**, on $CD4^+$ or **b,d**, $CD8^+$ T cells and **e**, frequency of $CD19^+$ B cells (n=5-12 mice per group from 3 independent experiments). **f-g**, Flow cytometric analysis of spleen and lymph nodes from MOG_{35-55} peptide immunized mice. $CD4^+CD20^+$ and $CD4^+CD20^-$ T cells analysed for activation (**f**, CD25, **g**, CD69) (n=3 mice per group, representative of 3 independent experiments). P values were calculated using two-way ANOVA with Holm-Sidak's post hoc analysis. **=p≤0.01, ****=p ≤ 0.0001

3.4.2. $CD20^+$ T cells exhibit an enhanced pathogenic phenotype upon MOG immunization

To further examine the effect of MOG immunization on $CD20^+$ T cell activation and expression of adhesion molecules, necessary to cross the blood-brain barrier, naïve and MOG_{1-117} protein immunized $CD20^+$ T cells were compared with each other and with naïve and MOG_{1-117} protein immunized $CD20^-$ T cells **(Fig.23)**. Cell activation **(Fig.23a-d)** and expression of adhesion molecules **(Fig.23e-h)** were measured to gauge the EAE-specific pathogenic potential of the T cell subsets. Therefore, MOG_{1-117} protein immunization was utilized, as it is an EAE model that more prominently engages B cells, while MOG_{35-55} peptide can also be presented by various antigen presenting cells and pathogenic B cell involvement is limited[29]. In general, MOG_{1-117} protein immunization led to an increased activation (measured by CD25 and CD69) and expression of adhesion molecules (CD11a = LFA-1 and CD49d = integrin α4) in both immunized T cell groups compared to their respective naïve counterparts. In addition, $CD20^+$ T cells showed a higher activation and expression of adhesion molecules in the naïve as well as the immunized group compared to the respective $CD20^-$ T cell group.

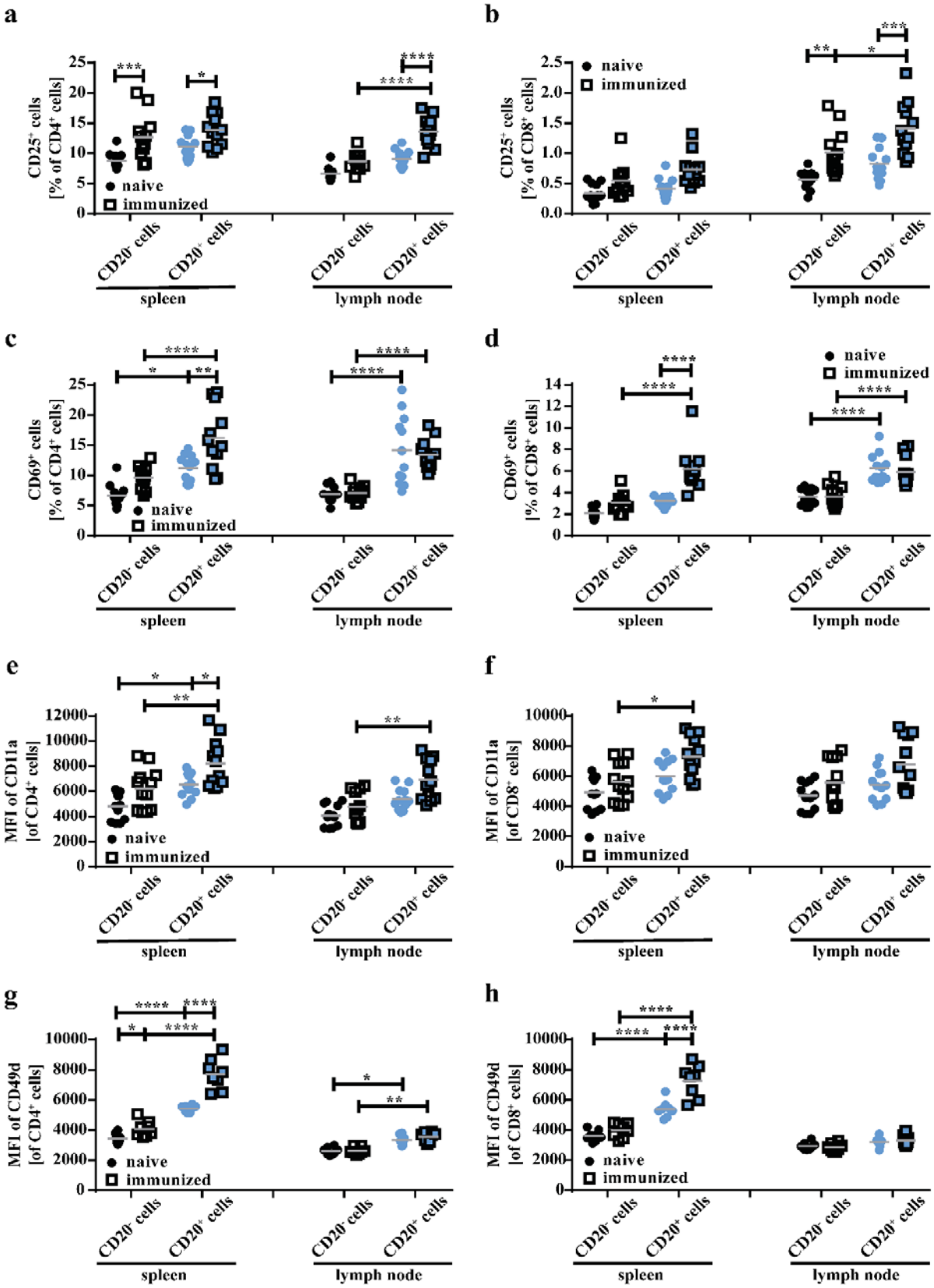

Fig.23: In EAE development, CD20$^+$ T cells express enhanced levels of activation markers and adhesion molecules. a-h, Flow cytometric analysis of spleen and lymph nodes of naïve or MOG_{1-117} protein-immunized mice (n=12 mice per group, combined from 3 independent experiments). Analysis of **a,c,e,g,** CD4$^+$ and **b,d,f,h,** CD8$^+$ T cells. Expression of activation markers (**a,b**, CD25, **c,d,** CD69) and adhesion molecules (**e,f,** CD11a and **g,h,** of CD49d) was evaluated on CD20$^-$ and CD20$^+$ T cells. P values were calculated using two-way ANOVA with Holm-Sidak's post hoc analysis. *=p≤0.05, **=p≤0.01, ***=p ≤ 0.001, ****=p ≤ 0.0001.

To further investigate the pathogenic potential of $CD20^+$ T cells, the expression of proinflammatory cytokines (IFNγ, GM-CSF and IL-17), which are known to be relevant in EAE development and progression[48, 49, 55, 120, 131], were measured in MOG immunized mice **(Fig.24a-c)**. When compared to $CD20^-$ T cells, the frequency of proinflammatory cytokine-producing cells was increased in the $CD20^+$ T cell population for all investigated cytokines in the spleen and lymph nodes. However, this increase only reached statistical significance for IFNγ- and GM-CSF-producing T cells in the spleen. Interestingly, there was also a slight increase in the frequency of $Foxp3^+$ regulatory T cells in the $CD20^+$ T cell population **(Fig.24d)**. Overall, these results are in line with the *in vitro* results from **3.3.1 (Fig.18c-e).**

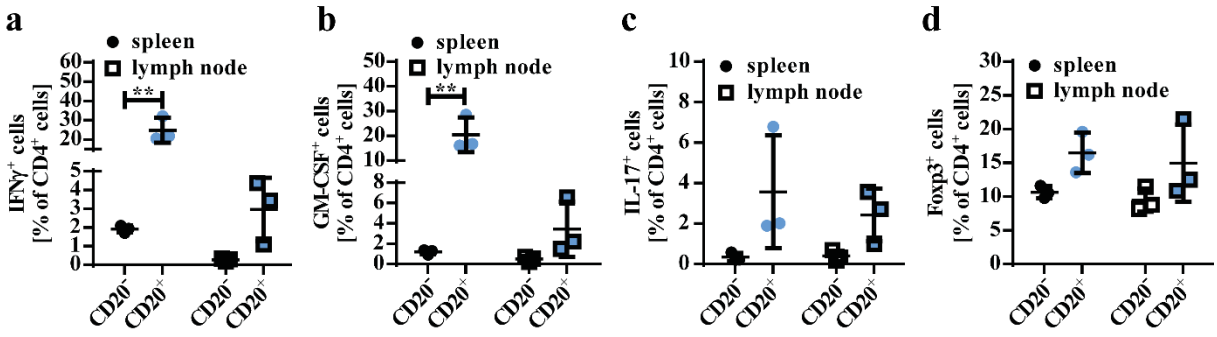

Fig.24: $CD20^+$ T cells produce enhanced amounts of cytokines in MOG immunization.
a-d, Flow cytometric analysis of spleen and lymph nodes from $MOG_{35\,55}$ peptide immunized mice. Analysis of $CD4^+CD20^+$ and $CD4^+CD20^-$ T cells for cytokine production (**a**, IFNγ, **b**, GM-CSF, **c**, IL-17 and **d**, Foxp3) (n=3 mice per group, representative of 3 independent experiments). P values were calculated using two-way ANOVA with Holm-Sidak's post hoc analysis. **=$p \leq 0.01$

3.4.3. CD20$^+$ T cells are depletable via anti-CD20 abs and play a role in EAE

In vitro and *ex vivo* mouse experiments confirmed CD20$^+$ T cells as highly activated, primarily proinflammatory T cells with a high expression of adhesion molecules **(see 3.3 and 3.5.1/2)**. However, there is nothing known about the potentially pathogenic role of CD20$^+$ T cells in MS, or EAE in that regard. Additionally, the depletion of CD20$^+$ T cells in anti-CD20 ab treatment of MS might be at least partially accountable for the positive therapeutic effect[117]. To examine if the CD20$^+$ T cells can be depleted in the murine model, wild type mice were treated with anti-CD20 abs. Depletion of CD19$^+$ B cells could be detected in the blood, spleen and inguinal lymph nodes **(Fig.25a)**. B cells were used to control for the depleting effect of the utilized anti-CD20 abs. As seen in human patients[117], and similar to B cells, CD20$^+$ T cells could be thoroughly depleted by anti-CD20 ab therapy in the blood and secondary lymphoid organs of wild type mice **(Fig.25b).**

To examine the potential pathogenic effects of CD20$^+$ T cells in EAE and the possible positive therapeutic effects of their depletion in anti-CD20 ab therapy, passive EAE was induced in CD20KO mice, where the CD20$^+$ T cell portion of transferred EAE-inducing T cells could be selectively depleted with anti-CD20 abs. Additional experiments are ongoing and are performed in collaboration with colleagues of the AG Weber **(Fig.25c)**. The mice receiving activated, EAE-inducing T cells were CD20KO to guarantee that solely transferred CD20$^+$ T cells were depleted, but no host B or T cells. Isotype control abs were used for the control group. The so far generated mean clinical scores corrected for a simultaneous onset show a clinical benefit for the selective depletion of CD20$^+$ T cells.

Before that, an on top experiment with CD20$^+$ T cells was performed to show a potential worsening of the EAE course via additional CD20$^+$ T cells. Therefore, FACS-sorted CD20$^+$ T cells were adoptively transferred to wild type mice after EAE induction. This occurred at day 5 and 8, during the stage of peripheral inflammation, before the development of the first EAE symptoms **(Fig.25d,e)**. The transfer of CD20$^-$ T cells was used as a control. Mice transferred with CD20$^+$ T cells showed a slightly higher mean clinical EAE score than CD20$^-$ T cell-transferred animals **(Fig.25d)**. In addition, CD20$^+$ T cell-transferred mice exhibited significantly more T cell infiltration into the spinal cord **(Fig.25e)**. The increased T cell infiltration in CD20$^+$ T cell-transferred mice combined with the heightened expression of adhesion molecules **(Fig.23)** indicates that CD20$^+$ T cells are exceedingly able to migrate into the CNS, where they potentially increase inflammation and CNS demyelination.

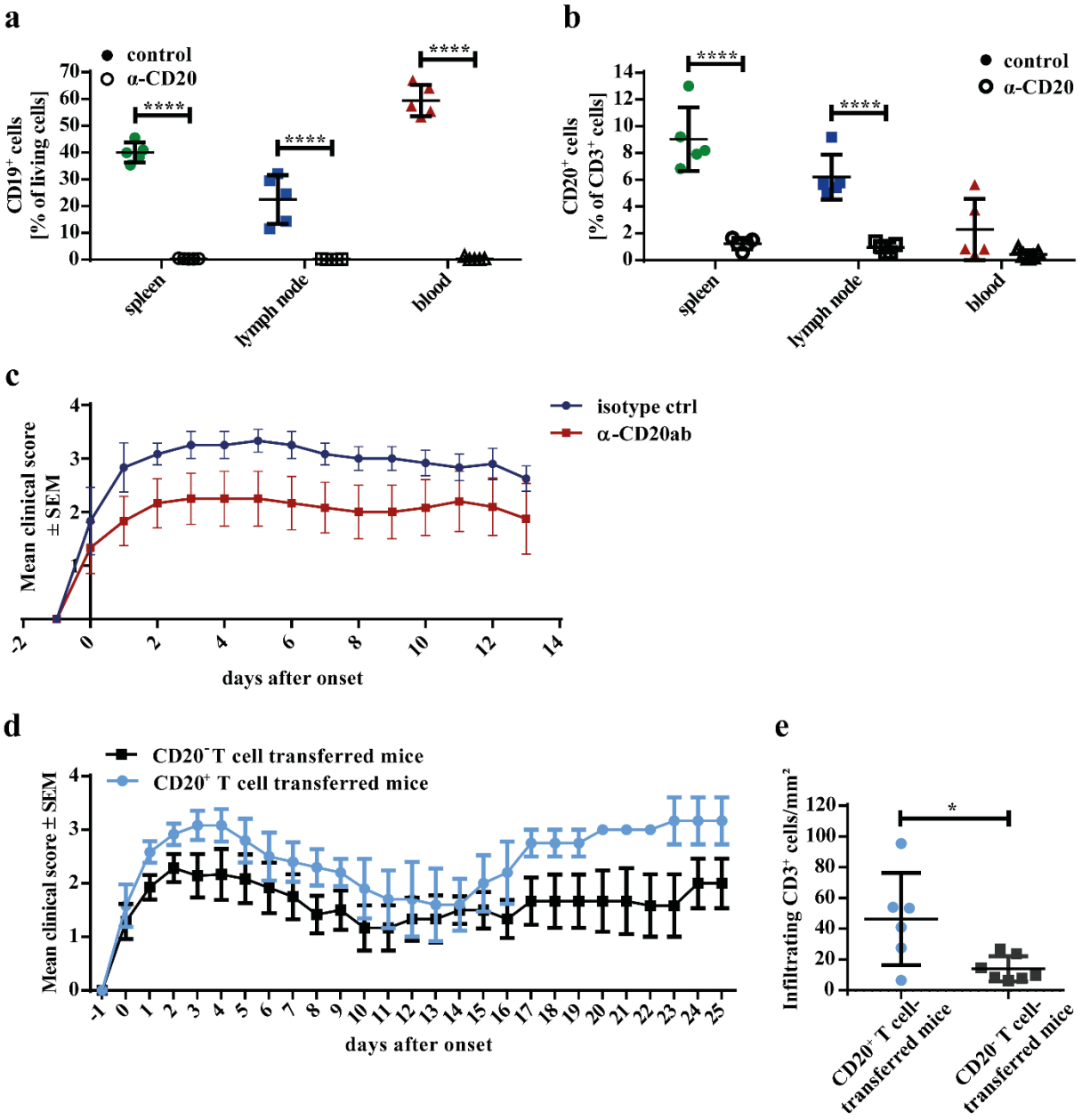

Fig.25: Anti-CD20 ab mediated depletion of CD20$^+$ T cells is therapeutically beneficial independent of B cells and adoptive transfer of CD20$^+$ T cells exacerbates clinical and histological EAE. a, b, Flow cytometric analysis of **a**, CD19$^+$ B cells and **b**, CD20$^+$ T cells of spleen, lymph nodes and blood of wild type mice treated with either anti-CD20 antibody or isotype control antibody. **c,** Passive EAE induction in CD20KO mice. EAE was induced by adoptive transfer of lymph node cells or splenocytes without B cells from MOG_{35-55} peptide immunized wt mice cultured for 3 days in the presence of MOG_{35-55} peptide, recombinant IL-12 and anti-IFNγ antibodies (n=6 mice per group). Recipient CD20KO mice were injected with 0.2 mg of anti-CD20 or isotype control antibody at d-1 and d1 of transfer. Mean EAE clinical score ± SEM, corrected for a simultaneous onset. **d,e,** Adoptive transfer of FACS-sorted CD20$^+$ or CD20$^-$ T cells into wild type mice at d5 and d8 after MOG_{35-55} peptide EAE induction (n=6/7). **c**, Mean EAE score ± SEM corrected for a simultaneous onset. **d**, Spinal cord infiltration of CD3$^+$ T cells displayed as CD3$^+$ T cells per mm^2; p value was calculated using unpaired t test with Welch's correction. p values were calculated using two-way ANOVA with Holm-Sidak's post hoc analysis. *=p≤0.05, ****=p ≤ 0.0001.

3.5. CD20$^+$ T cells could not be detected in relevant frequencies in the murine CNS

In **3.5.3.**, increased T cell infiltration into the CNS could be detected in CD20$^+$ T cell-transferred EAE mice. Since it could also be shown in MS patients that CD20$^+$ T cells accumulate in the CSF[115], the CNS of EAE mice was analyzed for infiltrated CD20$^+$ T cells **(Fig.26)**. Here, CD20KO EAE mice served as a negative control. The spleen and immunization draining lymph nodes served as a basis for CD20$^+$ T cells to determine a potential accumulation of CD20$^+$ T cells in the CNS. Interestingly, almost no CD20$^+$ T cells could be detected in the CNS when DNase I and Collagenase D followed by a percoll gradient were used to isolate lymphocytes from the CNS **(Fig.26a,b)**. Since it is known, that some surface markers can be affected by enzymatic tissue digestion, the multi tissue dissociation kit 1 and a gentleMACS™ Octo Dissociator were used as a different strategy for lymphocyte isolation from the CNS. However, this isolation process led to an unspecific increase of the CD20 signal on T cells, which also occurred in the samples that were not stained with the CD20 antibody (fluorescence minus one (FMO) staining for CD20) **(Fig.26c)**. In addition, no CD20$^+$ T cells could be detected in the samples of such treated EAE spinal cords **(Fig.26d).** Interestingly, CD19$^+$ B cells analyzed from those CNS samples exhibited a lower expression of CD20 on their surface **(Fig.26e)**. To further exclude potential influences of enzymes or components of the various gradient and removal solutions utilized for the extraction of lymphocytes from the CNS, CNS samples were stained and analyzed without enzyme or filtration treatments or without enzyme treatment but with one form of filtration **(Fig.27)**. Relevant amounts of CD20$^+$ T cells could merely be detected in samples treated with a ficoll gradient, but no accumulation of CD20$^+$ T cells in the CNS of EAE mice could be found.

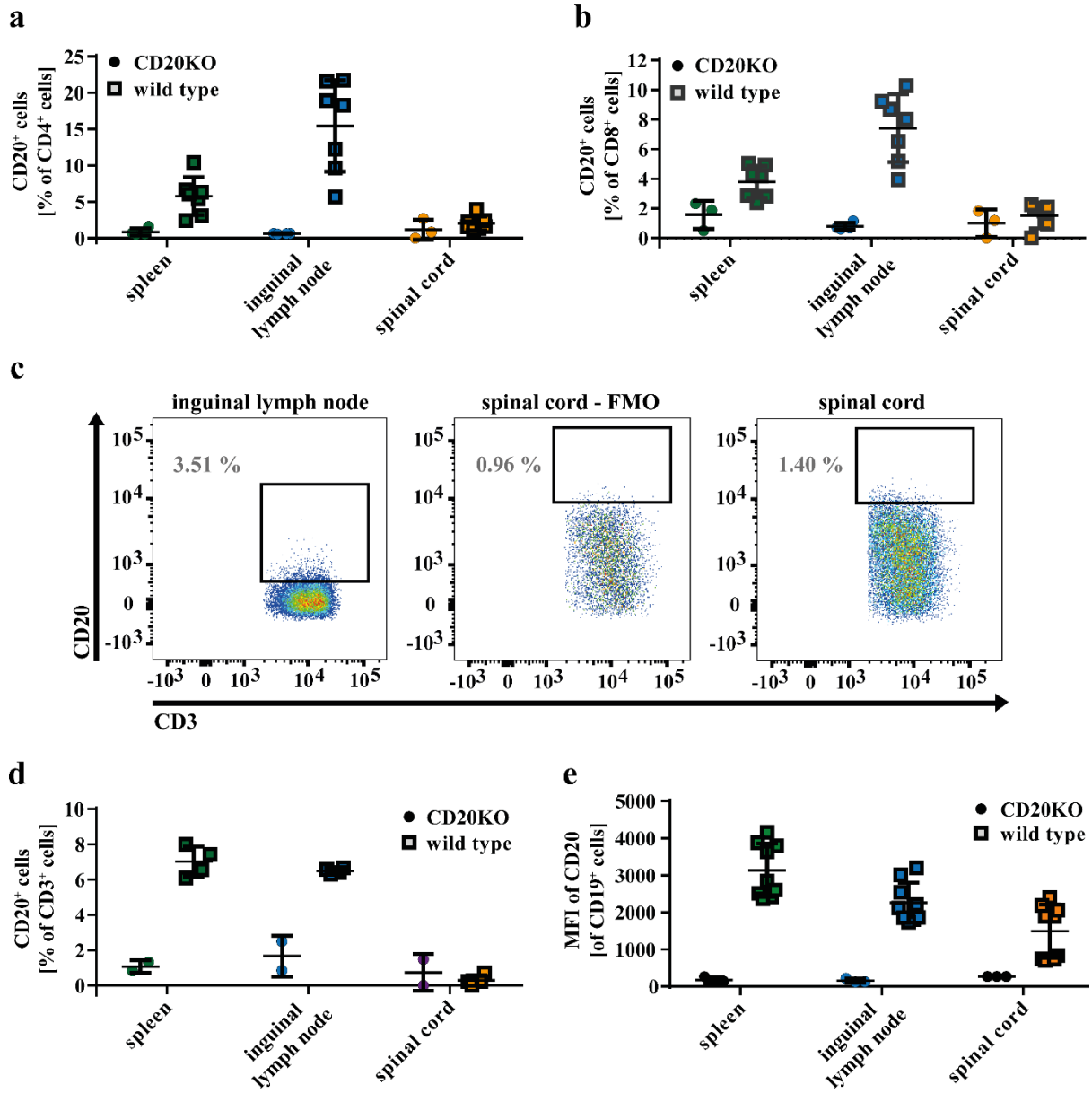

Fig.26: CD20 detection and/or expression is reduced in CNS-extracted lymphocytes.
a-e, Flow cytometric analysis of spleen, inguinal lymph nodes and spinal cord of MOG_{35-55} peptide immunized wild type or CD20KO mice (n=2-9 mice per group, combined from 2 independent experiments). Analysis of $CD20^+$ cells of **a**, $CD4^+$ and **b**, $CD8^+$ T cells from spinal cords digested with Collagenase D and DNAse I followed by a percoll gradient. **c-e**, Spinal cords lymphocytes isolated via digestion with the multi tissue dissociation kit 1 and a gentleMACS™ Octo Dissociator followed by debris and red blood cells removal. **c**, Exemplary flow cytometry blots for CD20 staining on T cells. Analysis of **d**, the percentage of CD20 on $CD3^+$ cells and **b**, MFI of CD20 on $CD19^+$ B cells.

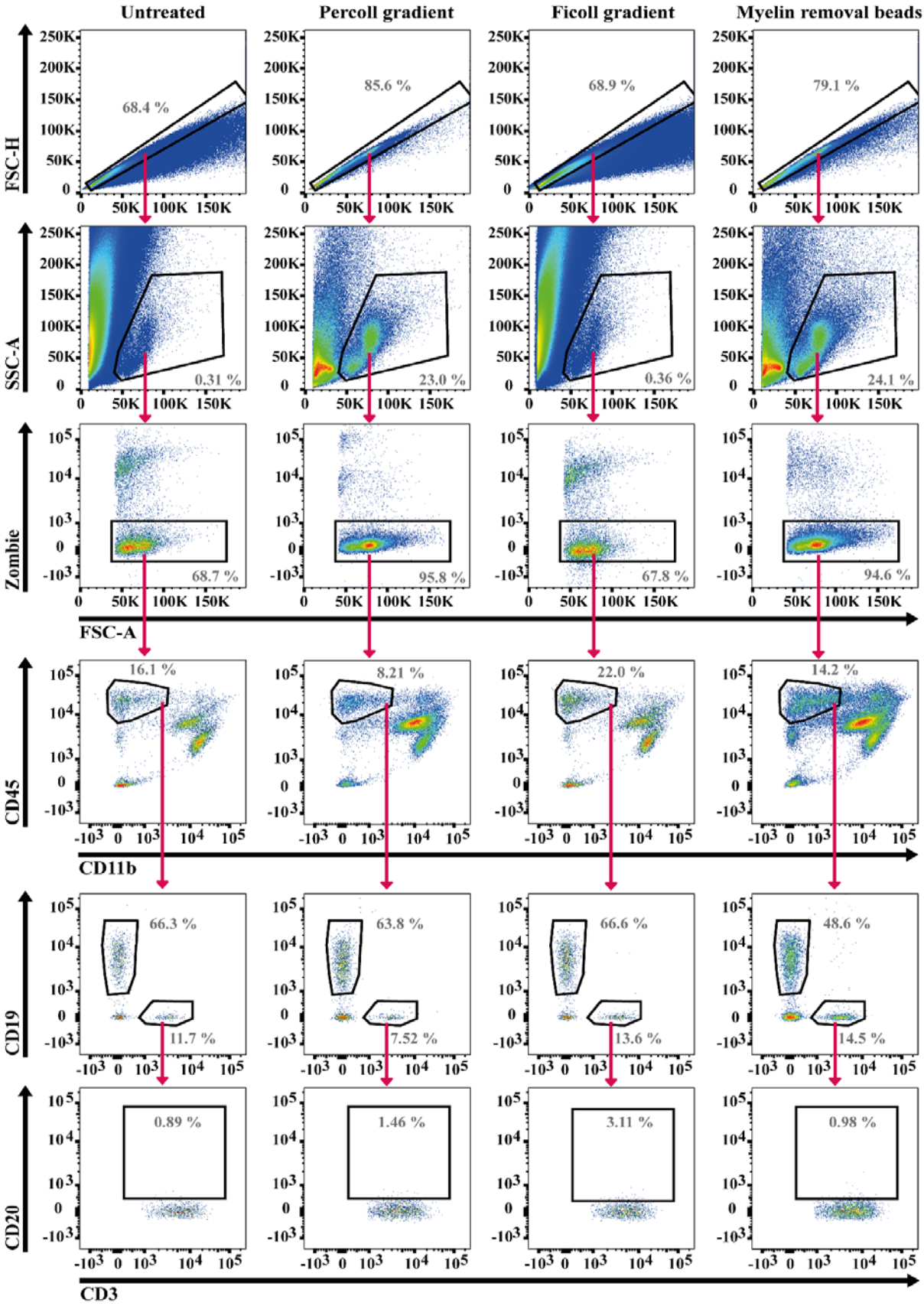

Fig.27: Comparison of different methods for CNS preparation and filtration for flow cytometry. Representative flow cytometric pregating and gating of pooled spinal cords from four mice at d20 post MOG_{35-55} peptide EAE induction. Spinal cord sample was separated equally in four groups (untreated or pre-treated with percoll gradient, ficoll gradient or myelin removal beads), stained and analysed.

3.6. CD20 on T cells is lost in T cell permeabilization

Not only enzymatic digestion in the lymphocyte isolation from the CNS can affect surface antigens, but also the necessary treatment for intracellular stainings. $CD20^+$ T cells needed to be fixated and their cell membrane permeabilized to examine them for their phenotype and cytokine expression. A loss in the percentage of $CD20^+$ T cells in fixated and permeabilized splenocytes, lymph node cells and PBMCs could be measured when compared to the frequency of their respective non-fixated, non-permeabilized counterparts **(Fig.28a-g)**.

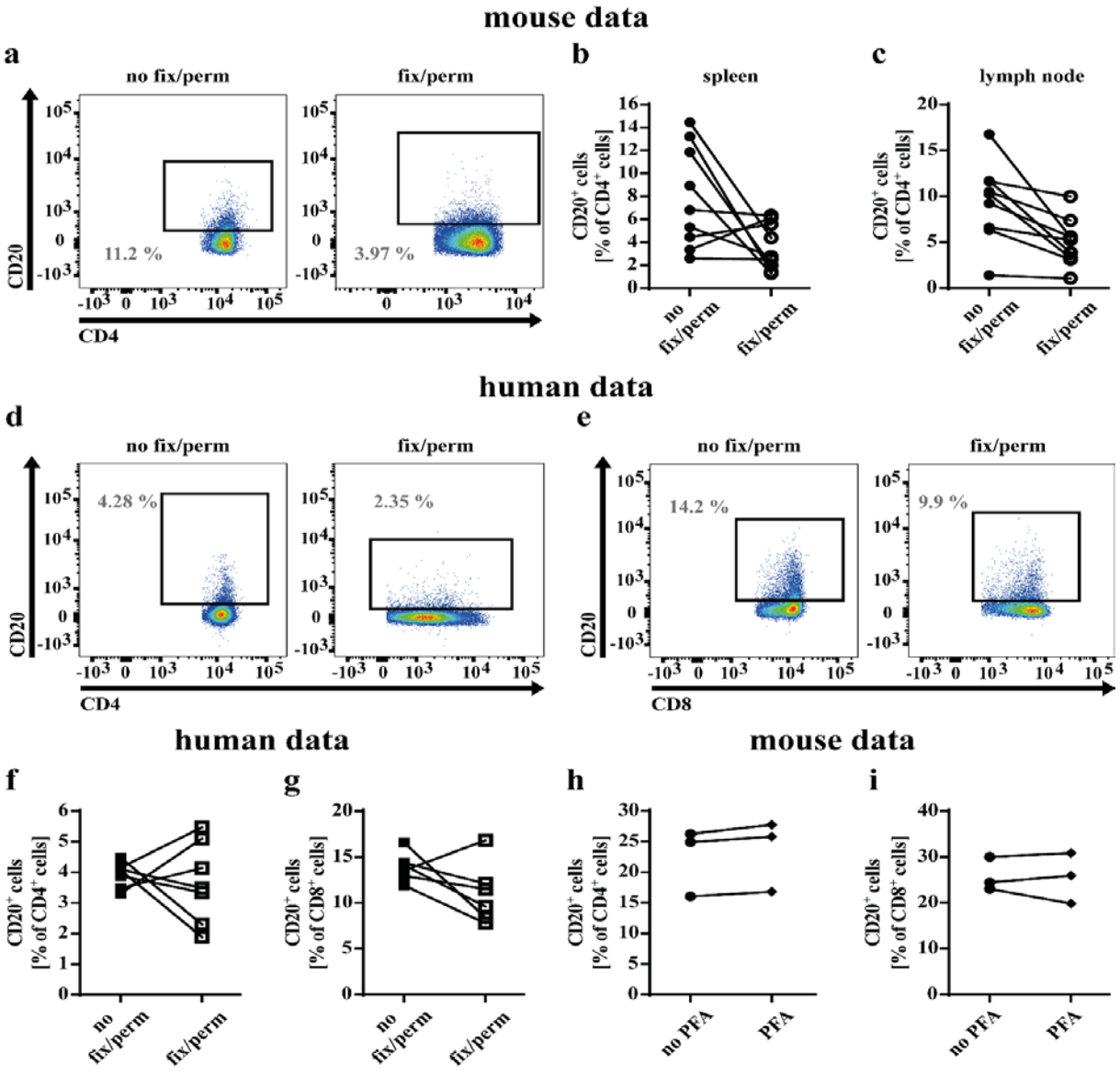

Fig.28: Permeabilization, but not fixation reduces CD20 signal on T cells.
a, Representative CD20 staining on murine $CD4^+$ T cells with and without permeabilisation/ fixation. Percentage of CD20 on $CD4^+$ T cells with and without permeabilisation/fixation in murine **b**, spleens and **c**, lymph nodes (n=8-9 per group, representative of three independent experiments). Representative CD20 staining on human **d**, $CD4^+$ and **e**, $CD8^+$ T cells with and without permeabilisation/fixation. Percentage of CD20 on **f**, $CD4^+$ and **g**, $CD8^+$ T cells with and without permeabilisation/fixation in human PBMCs (n=6-7 per group, representative of 6-7 independent experiments). Flow cytometric analysis of CD20 staining on murine **h**, $CD4^+$ and **i**, $CD8^+$ T cells with and without PFA fixation. Lines connect values from the identical mouse respectively patient.

To examine whether the loss of $CD20^+$ T cells occurs due to fixation or permeabilisation, sole PFA fixation of the cells was performed. PFA fixation alone seemed to have no relevant effect on the frequency of $CD20^+$ T cells **(Fig.28h,i).** The loss of $CD20^+$ T cells due to handling did not affect murine experiments, because sufficient amounts of cells were available to counteract the loss. In experiments analyzing PBMCs, loss of $CD20^+$ T cells led to a reduction of examinable samples **(see 3.8.3)**.

3.7. $CD20^+$ T cells show pathogenic potential in MS

3.7.1. $CD20^+$ T cells show an activated, proinflammatory phenotype in MS

Results generated in animal models are not entirely transferable to the human. Therefore, $CD20^+$ T cells from the blood of MS patients were analyzed for their potential pathogenicity. Here, $CD8^+$ T cells showed a significantly higher frequency of $CD20^+$ cells compared to $CD4^+$ T cells in the individual patients **(Fig.29a)**. In comparison to $CD4^+CD20^-$ T cells, $CD4^+CD20^+$ T cells showed a significant increase in the expression of CD69 as well as the differentiation into $CXCR3^+$ Th1 and $CCR4^+$ Th2 T cells **(Fig.29b)**. Additionally, $CD20^+$ T cells exhibited a significantly higher frequency and expression of the adhesion molecule integrin α-4 (CD49d) **(Fig.29c)**. Furthermore, we consistently observed a significantly higher frequency of cells expressing the proinflammatory cytokines IFNγ, GM-CSF, TNFα and IL-17, which are known to play a role in MS pathology[17, 40, 48, 49, 55, 120, 131] **(Fig.29d).** Analyzing the maturation and developmental status, $CD20^+$ T cells were composed of significantly lower frequencies of naïve cells ($CCR7^+CD45RO^-$) and accordingly significantly higher frequencies of differentiated central memory ($CCR7^+CD45RO^+$) and effector memory ($CCR7^-CD45RO^+$) T cells compared to $CD20^-$ T cells **(Fig.29e).** Exemplary T cell differentiation, activation and cytokine stainings gated on isotype controls or fluorescence minus one stainings are displayed in **Fig.30.** Overall, $CD20^+$ T cells in MS patients exhibited a similar pathogenic potential as observed in EAE, due to their differentiated state, adhesion molecule expression and proinflammatory cytokine production.

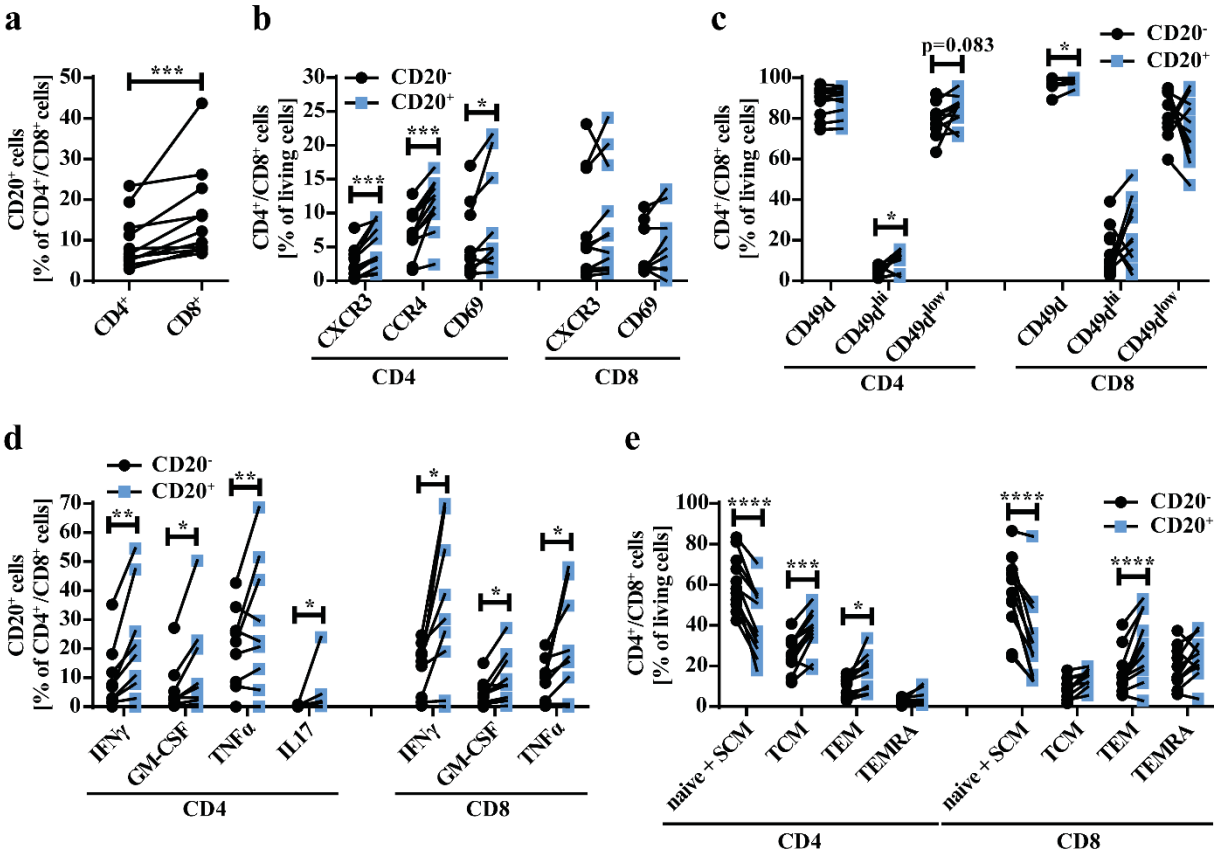

Fig.29: In MS patients, CD20⁺ T cells display an activated, mature phenotype with enhanced pathogenic properties. a-e, Flow cytometric analysis of human PBMCs from MS patients prior to rituximab treatment (n=9-11 MS patients). **a**, Relative frequency of $CD4^+$- vs. $CD8^+CD20^+$ T cells. **b-e**, Comparison of $CD20^+$ vs. $CD20^-$ T cells (separated into $CD4^+$ and $CD8^+$) in regard to **b**, differentiation ($CXCR3^+$, $CCR4^+$) and activation ($CD69^+$); **c**, adhesion capability (integrin α-4 = CD49d); **d**, cytokine production (IFNγ, GM-CSF, TNFα and IL-17) and **e**, developmental state ($CCR7^+CD45RO^-$ = naïve and SCM (stem cell-like memory), $CCR7^+CD45RO^+$ = TCM (central memory), $CCR7^-CD45RO^+$ = TEM (effector memory), $CCR7^-CD45RO^-$ = TEMRA (terminally differentiated)). Lines connect values from the identical patient. p values were calculated using Wilcoxon matched-pairs signed rank test.*=$p \leq 0.05$,**=$p \leq 0.01$,***=$p \leq 0.001$, ****=$p \leq 0.0001$.

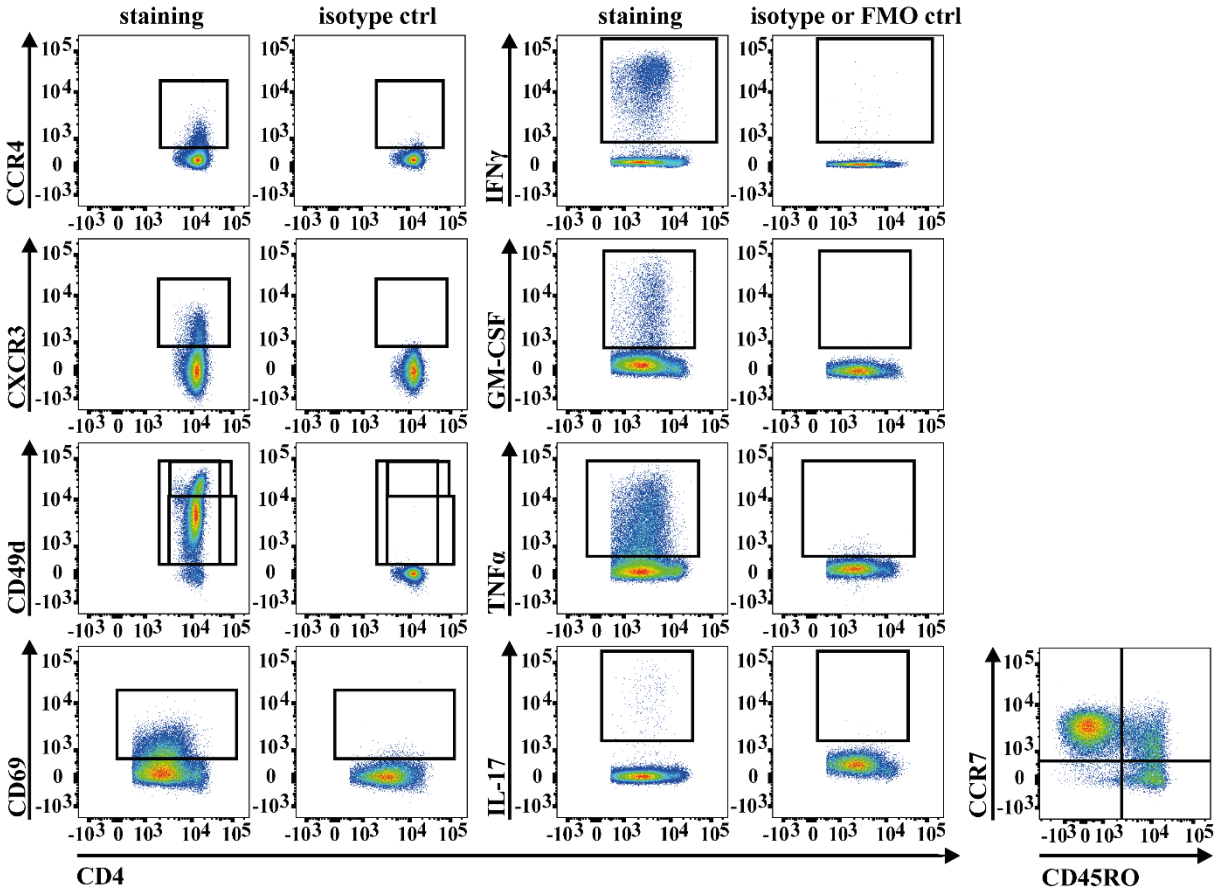

Fig.30: Characterization staining of human T cells.
Representative flow cytometric staining of CCR4, CXCR3, CD49d, CD69, IFNγ, GM-CSF, TNFα, IL-17, CCR7 and CD45RO staining on $CD4^+$ T cells from human PBMCs, gated on respective isotype controls or fluorescence minus one.

3.7.2. $CD20^+$ T cells can be depleted in MS patient blood and reoccur after anti-CD20 ab treatment stop

Anti-CD20 ab treatment belongs to the most effective MS therapies[108, 109, 132], therefore we were interested if anti-CD20 abs are able to not only effectively deplete $CD20^+$ B cells but also $CD20^+$ T cells in the blood of MS patients. We analyzed the blood of 14 MS patients on average over 4.07 ± 0.83 years. **Fig.31** depicts four MS patients with conventional anti-CD20 ab treatment courses. We observed that $CD20^+$ T cells as well as $CD20^+$ B cells reoccur in the blood within weeks to months after anti-CD20 ab treatment. Interestingly, $CD20^+$ T cells reoccurred considerably earlier and to a higher extent than $CD20^+$ B cells in the blood. The patient displayed in **Fig.31b** did not show a complete depletion of $CD20^+$ cells. However, since

PBMCs from only two time points were available from this patient, likely none was close enough after the anti-CD20 ab treatment to show complete depletion.

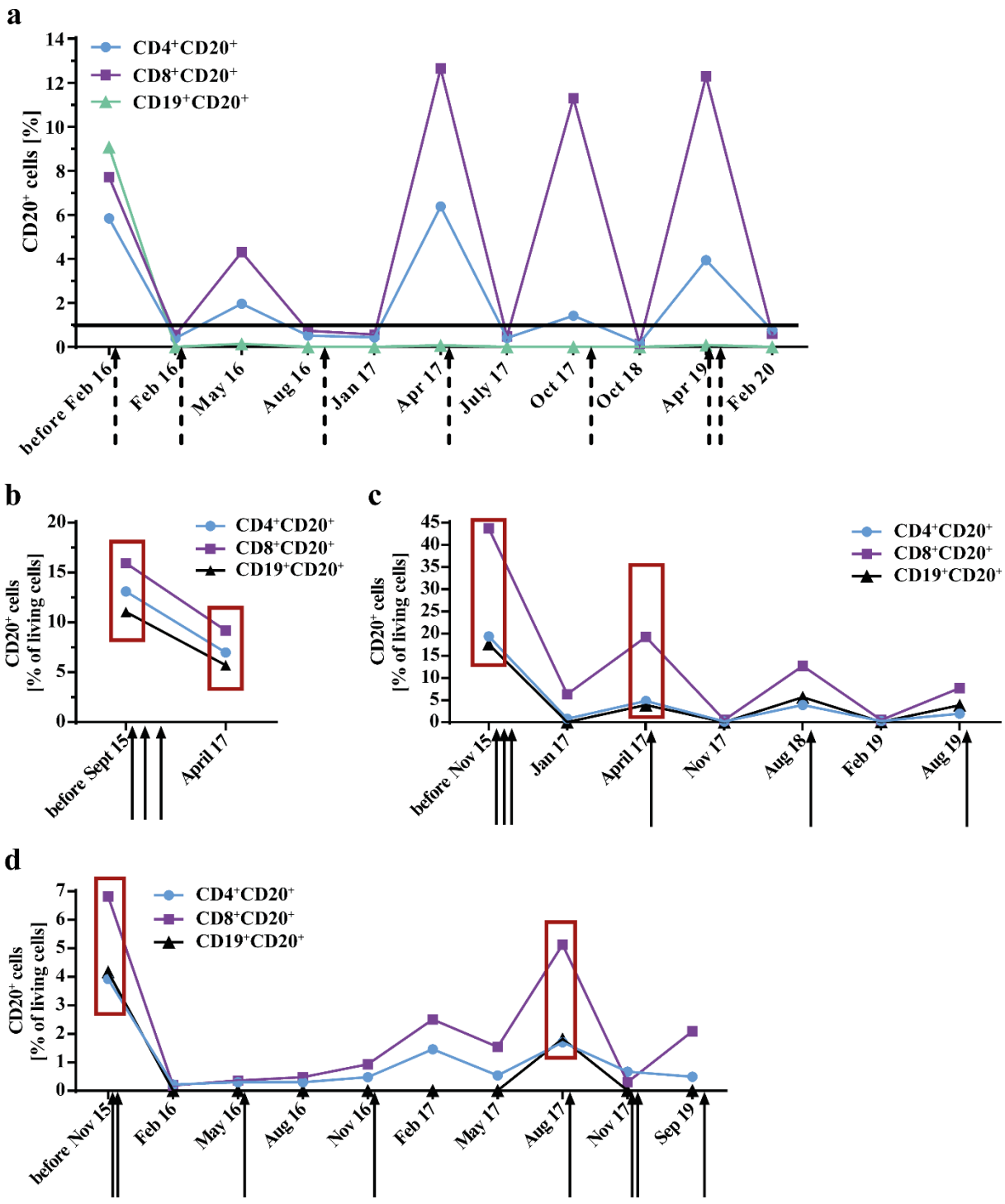

Fig.31: Anti-CD20 ab treatment courses of longitudinally tested MS patients.
a-d, Flow cytometric analysis of percentages of $CD20^+$ cells of human PBMCs from 4 MS patients at different time points before and during rituximab therapy. Arrows mark rituximab treatment while the red rimmed values are the before and after time points of **Fig.32**.

3.7.3. CD20$^+$ T cells reoccur more activated and differentiated

In the anti-CD20 ab treatment courses from **3.8.2 (Fig.31)**, it was detected that CD20$^+$ T cells are depleted, but that they also reoccur after depletion. For B cells, it is known that they mostly reoccur with a more differentiated, proinflammatory phenotype[127]. Therefore, reoccurring CD20$^+$ T cells were compared to CD20$^+$ T cells present before depletion to look for possible analog effects in these cells **(Fig.32)**. Unfortunately, only three patients **(Fig.31b-d**) passed the inclusion criteria (before depletion sample available, more than 100 CD20$^+$ T cells per sample, no cortisone-obligatory relapse within the last three months before sample collection) needed to reliably examine their reoccurring CD20$^+$ T cells. Reoccurring CD20$^+$ T cells exhibited trends towards CXCR3$^+$ Th1 and CXCR3$^+$ Tc1 differentiation and a higher expression of the adhesion molecule integrin α-4 (CD49d) **(Fig.32a)**. The frequency of proinflammatory cytokine (IFNγ, GM-CSF, IL-17, TNFα)-expressing cells was strongly increased in reoccurring CD20$^+$ T cells compared to CD20$^+$ T cells before depletion **(Fig.32b)**. The developmental stage of reoccurring CD20$^+$ T cells tended to a less naïve and more differentiated, especially in the CD8$^+$ T cell population **(Fig.32c)**. Additional samples might strengthen the trends observed in the three analyzed MS patients, which portrayed reoccurring CD20$^+$ T cells as an even more differentiated, activated, proinflammatory and therefore pathogenic population than before depletion. In conclusion, CD20$^+$ T cells exhibit a highly pathogenic potential in MS, are depletable by anti-CD20 ab therapy, and seem to regenerate even more pathogenic.

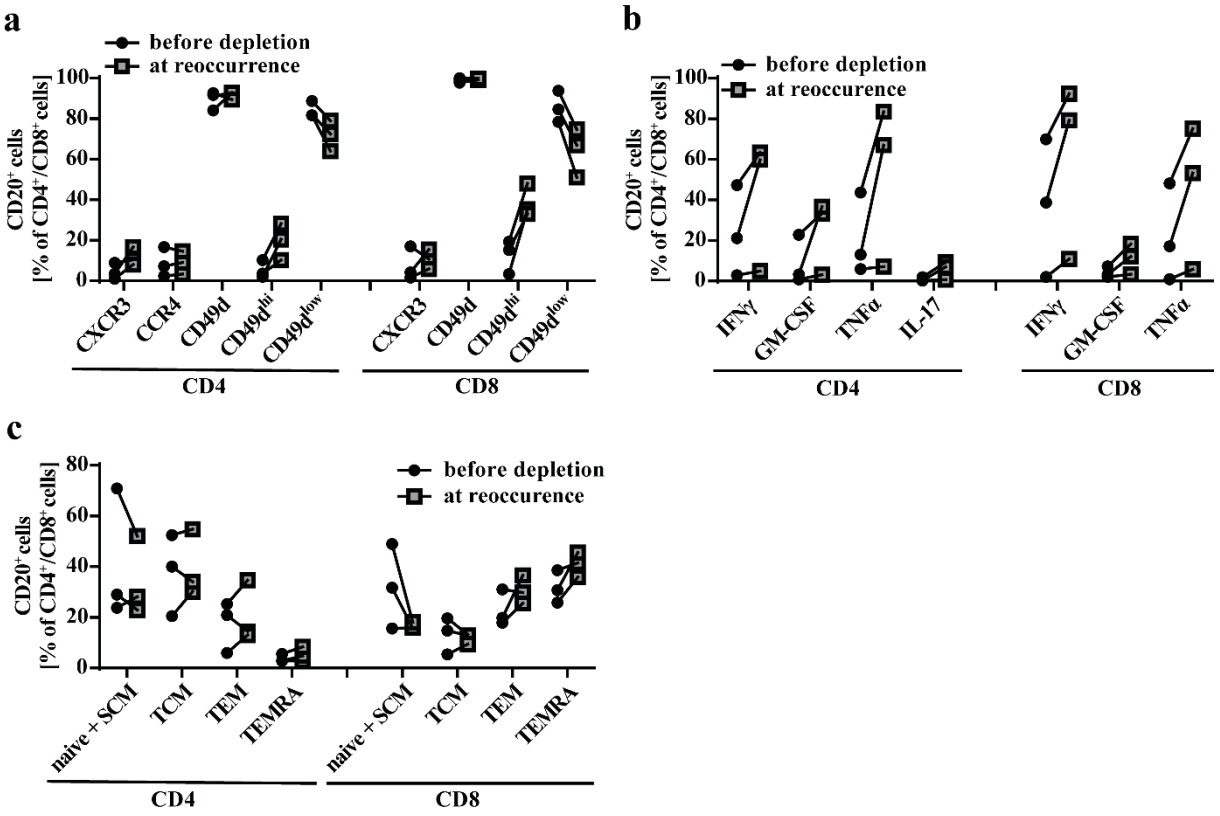

Fig.32: After depletion, CD20$^+$ T cells reoccur with enhanced pathogenic properties in MS patients.
a-c, Comparison of CD20$^+$ T cells obtained human PBMCs from the identical MS patient via flow cytometry prior to depletion and after reconstitution (n=3; depletion course in **Fig.31**) in regard to **a**, differentiation (CXCR3$^+$, CCR4$^+$) and adhesion capability (integrin α-4 = CD49d); **b**, cytokine production (IFNγ, GM-CSF, TNFα and IL-17) and **c**, developmental state. Lines connect values from the identical patient.

4. Discussion

CD20 is a transmembrane protein that was considered a B cell lineage marker due to its high expression on only B cells. Its function or any potential ligands still remain unknown. Due to its expression on B cells in all stages of antigen-dependent activity, anti-CD20 ab therapy was developed to deplete B cells in diseases where they are pathogenic[107]. Interestingly, anti-CD20 ab treatment showed a positive treatment effect in MS[108], which was considered a T cell-driven disease[23]. Consequently, a small population of $CD20^+$ T cells, which were first discovered in 1993[112], were analyzed in MS. They were found to be increased in MS patients compared to healthy controls[117] and exhibit a proinflammatory phenotype[114]. Additionally, it could be demonstrated that $CD20^+$ T cells are depleted as effectively as B cells in anti-CD20 ab treatment in MS patients[117, 125]. Therefore, we were interested in the question if $CD20^+$ T cells play a role in MS development and progression and if their depletion by anti-CD20 ab treatment has a part in the positive therapeutic effect in MS. We determined the existence of $CD20^+$ T cells in mice and analyzed them for their pathogenic potential in EAE. In addition, we examined $CD20^+$ T cells for their pathogenic potential, depletion and their phenotype at reoccurrence after depletion in up to 14 MS patients.

4.1. Trogocytotic transfer of CD20

Since their discovery, $CD20^+$ T cells have been found in various components of healthy human donors, as wells as in patients with autoimmune diseases like MS[112, 114], psoriasis[129] or rheumatoid arthritis[130]. Until now, $CD20^+$ T cells have been exclusively studied in the human due to the fact that their existence in other species was unknown. By analyzing wild type and CD20KO mice, we could detect the existence of $CD20^+$ T cells in mice **(Fig.8)**. By then, it was merely suggested, that T cells in mice express some CD20 homolog called MS4a4B that differs from the CD20 found on B cells[133, 134]. Since in humans, the existence of $CD20^+$ T cells was first put into question and it was claimed that $CD20^+$ T cells are merely a flow cytometry artefact due to T cell-B cell doublets[113]. To avoid potential false positive signals due to doublets with B cells, flow cytometry data was always gated for single cells and B cells were excluded by CD19 B cell staining **(Fig.7)**. It was also observed that the fluorescence intensity of CD20 on B cells is generally a great deal higher than the signal found on $CD20^+$ T cells and would therefore most likely expose B cell contamination. $CD20^+$ T cells could be detected in two different wild type mouse strains, which confirms, that this cell population is not solely present in the B6J mouse strain.

The hypothesis of $CD20^+$ T cells are flow cytometry artefacts was mainly based on the fact that the group was unable to expand the $CD20^+$ T cell population via direct α-CD3/α-CD28 T cell stimulation[113]. Similar results could be observed in this study: T cells proliferated, but the frequency of $CD20^+$ T cells did not change **(Fig.10)**. At this point, we put in question if $CD20^+$ T cells have the ability to endogenously express CD20. This hypothesis was reinforced due to the fact that two different strains of B cell-deficient mice did not contain any $CD20^+$ T cells **(Fig.9)**, indicating a connection between the incidence of CD20-expressing B cells and $CD20^+$ T cells. We did not detect any CD20 RNA expression in murine FACS-sorted $CD20^+$ T cells, although two primer pairs, binding in different areas of the MS4A1 gene, were utilized **(Fig.11)**. In human $CD20^+$ T cells, some groups found a slight CD20 mRNA expression signal[114]. We cannot exclude the possibility, that in the human some $CD20^+$ T cells endogenously express CD20, since we have not yet analyzed human $CD20^+$ T cells. However, qRT-PCR is a highly sensitive method, where contamination with even one B cell might cause a CD20 signal in sorted T cells. B cell contamination however little might also be a possibility since a slight CD19 signal can be seen in their $CD20^+$ T cell population. This might only be background signal due to e.g. non-specific primer binding, but we generally observed that CD20 expression was higher than CD19 expression in B cells. Therefore, CD19 expression of contaminating B cells might not be sufficient for detection at this stage. In our mouse model, $CD20^+$ T cells did not endogenously express CD20.

These results led to the hypothesis of a trogocytotic transfer of CD20 from CD20-highly expressing B cells during B cell-T cell interaction, which was already suggested by various groups[115, 135]. This hypothesis would build on the trogocytotic transfer of the B cell surface protein MHC II to T cells, which is already well-established[136, 137, 138, 139]. CD20 was also found to be physically associated with the B cell antigen receptor[140] and physically and functionally coupled to MHC class II on human B cell lines[141]. The proximity of CD20 to the B cell receptor and MHC II, which is known to be transferred[139], especially suggests that CD20 is transferred as well.

The first result pointing to a trogocytotic transfer was the expansion of the $CD20^+$ T cell population that could be achieved by APC-dependent stimulation of T cells in splenocyte cultures **(Fig.12b)**. A necessity of B cells in the expansion of $CD20^+$ T cells was determined since no expansion of the $CD20^+$ T cell population could be detected in cultures lacking CD20-expressing B cells **(Fig.12d)**. To exclude the possibility that only the interaction with B cells, but not their CD20 expression, led to an increase of $CD20^+$ T cells, B cell-T cell cocultures with wild type or CD20KO B cells were performed. These cultures

confirmed the necessity of T cells to interact with CD20-expressing B cells for the expansion of the $CD20^+$ T cell population **(Fig.14a-f)**. Cultures with other antigens were performed to investigate whether the observed effects are antigen-specific **(Fig.13)**. Subsequently, the need for $CD20^+$ T cells to have interacted with $CD20^+$ B cells in a direct, antigen-dependent manner to become CD20 was analyzed. Therefore, cocultures with MHC IIKO B cells were conducted, since those B cells cannot present antigen to the mainly $CD4^+$ T cells in MOG_{35-55} TCR transgenic 2D2 T cells **(Fig.14g-i)**. Additionally, transwell cocultures were performed, where a membrane prevented direct T cell interaction **(Fig.14j)**. These experiments excluded the possibility of a CD20 transfer from B cells to T cells via B cell vesicles. Therefore, the necessity of direct, antigen-dependent interaction between B cells and T cells was confirmed. In trogocytosis not only surface proteins are transferred, but entire spots of cell membrane[136, 139]. On that account, trogocytotic transfer of CD20 from B cells to T cells could be further verified by staining B cells with a membrane stain and measuring the signal of transferred membrane stain on T cells. Here, membrane $stain^{hi}$ T cells had to be excluded, since they originate from the <1 % T cell contamination in the MACS-isolated membrane-stained B cells **(Fig.15)**. Another indication that these T cells were membrane-stained together with the B cells was their high fluorescence intensity, which equals the fluorescence intensity of membrane-stained B cells, compared to the membrane stain-transferred T cells. Additionally, transwell experiments with membrane-stained B cells were conducted to exclude the possibility that the membrane stain leaks from stained B cells to stain T cells **(Fig.16)**.

In the end, the higher amount of membrane stain on $CD20^+$ T cells and the significant positive correlation between the fluorescence intensity of transferred membrane stain and CD20 on membrane stain-transferred T cells point towards the trogocytotic transfer of stained membrane and CD20. Fluorescence microscopic analysis additionally displayed a “patchy” signal of CD20, as well as membrane stain, in the same location on the surface of a T cell. Similar “patchy” signals were found in other groups, further confirming the trogocytotic transfer of CD20[130].

Since results produced *in vitro* do not always completely translate to equal effects *in vivo*, the possible generation of $CD20^+$ T cells needs to be confirmed *in vivo*. For *in vivo* analysis, $CD20^+$ B cells were transferred into B cell-deficient, $CD20^+$ T cell-lacking mice **(Fig.17)**. Trogocytosis of CD20 could be demonstrated in these experiments due to the detection of newly generated $CD20^+$ T cells only in mice who were transferred with CD20-expressing B cells. In addition, the frequency of newly generated $CD20^+$ T cells positively correlated with the frequency of newly accumulated B cells. MOG_{1-117} protein immunization was performed

following B cell accumulation to further B cell-T cell interaction in the animals, since MOG_{1-117} protein immunization leads to pathogenic B cell interaction[29]. Increased B cell-T cell interaction should have led to an increased trogocytotic transfer of CD20 to T cells and therefore an increased frequency of $CD20^+$ T cells. Furthermore, in MOG_{1-117} protein immunized mice, B cells were also recruited to the immunization draining lymph nodes. The immunized mice confirmed the need for direct B cell interaction, since $CD20^+$ T cells did not occur in the lymph nodes of naïve mice, where no CD20-expressing B cells were recruited to. These results confirm that trogocytotic transfer of CD20 to T cells during direct, antigen-dependent B cell-T cell interaction is the sole origin of $CD20^+$ T cells in mice.

This concludes that every $CD20^+$ T cell is a T cell that recently interacted and was probably activated by a B cell. Therefore, CD20 might serve as a marker for T cell activation by a B cell and an increased amount of $CD20^+$ T cells in patients[117] might indicate a substantial participation of B cells in the development and progression of various diseases.

4.2. $CD20^+$ T cells may play a pathogenic role in EAE, respectively MS

$CD20^+$ T cells were found to be increased in the blood of untreated MS patients[117]. We were able to reproduce similar results in MOG immunized mice by expanding the $CD20^+$ T cell population significantly in the immunization draining lymph nodes, the points of T cell activation **(Fig.22a-d**). An increased amount of $CD20^+$ T cells alone would not lead to the development and progression of MS, respectively EAE, if $CD20^+$ T cells would not show pathogenic potential. In MS patients, it could be shown that $CD20^+$ T cells express higher frequencies of proinflammatory cytokine IL-17, TNFα, GM-CSF and IFNγ-expressing cells than $CD20^-$ T cells[114, 115]. In rheumatoid arthritis, a greater portion of Th17 cells was $CD20^+$ than in healthy controls in the blood[130]. Furthermore, $CD20^+$ T cells expressed higher levels of activation markers like CD69 and HLA-DR in psoriasis[129]. In ovarian cancer, $CD20^+$ T cells are expanded in the ascites of patients and exhibited a predominantly Tc1 effector memory phenotype[118]. All those data points to a potential pathogenic role of $CD20^+$ T cells. *In vitro* and *ex vivo* experiments in naïve and MOG immunized mice in this study confirmed $CD20^+$ T cells to be primarily highly activated T cells with a significantly higher expression of proinflammatory cytokines like IL-17, TNFα, GM-CSF and IFNγ as compared to $CD20^-$ T cells **(Fig.18,19,22f-g,23a-d,24a-c)**. Similar results could be detected in PBMCs from our MS patient cohort **(Fig.29b,d)**. These results portray $CD20^+$ T cells as highly proinflammatory, potentially pathogenic cells. Interestingly, increased expression of anti-inflammatory cytokines

could also be detected in CD20$^+$ T cells **(Fig.20)**. Since we hypothesize that CD20$^+$ T cells are generated during antigen-dependent B cell-T cell interaction, they would not represent a separate T cell population. Being activated by a B cell might be their only uniformity. Therefore, the phenotype of a CD20$^+$ T cell might be determined by the type of B cell it was activated by. However, the frequency of anti-inflammatory CD20$^+$ T cells and their cytokine expression is relatively small compared to the frequency and cytokine expression of proinflammatory CD20$^+$ T cells.

Another pathogenic trademark we detected in murine and human CD20$^+$ T cells was the increased expression of the adhesion molecules integrin α4 (CD49d, mouse and human) and LFA-1 (CD11a, mouse) **(Fig.23e-h, 29c).** The frequency of CD49d-expressing cells was even further increased in mice by EAE induction. The group around von Essen et al. also detected the increased CD49d expression of CD20$^+$ T cells[115]. The expression of adhesion molecules is especially important in MS, respectively EAE, development and progression since autoreactive T cells need to be able to cross the blood-brain barrier to attack the myelin sheath in the CNS[97]. Von Essen et al. were able to detect high amounts of CD20$^+$ T cells in the CSF of MS patients[115]. In EAE, we were unable to detect relevant frequencies of CD20$^+$ T cells in the CNS and especially no accumulation with frequencies higher than in the blood as was published by von Essen in MS patients[115] **(Fig.26,27)**. The differences in the results could for one be due to the different compartments analyzed. CSF results might differ from the results in CNS. To ascertain this difference, either CSF from EAE mice or CNS lesion samples from MS patients would need to be examined for CD20$^+$ T cells. However, it would not be plausible to claim that CD20$^+$ T cells play a role in MS, respectively EAE, pathology if they do not occur in the damaged compartment. To detect CD20$^+$ T cells, we tested various methods for lymphocyte isolation from the murine CNS.

Our first hypothesis was that CD20, like so many other surface proteins, might be destroyed in the enzymatic digestion utilized to isolate lymphocytes from the CNS. This might still be the case, but no relevant frequencies of CD20$^+$ T cells could be detected even without enzymatic digestion, various different filtration methods tested or in completely untreated CNS cell suspensions. One might argue that without enzymatic digestion, CD20$^+$ T cells might not be sufficiently isolated from the CNS tissue. However, even if enzymatic digestion is needed to isolate CD20$^+$ T cells they might simultaneously lose their surface CD20 due to digestion.

Another hypothesis we considered is that the loss of CD20 on the CD20$^+$ T cell surface might be due to membrane turnover. In our trogocytosis model, CD20$^+$ T cells receive the CD20 on their surface during B cell-dependent activation in the periphery and then travel to the CNS.

There they become reactivated by various antigen-presenting cells and attack the myelin sheath[15]. In our experiments with membrane-stained B cells, we could observe that at the latest after 48 h, membrane stain could solely be detected inside the cell, but no longer on the surface. Since $CD20^+$ T cells are unable to endogenously express CD20 **(Fig.11)**, CD20 might be internalized after a while due to membrane turnover, making the cells undetectable as former $CD20^+$ T cells. The B cell frequency and their expression of CD20 was found to be lower in the CNS compared to the blood, the spleen and especially the immunization draining lymph nodes, where most $CD20^+$ T cells were generated in EAE **(Fig.26e)**. These findings indicate that T cells might only infrequently interact and be reactivated by a B cell and more commonly by CNS-resident cells or e.g. dendritic cells. Thus, former B cell-activated $CD20^+$ T cells would be unable to reacquire CD20 on their surface since interaction with CD20-expressing B cells might occur too infrequently. Further experiments in the mouse model, but also in MS patients would need to be performed to conclusively determine, whether $CD20^+$ T cells accumulate in the CNS.

At this point, the CSF results from von Essen et al.[115] seem more reliable, since the CSF cells they analyzed were processed to a lesser extent than our murine CNS samples. Moreover, in EAE mice adoptively transferred with $CD20^+$ T cells, increased T cell infiltration into the CNS could be observed compared to $CD20^-$ T cell transferred mice **(Fig.25c,d).** This finding suggests increased infiltration of $CD20^+$ T cells in the CNS of EAE mice even though we could not yet detect it.

In combination, the enhanced expression of proinflammatory markers and cytokines, that were found to play a role in MS, respectively EAE, strongly suggests a pathogenic potential of $CD20^+$ T cells in this disease.

4.3. Depletion of $CD20^+$ T cells is likely of clinical benefit

The potential importance of $CD20^+$ T cells in MS emerged of late since anti-CD20 ab therapy led to a substantial treatment success in MS patients[108]. The treatment success of anti-CD20 ab therapy was at first considered the sole result of B cell depletion. This hypothesis indicated a considerably greater role of B cells in a disease that was formerly thought to be mainly T cell-driven[23]. In the following years, $CD20^+$ T cells were contemplated as a T cell population that was also depletable by anti-CD20 ab therapy and its depletion was debated to also play a role in the positive anti-CD20 ab treatment effects[117, 125]. We were able to reproduce the complete depletion of $CD20^+$ T cells in various compartments in the mouse **(Fig.25a,b)**, but were until now unable to deplete $CD20^+$ T cells apart from B cells to examine the sole effect of

$CD20^+$ T cell depletion in EAE. In collaboration with other members of the AG Weber, transfer EAE experiments, where MOG-activated T cells are transferred to induce EAE in naïve CD20KO mice, now offer a model to separately deplete $CD20^+$ T cells and are currently in progress with promising results **(Fig.25c)**.

In MS patients, $CD20^+$ T cell depletion was already published with various anti-CD20 abs[117, 125]. Blood samples from our MS patient cohort were analyzed longitudinally throughout anti-CD20 ab therapy **(Fig.31)**. Complete depletion of CD20-expressing B cells and $CD20^+$ T cells could be observed directly following anti-CD20 ab treatment. However, reoccurrence of $CD20^+$ B and T cells could also be observed, as was already published by Palanichamy et.al[117]. Interestingly, $CD20^+$ T cells reoccurred generally earlier and at a higher frequency than B cells after anti-CD20 ab treatment. Similar results were published by Schuh et al.[114], who observed three patients with relapses 4-8 months after the last rituximab infusion, at a time when there were more $CD20^+$ T cells than B cells in the blood. Additionally, they described one patient with a relapse when $CD20^+$ T cells had reached 4 % of all lymphocytes, while $CD20^+$ B cells were hardly detectable in the blood. These results further strengthen the hypothesis that $CD20^+$ T cells play an important role in MS pathology.

However, if we claim that direct interaction with $CD20^+$ B cells is necessary to generate $CD20^+$ T cells the question emerges how $CD20^+$ T cells can be found in the blood while no $CD20^+$ B cells are detectable. A possible explanation for the earlier return of $CD20^+$ T cells might be the analyzed compartment. Reoccurring B cells generally first accumulate in the spleen and secondary lymphatic organs before they are flushed into the blood. Mouse experiments from our group confirmed that B cells in the spleen were replenished weeks earlier as in the blood[127]. Unpublished data from our group also discovered that $CD20^+$ T cells occur in the spleen slightly earlier than in the blood of anti-CD20-depleted mice (unpublished data Ochs et al.). With these data, we conclude that $CD20^+$ B cells newly generated in the bone marrow first accumulate in the spleen, where they fill up the vacant B cell follicles, before they are flushed into the blood. At the same time, T cells remained a complete, functional population since the depleted $CD20^+$ T cells only account for 3-5 % of the overall T cells in the blood[114]. Therefore, plenty mature T cells are present in the spleen of depleted mice and MS patients, where they could interact with newly generated $CD20^+$ B cells and are afterwards directly flushed out into the blood. This model of $CD20^+$ B and T cell-regeneration would also explain the findings that at the time of reoccurrence both populations show a more activated and possibly differentiated phenotype in the blood[142]. In the case of $CD20^+$ T cells an even more proinflammatory phenotype than before depletion was detected **(Fig.32).** The background here

would be that $CD20^+$ T cells would have recently been activated by B cells and in the smaller proportion of regenerated B cells, the percentage of B cells having directly interacted with a T cell would be enhanced. Unfortunately, the shortage of MS patient samples that fulfilled all criteria for analysis impeded significant results. The number of patients, who could be used for longitudinal analysis of $CD20^+$ T cells, was reduced to three due to exclusion criteria. The fact that the MS patients had to be treated regularly with anti-CD20 antibodies to control their disease reduced the amount of samples with more than 100 $CD20^+$ T cells. To be able to analyze tiny populations like e.g. $CD20^+$ Th17 cells, at least 100 $CD20^+$ T cells were necessary to acquire reliable results.

Another challenge was the necessity to permeabilized the cell membrane to stain cells for their phenotype and cytokine expression. Since this treatment reduces the membrane surface, loss of surface molecules was inevitable. Unfortunately, CD20 on T cells is a "patchy", dim staining due to the trogocytotic transfer. Thus, loss of CD20 on the cell surface was unavoidable and resulted in a lower frequency of detectable and therefore analyzable $CD20^+$ T cells **(Fig.28).** Another exclusion criterion was the treatment with cortisol in the last three months before sample collection. Cortisol has an immunosuppressive effect and would thus falsify our results. Longitudinal analysis of additional MS patients might be included throughout the years and strengthen the trends observed in this study that already depict the phenotype of reoccurring $CD20^+$ T cells as more proinflammatory and more differentiated. Consequentially, as was already suggested due to the more activated phenotype of reoccurring B cells[127, 142] and these reoccurring, even more pathogenic $CD20^+$ T cells, a follow up therapy after treatment stop of anti-CD20 ab therapy like e.g. BTK-inhibitors needs to be considered.

In conclusion, $CD20^+$ T cells were determined to be primarily highly activated, proinflammatory cells with a high expression of adhesion molecules and enhanced occurrence in MS and EAE. As a result, they possess most features necessary to play a pathogenic role in MS, respectively EAE. Ongoing experiments indicate an additional clinical benefit of the selective depletion of $CD20^+$ T cells and together with the results in this study strongly suggest the pathogenic influence of $CD20^+$ T cells. At the very least, anti-CD20 ab therapy would deplete a population of B cell-activated, proinflammatory T cells on top of B cells[91, 126].

5. Outlook

In this study, we found that $CD20^+$ T cells cannot endogenously express CD20 in mice and that they receive CD20 from CD20-expressing B cells via trogocytosis. A trogocytotic transfer of MHC II from B to T cells is already established[139]. It might be interesting, in this context, to further investigate if CD20 and MHC II are the only B cell markers transferred to T cells and if other B cell membrane proteins are also transferred. The B cell marker B220 could be a potential candidate. In addition, trogocytotic membrane transfer might also occur in both directions. This would mean that B cells also receive membrane and membrane proteins from T cells. Since it was described that T cells that received MHC II are able to present antigen to other T cells[143, 144], the transfer of other B cell antigens to T cells or the transfer of T cell antigens to B cells might also affect and possibly potentiate immune responses. Furthermore, the trogocytotic transfer of membrane proteins might not be limited to B and T cells, but could also occur in the direct interaction with various other cells, e.g. monocytes or CNS-inherent cells. Trogocytotic transfer of CD20 to such other cells could have so far unconsidered implications for anti-CD20 ab therapy.

If $CD20^+$ T cells develop due to direct B cell-T cell interaction, it would also be interesting to observe the generation and occurrence of $CD20^+$ T cells in other models of infectious diseases. In the future, we want to further confirm our results about the origin of $CD20^+$ T cells in the mouse via single cell analysis to examine, whether T cells that have CD20 proteins on their surface are actually all negative for CD20 RNA. Additionally, we would like to look into human $CD20^+$ T cells, to analyze whether similar results can be found there.

In this study, we barely started to analyze the clinical role of $CD20^+$ T cells in EAE, respectively MS. We already performed the transfer of $CD20^+$ or $CD20^-$ T cells on top of an already developing EAE. Here, a worsening of the disease course and an increased infiltration of $CD3^+$ T cells could be observed in $CD20^+$ T cell-transferred mice. Another attempt at this strategy might result in a more distinct effect of $CD20^+$ T cells, if more T cells are transferred than the two times 200 000 cells from the previous experiments. Moreover, it would be preferable to transfer $CD20^+$ and $CD20^-$ T cells from a mouse line with genetically fluorescent cells to be able to distinguish the CNS-infiltrated T cells from host T cells. This would help to understand, if the transferred T cells are also the infiltrated T cells. So far, we are unable to make that distinction otherwise, since we cannot detect or isolate and stain $CD20^+$ T cells in the CNS.

Pilot experiments selectively depleting $CD20^+$ T cells in passive EAE are ongoing and need to be completed, but they already show promising results. Here, CNS-antigen reactive T cells are

transferred to naïve mice to induce EAE in CD20KO. Thus, only the transferred $CD20^+$ T cells are depleted, which would demonstrate the effect of $CD20^+$ T cells in EAE development and progression.

In perspective and summary, in case the depletion of $CD20^+$ T cells shows a positive therapeutic effect, the clinical benefit of anti-CD20 ab treatment may refer to the depletion of both B and T cells and may disrupt pathogenic B cell-T cell interaction far more thoroughly than previously thought.

6. Bibliography

1. Alastair Compston, A.C. Multiple sclerosis. *Lancet* (2008).

2. MS international federation. What is MS? 2020, September 14 [cited]Available from: https://www.msif.org/about-ms/what-is-ms/

3. Nils Koch-Henriksen, P.S.S. The changing demographic pattern of multiple sclerosis epidemiology. *Lancet Neurol* (2010).

4. Dendrou, C.A., Fugger, L. & Friese, M.A. Immunopathology of multiple sclerosis. *Nat Rev Immunol* **15**, 545-558 (2015).

5. Lublin, F.D. & Reingold, S.C. Defining the clinical course of multiple sclerosis: results of an international survey. National Multiple Sclerosis Society (USA) Advisory Committee on Clinical Trials of New Agents in Multiple Sclerosis. *Neurology* **46**, 907-911 (1996).

6. Fred D. Lublin, S.C.R., Jeffrey A. Cohen, Gary R. Cutter, Per Soelberg Sørensen, *et al.* Defining the clinical course of multiple sclerosis. *Neurology* (2014).

7. MS international federation. Types of MS. 2019 October 5 [cited]Available from: https://www.msif.org/about-ms/types-of-ms/

8. Frischer, J.M. *et al.* The relation between inflammation and neurodegeneration in multiple sclerosis brains. *Brain* **132**, 1175-1189 (2009).

9. de Vos, A.F. *et al.* Transfer of central nervous system autoantigens and presentation in secondary lymphoid organs. *J Immunol* **169**, 5415-5423 (2002).

10. Ransohoff, R.M. & Engelhardt, B. The anatomical and cellular basis of immune surveillance in the central nervous system. *Nature Reviews Immunology* **12**, 623-635 (2012).

11. Louveau, A. *et al.* Structural and functional features of central nervous system lymphatic vessels. *Nature* **523**, 337-341 (2015).

12. Harkiolaki, M. *et al.* T cell-mediated autoimmune disease due to low-affinity crossreactivity to common microbial peptides. *Immunity* **30**, 348-357 (2009).

13. Munz, C., Lunemann, J.D., Getts, M.T. & Miller, S.D. Antiviral immune responses: triggers of or triggered by autoimmunity? *Nat Rev Immunol* **9**, 246-258 (2009).

14. Olson, J.K., Croxford, J.L., Calenoff, M.A., Dal Canto, M.C. & Miller, S.D. A virus-induced molecular mimicry model of multiple sclerosis. *Journal of Clinical Investigation* **108**, 311-318 (2001).

15. Baecher-Allan, C., Kaskow, B.J. & Weiner, H.L. Multiple Sclerosis: Mechanisms and Immunotherapy. *Neuron* **97**, 742-768 (2018).

16. Hemmer, B., Archelos, J.J. & Hartung, H.P. New concepts in the immunopathogenesis of multiple sclerosis. *Nat Rev Neurosci* **3**, 291-301 (2002).

17. Wagner, C.A., Roque, P.J. & Goverman, J.M. Pathogenic T cell cytokines in multiple sclerosis. *J Exp Med* **217** (2020).

18. Burrows, D.J. *et al.* Animal models of multiple sclerosis: From rodents to zebrafish. *Mult Scler* **25**, 306-324 (2019).

19. Bjelobaba, I., Begovic-Kupresanin, V., Pekovic, S. & Lavrnja, I. Animal models of multiple sclerosis: Focus on experimental autoimmune encephalomyelitis. *J Neurosci Res* **96**, 1021-1042 (2018).

20. Tompkins, S.M. *et al.* De novo central nervous system processing of myelin antigen is required for the initiation of experimental autoimmune encephalomyelitis. *J Immunol* **168**, 4173-4183 (2002).

21. Procaccini, C., De Rosa, V., Pucino, V., Formisano, L. & Matarese, G. Animal models of Multiple Sclerosis. *Eur J Pharmacol* **759**, 182-191 (2015).

22. Croxford, A.L., Kurschus, F.C. & Waisman, A. Mouse models for multiple sclerosis: historical facts and future implications. *Biochim Biophys Acta* **1812**, 177-183 (2011).

23. Glaucia C. Furtado, M.C.G.M., Jo-Ann Latkowski, Julia Tsai, Allen Wensky, and Juan J. Lafaille. Swift Entry of Myelin-Specific T Lymphocytes into the central nervous system in spontaneous autoimmune encephalomyelitis. *The Journal of Immunology* (2008).

24. Hofstetter, H.H., Shive, C.L. & Forsthuber, T.G. Pertussis toxin modulates the immune response to neuroantigens injected in incomplete Freund's adjuvant: induction of Th1 cells and experimental autoimmune encephalomyelitis in the presence of high frequencies of Th2 cells. *J Immunol* **169**, 117-125 (2002).

25. Carbajal, K.S. *et al.* Th Cell Diversity in Experimental Autoimmune Encephalomyelitis and Multiple Sclerosis. *J Immunol* **195**, 2552-2559 (2015).

26. Langrish, C.L. *et al.* IL-23 drives a pathogenic T cell population that induces autoimmune inflammation. *J Exp Med* **201**, 233-240 (2005).

27. Voskuhl, R.R. *et al.* T helper 1 (Th1) functional phenotype of human myelin basic protein-specific T lymphocytes. *Autoimmunity* **15**, 137-143 (1993).

28. Miller, S.D. & Karpus, W.J. Experimental autoimmune encephalomyelitis in the mouse. *Curr Protoc Immunol* **Chapter 15**, Unit 15 11 (2007).

29. Weber, M.S. *et al.* B-cell activation influences T-cell polarization and outcome of anti-CD20 B-cell depletion in central nervous system autoimmunity. *Ann Neurol* **68**, 369-383 (2010).

30. Avraham Ben-Nuno, H.W.a.I.R.C. The rapid isolation of clonable antigen-specific T lymphocyte lines capable of mediating autoimmune encephalomyelitis. *Eur. J. Immunol.* (1981).

31. Hohlfeld, R. & Steinman, L. T Cell-Transfer Experimental Autoimmune Encephalomyelitis: Pillar of Multiple Sclerosis and Autoimmunity. *J Immunol* **198**, 3381-3383 (2017).

32. Batoulis, H., Recks, M.S., Addicks, K. & Kuerten, S. Experimental autoimmune encephalomyelitis--achievements and prospective advances. *APMIS* **119**, 819-830 (2011).

33. Wagner, C.A., Roque, P.J., Mileur, T.R., Liggitt, D. & Goverman, J.M. Myelin-specific CD8+ T cells exacerbate brain inflammation in CNS autoimmunity. *J Clin Invest* **130**, 203-213 (2020).

34. Luckheeram, R.V., Zhou, R., Verma, A.D. & Xia, B. CD4(+)T cells: differentiation and functions. *Clin Dev Immunol* **2012**, 925135 (2012).

35. Kim, C.H., Nagata, K. & Butcher, E.C. Dendritic Cells Support Sequential Reprogramming of Chemoattractant Receptor Profiles During Naive to Effector T Cell Differentiation. *The Journal of Immunology* **171**, 152-158 (2003).

36. Coffman, T.R.M.o.a.R.L. THI AND TH2 CELLS: different patterns of lymphokine secretion lead to different functional properties. *Ann. Rev. Immunol.* (1989).

37. Korn, T., Bettelli, E., Oukka, M. & Kuchroo, V.K. IL-17 and Th17 Cells. *Annu Rev Immunol* **27**, 485-517 (2009).

38. Golubovskaya, V. & Wu, L. Different Subsets of T Cells, Memory, Effector Functions, and CAR-T Immunotherapy. *Cancers (Basel)* **8** (2016).

39. Fletcher, J.M., Lalor, S.J., Sweeney, C.M., Tubridy, N. & Mills, K.H. T cells in multiple sclerosis and experimental autoimmune encephalomyelitis. *Clin Exp Immunol* **162**, 1-11 (2010).

40. Willenborg, R.D.S.a.D.O. Direct injection of cytokines into the spinal cord causes autoimmune encephalomyelitis-like inflammation. *Journal of the Neurological Sciences* (1990).

41. Lassmann, K.V.a.H. Intrathecal Application of Interferon Gamma. *AmericanJournal ofPathology* (1990).

42. Lampson, M.P.S.a.L.A. Immune modulation within the brain; recruitment of inflammatory cells and increased major histocompatibility antigen expression following intracerebral injection of interferon-g. *Journal of Neuroimmunology* (1991).

43. Sonar, S.A., Shaikh, S., Joshi, N., Atre, A.N. & Lal, G. IFN-gamma promotes transendothelial migration of CD4(+) T cells across the blood-brain barrier. *Immunol Cell Biol* **95**, 843-853 (2017).

44. Ding, X. *et al.* Silencing IFN-gamma binding/signaling in astrocytes versus microglia leads to opposite effects on central nervous system autoimmunity. *J Immunol* **194**, 4251-4264 (2015).

45. Arellano, G. *et al.* Th1 and Th17 Cells and Associated Cytokines Discriminate among Clinically Isolated Syndrome and Multiple Sclerosis Phenotypes. *Front Immunol* **8**, 753 (2017).

46. Beck, J. *et al.* Increased production of interferon gamma and tumor necrosis factor precedes clinical manifestation in multiple sclerosis: Do cytokines trigger off exacerbations? *Acta Neurologica Scandinavica* **78**, 318-323 (1988).

47. Joanne Link, M., PhD, Mats Soderstrom, MD, PhD, Tomas Olsson, MD, PhD, Bo Hojeberg, MD, PhD, Ake Ljungdahl, MD, PhD, and Hans Link, MD, PhD. Increased Transforming Growth Factor-b, Interleulun-4, and Interferon-y in Multiple Sclerosis. *Ann Neurol* (1994).

48. HALEY, H.S.P.A.S. & JOHNSON, R.L.H.K.P. EXACERBATIONS OF MULTIPLE SCLEROSIS in patients trested with gamma interferon. *The Lancet* (1987).

49. Bettelli, E. *et al.* Loss of T-bet, but not STAT1, prevents the development of experimental autoimmune encephalomyelitis. *J Exp Med* **200**, 79-87 (2004).

50. Birgit Oppmann, R.L., Bianca Blom, Jackie C. Timans, Yuming Xu, Brisdell Hunte, Felix Vega, Nancy Yu, Jing Wang, Komal Singh, Francesca Zonin, Elena Vaisberg, Tatyana Churakova, Man-ru Liu, Daniel Gorman, Janet Wagner, Sandra Zurawski, Yong-Jun Liu, John S. Abrams,, Kevin W. Moore, D.R., Rene de Waal-Malefyt, Charles Hannum, & J. Fernando Bazan, a.R.A.K. Novel p19 Protein Engages IL-12p40 to Form a cytokine, IL-23, with biological activities similar as well as distinct from IL-12. *Immunity* (2000).

51. Daniel J. Cua, J.S., Yi Chen, Craig A. Murphy, Barbara Joyce, Brian Seymour, Linda Lucian, Wayne To, Sylvia Kwan, Tatyana Churakova, Sandra Zurawski, Maria Wiekowski, Sergio A. Lira, Daniel Gormank, Robert A. Kasteleink & Jonathon D. Sedgwick. Interleukin-23 rather than interleukin-12 is the critical cytokine for autoimmune inflammation of the brain. *NATURE* (2003).

52. Becher, B., Durell, B.G. & Noelle, R.J. Experimental autoimmune encephalitis and inflammation in the absence of interleukin-12. *J Clin Invest* **110**, 493-497 (2002).

53. Gran, B. *et al.* IL-12p35-deficient mice are susceptible to experimental autoimmune encephalomyelitis: evidence for redundancy in the IL-12 system in the induction of central nervous system autoimmune demyelination. *J Immunol* **169**, 7104-7110 (2002).

54. Stromnes, I.M., Cerretti, L.M., Liggitt, D., Harris, R.A. & Goverman, J.M. Differential regulation of central nervous system autoimmunity by T(H)1 and T(H)17 cells. *Nat Med* **14**, 337-342 (2008).

55. Huppert, J. *et al.* Cellular mechanisms of IL-17-induced blood-brain barrier disruption. *FASEB J* **24**, 1023-1034 (2010).

56. Kang, Z. *et al.* Astrocyte-restricted ablation of interleukin-17-induced Act1-mediated signaling ameliorates autoimmune encephalomyelitis. *Immunity* **32**, 414-425 (2010).

57. Simmons, S.B., Liggitt, D. & Goverman, J.M. Cytokine-regulated neutrophil recruitment is required for brain but not spinal cord inflammation during experimental autoimmune encephalomyelitis. *J Immunol* **193**, 555-563 (2014).

58. Brucklacher-Waldert, V., Stuerner, K., Kolster, M., Wolthausen, J. & Tolosa, E. Phenotypical and functional characterization of T helper 17 cells in multiple sclerosis. *Brain* **132**, 3329-3341 (2009).

59. Segal, B.M. *et al.* Repeated subcutaneous injections of IL12/23 p40 neutralising antibody, ustekinumab, in patients with relapsing-remitting multiple sclerosis: a phase II, double-blind, placebo-controlled, randomised, dose-ranging study. *The Lancet Neurology* **7**, 796-804 (2008).

60. Haak, S. *et al.* IL-17A and IL-17F do not contribute vitally to autoimmune neuro-inflammation in mice. *J Clin Invest* **119**, 61-69 (2009).

61. Grifka-Walk, H.M., Giles, D.A. & Segal, B.M. IL-12-polarized Th1 cells produce GM-CSF and induce EAE independent of IL-23. *Eur J Immunol* **45**, 2780-2786 (2015).

62. Codarri, L. *et al.* RORgammat drives production of the cytokine GM-CSF in helper T cells, which is essential for the effector phase of autoimmune neuroinflammation. *Nat Immunol* **12**, 560-567 (2011).

63. El-Behi, M. *et al.* The encephalitogenicity of T(H)17 cells is dependent on IL-1- and IL-23-induced production of the cytokine GM-CSF. *Nat Immunol* **12**, 568-575 (2011).

64. Shi, Y. *et al.* Granulocyte-macrophage colony-stimulating factor (GM-CSF) and T-cell responses: what we do and don't know. *Cell Res* **16**, 126-133 (2006).

65. Ponomarev, E.D. *et al.* GM-CSF production by autoreactive T cells is required for the activation of microglial cells and the onset of experimental autoimmune encephalomyelitis. *J Immunol* **178**, 39-48 (2007).

66. Duncker, P.C., Stoolman, J.S., Huber, A.K. & Segal, B.M. GM-CSF Promotes Chronic Disability in Experimental Autoimmune Encephalomyelitis by Altering the Composition of Central Nervous System-Infiltrating Cells, but Is Dispensable for Disease Induction. *J Immunol* **200**, 966-973 (2018).

67. Rasouli, J. *et al.* Expression of GM-CSF in T Cells Is Increased in Multiple Sclerosis and Suppressed by IFN-beta Therapy. *J Immunol* **194**, 5085-5093 (2015).

68. LESLEY PROBERT, K.A., MANOLIS PASPARAKIS, GEORGE KONTOGEORGO, AND GEORGE KOLLIAS. Spontaneous inflammatory demyelinating disease in transgenic mice showing central nervous system-specific expression of tumor necrosis factor alpha. *Proc. Natl. Acad. Sci.* (1995).

69. Akassoglou, K. *et al.* Oligodendrocyte Apoptosis and Primary Demyelination Induced by Local TNF/p55TNF Receptor Signaling in the Central Nervous System of Transgenic Mice. *The American Journal of Pathology* **153**, 801-813 (1998).

70. Nancy H. Ruddle, C.M.B., Katherine M . McGrath, Elizabeth G. & Lingenheld, M.L.G., S Steven J. Padula,$ and Robert B. Clark. An Antibody to Lymphotoxin and Tumor necrosis factor prevents transfer of EAE. *J . Exp. Med* (1990).

71. Krzysztof Selmaj , W.P., Andrzej Glabifiski , Tadahiko Kohno Prevention of chronic relapsing experimental autoimmune encephalomyelitis by soluble tumor necrosis factor receptor I. *Journal of Neuroimmunology* (1995).

72. Suvannavejh, G.C. *et al.* Divergent roles for p55 and p75 tumor necrosis factor receptors in the pathogenesis of MOG(35-55)-induced experimental autoimmune encephalomyelitis. *Cell Immunol* **205**, 24-33 (2000).

73. Hans-Pietro Eugster, K.F., Rosilla Bachmann , Horst Bluethmann ,Hans Lassmann & Fontana, a.A. Severity of symptoms and demyelination in MOG-induced EAE depends on TNFR1. *Eur. J. Immunol.* (1999).

74. Gimenez, M.A., Sim, J., Archambault, A.S., Klein, R.S. & Russell, J.H. A tumor necrosis factor receptor 1-dependent conversation between central nervous system-specific T cells and the central nervous system is required for inflammatory infiltration of the spinal cord. *Am J Pathol* **168**, 1200-1209 (2006).

75. P. Rieckmann, M., M. Albrecht, BA, B. Kitze, MD, T. Weber, MD, H. Tumani, MD, A. Broocks, MD, W. Luer, MD, A. Helwig, MD, and S. Poser, MD. Tumor Necrosis Factor-a Messenger RNA expression in patients with Relapsing-Remitting Multiple Sclerosis Is Associated with Disease Activity. *Ann Neurol* (1995).

76. Mohammad K. Sharief, M.B., Ch.B., M.Phil., and Romain Hentges, M.D. Association between Tumor Necrosis Factor-α and Disease Progression in Patients with Multiple Sclerosis. *N Engl J Med* (1991).

77. Shimon Sakaguchi, N.S., Masanao Asano, Misako Itoh, and Masaaki Toda. Immunologic Self-Tolerance Maintained by Activated T Cells Expressing 11-2 Receptor a-Chains (CD25). *The lournal of Immunology* (1995).

78. Fontenot, J.D., Gavin, M.A. & Rudensky, A.Y. Foxp3 programs the development and function of CD4+CD25+ regulatory T cells. *Nat Immunol* **4**, 330-336 (2003).

79. Hori, S. & Sakaguchi, S. Foxp3: a critical regulator of the development and function of regulatory T cells. *Microbes and Infection* **6**, 745-751 (2004).

80. Kohm, A.P., Carpentier, P.A., Anger, H.A. & Miller, S.D. Cutting edge: CD4+CD25+ regulatory T cells suppress antigen-specific autoreactive immune responses and central nervous system inflammation during active experimental autoimmune encephalomyelitis. *J Immunol* **169**, 4712-4716 (2002).

81. Zhang, X. *et al.* IL-10 is involved in the suppression of experimental autoimmune encephalomyelitis by CD25+CD4+ regulatory T cells. *Int Immunol* **16**, 249-256 (2004).

82. Walsh, K.P., Brady, M.T., Finlay, C.M., Boon, L. & Mills, K.H. Infection with a helminth parasite attenuates autoimmunity through TGF-beta-mediated suppression of Th17 and Th1 responses. *J Immunol* **183**, 1577-1586 (2009).

83. Estelle Bettelli, M.P.D., Edward D. Howard, Howard L. Weiner, Raymond A. Sobel and Vijay K. Kuchroo. IL-10 Is Critical in the Regulation of Autoimmune Encephalomyelitis as Demonstrated by Studies of IL-10- and IL-4-Deficient and Transgenic Mice. *J Immunol* (1998).

84. Daniel J. Cua, H.G., David R. Hinton, Stephen A. Stohlman, and Robert L. Coffman. Transgenic Interleukin 10 Prevents Induction of Experimental Autoimmune Encephalomyelitis. *J. Exp. Med* (1999).

85. Al-Banna, N.A., Vaci, M., Slauenwhite, D., Johnston, B. & Issekutz, T.B. CCR4 and CXCR3 play different roles in the migration of T cells to inflammation in skin, arthritic joints, and lymph nodes. *Eur J Immunol* **44**, 1633-1643 (2014).

86. Groom, J.R. & Luster, A.D. CXCR3 in T cell function. *Exp Cell Res* **317**, 620-631 (2011).

87. Subash Sad, R.M., Tim R. Mosmann. Cytokine-induced differentiation of precursor mouse CD8+ T cells into cytotoxic CD8+ T cells secreting Th1 or Th2 cytokines. *Immunity*, (1995).

88. Liang, Y., Pan, H.-F. & Ye, D.-Q. Tc17 Cells in Immunity and Systemic Autoimmunity. *International Reviews of Immunology* **34**, 318-331 (2015).

89. Hamada, H. *et al.* Tc17, a unique subset of CD8 T cells that can protect against lethal influenza challenge. *J Immunol* **182**, 3469-3481 (2009).

90. Friese, M.A. & Fugger, L. Pathogenic CD8(+) T cells in multiple sclerosis. *Ann Neurol* **66**, 132-141 (2009).

91. Sabatino, J.J., Jr. *et al.* Anti-CD20 therapy depletes activated myelin-specific CD8(+) T cells in multiple sclerosis. *Proc Natl Acad Sci U S A* **116**, 25800-25807 (2019).

92. SMITH, K.A. Interleukin-2: inception, impact, and implications. *SCIENCE*, (1988).

93. Ross, S.H. & Cantrell, D.A. Signaling and Function of Interleukin-2 in T Lymphocytes. *Annu Rev Immunol* **36**, 411-433 (2018).

94. Lopez-Cabrera M, S.A., Fernandez-Ruiz E, Blacher R, Esch P,Sanchez-Mateos P, Sanchez-Madrid Molecular cloning, expression,and chromosomal localization of the human earliest lymphocyteactivation antigen AIM/CD69, a new member of the C-type animallectin superfamily of signal transmitting receptors. *J. Exp. Med* (1993).

95. A. Caruso, S.L., M. Corulli, A.D. Canaris, M.A. De Francesco, S. Fiorentini, L. Peroni, F. Fallacara, F. Dima, A. Balsari, and A. Turano. Flow Cytometric Analysis of Activation Markers on Stimulated T Cells and Their Correlation With Cell Proliferation. *Cytometry* (1997).

96. Raine, B.C.a.C.S. The Adhesion Molecule and Cytokine profile of multiple sclerosis lesions. *Ann Neurol* **37** (1995).

97. Irina Elovaara, M., PhD; Maritta Ukkonen, MD; Minna Leppäkynnäs, MD; Terho Lehtimäki, MD, PhD; Mari Luomala, MSc; Jukka Peltola, MD; Prasun Dastidar, MD. Adhesion molecules in MS. *ARCH NEUROL* (2000).

98. P Stashenko, L.M.N., R Hardy and S F Schlossman. Characterization of a human B lymphocyte-specific antigen. *The Journal of Immunology* (1980).

99. Glennie, M.J., French, R.R., Cragg, M.S. & Taylor, R.P. Mechanisms of killing by anti-CD20 monoclonal antibodies. *Mol Immunol* **44**, 3823-3837 (2007).

100. Leandro, M.J. B-cell subpopulations in humans and their diff erential susceptibility to depletion with anti-CD20 monoclonal antibodies *Arthritis Research & Therap* (2013).

101. A. Bar-Or, R.B., M. Weber, R. Hughes, C. Lin, J. Wang, A. Sauter, H. Koendgen, L. Craveiro, S. Hauser, T. Derfuss Serum Ig Levels and Risk of Serious Infections by Baseline Ig Quartile in the Pivotal Phase III Trials and Open-Label Extensions of Ocrelizumab in Multiple Sclerosis. *Annual Meeting of the American Academy of Neurology* Toronto, ON, Canada; 2020.

102. McLaughlin, P. *et al.* Rituximab chimeric anti-CD20 monoclonal antibody therapy for relapsed indolent lymphoma: half of patients respond to a four-dose treatment program. *Journal of Clinical Oncology* **16**, 2825-2833 (1998).

103. U.S. Food and Drug administration. Drugs@FDA: FDA-Approved Drugs. 1997 [cited]Available from: https://www.accessdata.fda.gov/scripts/cder/daf/index.cfm?event=overview.process&varApplNo=103705

104. Reff, M.E. *et al.* Depletion of B cells in vivo by a chimeric mouse human monoclonal antibody to CD20. *Blood* **83**, 435-445 (1994).

105. Jonathan C.W. Edwards, M.D., Leszek Szczepa´nski, M.D., Ph.D., & Jacek Szechi´nski, M.D., Ph.D., Anna Filipowicz-Sosnowska, M.D., Ph.D., Paul Emery, M.D., David R. Close, Ph.D., Randall M. Stevens, M.D., and Tim Shaw, B.Sc. Efficacy of B-Cell–Targeted Therapy with Rituximab in Patientswith Rheumatoid Arthritis. *The new england journal of medicine* (2004).

106. Cambridge, J.C.W.E.a.G. Sustained improvement in rheumatoid arthritis following a protocol designed to deplete B lymphocytes. *Rheumatology* (2001).

107. Casan, J.M.L., Wong, J., Northcott, M.J. & Opat, S. Anti-CD20 monoclonal antibodies: reviewing a revolution. *Hum Vaccin Immunother* **14**, 2820-2841 (2018).

108. Stephen L. Hauser, M.D., Emmanuelle Waubant, M.D., Ph.D., Douglas L. Arnold, M.D., Timothy Vollmer, M.D., Jack Antel, M.D., Robert J. Fox, M.D., Amit Bar-Or, M.D., Michael Panzara, M.D., & Neena Sarkar, P.D., Sunil Agarwal, M.D., Annette Langer-Gould, M.D., Ph.D., and Craig H. Smith, M.D. B-Cell Depletion with

Rituximab in Relapsing–Remitting Multiple Sclerosis. *Th e new engl and journal o f medicine* (2008).

109. Alcala, C. *et al.* Efficacy and safety of rituximab in relapsing and progressive multiple sclerosis: a hospital-based study. *J Neurol* **265**, 1690-1697 (2018).

110. Kappos, L. *et al.* Ocrelizumab in relapsing-remitting multiple sclerosis: a phase 2, randomised, placebo-controlled, multicentre trial. *The Lancet* **378**, 1779-1787 (2011).

111. Lin, T.S. Ofatumumab- a novel monoclonal anti-CD20 antibody. *Pharmacogenomics and Personalized Medicine* (2010).

112. Lance E. Hultin, M.A.H., Patricia M. Hultin, and Janis V. Giorgi. CD20 (pan-B cell) antigen is expressed at a low level on a subpopulation of human T lymphocytes. *Cytometry* (1993).

113. Henry, C. *et al.* CD3+CD20+ cells may be an artifact of flow cytometry: comment on the article by Wilk et al. *Arthritis Rheum* **62**, 2561-2563; author reply 2563-2565 (2010).

114. Schuh, E. *et al.* Features of Human CD3+CD20+ T Cells. *J Immunol* **197**, 1111-1117 (2016).

115. von Essen, M.R. *et al.* Proinflammatory CD20+ T cells in the pathogenesis of multiple sclerosis. *Brain* **142**, 120-132 (2019).

116. Wilk, E. *et al.* Depletion of functionally active CD20+ T cells by rituximab treatment. *Arthritis Rheum* **60**, 3563-3571 (2009).

117. Palanichamy, A. *et al.* Rituximab efficiently depletes increased CD20-expressing T cells in multiple sclerosis patients. *J Immunol* **193**, 580-586 (2014).

118. de Bruyn, M. *et al.* CD20(+) T cells have a predominantly Tc1 effector memory phenotype and are expanded in the ascites of patients with ovarian cancer. *Oncoimmunology* **4**, e999536 (2015).

119. Alunno, A. *et al.* Interleukin (IL)-17-producing pathogenic T lymphocytes co-express CD20 and are depleted by rituximab in primary Sjogren's syndrome: a pilot study. *Clin Exp Immunol* **184**, 284-292 (2016).

120. Komiyama, Y. *et al.* IL-17 plays an important role in the development of experimental autoimmune encephalomyelitis. *J Immunol* **177**, 566-573 (2006).

121. Milovanovic, J. *et al.* Interleukin-17 in Chronic Inflammatory Neurological Diseases. *Front Immunol* **11**, 947 (2020).

122. Cohen, S.B. *et al.* Rituximab for rheumatoid arthritis refractory to anti-tumor necrosis factor therapy: Results of a multicenter, randomized, double-blind, placebo-controlled, phase III trial evaluating primary efficacy and safety at twenty-four weeks. *Arthritis Rheum* **54**, 2793-2806 (2006).

123. Montalban, X. *et al.* Ocrelizumab versus Placebo in Primary Progressive Multiple Sclerosis. *N Engl J Med* **376**, 209-220 (2017).

124. Edwards, J.C. & Cambridge, G. B-cell targeting in rheumatoid arthritis and other autoimmune diseases. *Nat Rev Immunol* **6**, 394-403 (2006).

125. Gingele, S. *et al.* Ocrelizumab Depletes CD20(+) T Cells in Multiple Sclerosis Patients. *Cells* **8** (2018).

126. Datta, S.K. Anti-CD20 antibody is an efficient therapeutic tool for the selective removal of autoreactive T cells. *Nat Clin Pract Rheumatol* **5**, 80-82 (2009).

127. Hausler, D. *et al.* Functional characterization of reappearing B cells after anti-CD20 treatment of CNS autoimmune disease. *Proc Natl Acad Sci U S A* **115**, 9773-9778 (2018).

128. Daisuke Kitamura, J.R., Ralf Kühn and Klaus Rajewsky. A B cell-deficient mouse targeted disruption of the membrane exon of the immunoglobulin mu chain gene. *letters to nature* (1991).

129. Niu, J. *et al.* Dissection of a circulating CD3(+) CD20(+) T cell subpopulation in patients with psoriasis. *Clin Exp Immunol* **192**, 206-212 (2018).

130. Eggleton, P. *et al.* Frequency of Th17 CD20+ cells in the peripheral blood of rheumatoid arthritis patients is higher compared to healthy subjects. *Arthritis Res Ther* **13**, R208 (2011).

131. Uyttenhove, C. *et al.* Prophylactic treatment against GM-CSF, but not IL-17, abolishes relapses in a chronic murine model of multiple sclerosis. *Eur J Immunol* **48**, 1883-1891 (2018).

132. Pierre de Flon, M.M.G., MD, PhD, Katarina Laurell, M., PhD, Lars Söderström, M.R.B., MD, PhD, Thomas Lindqvist, M.W.K., MD Ann Dring, PhD Joakim Bergman, MSc Peter Sundström, MD, PhD & Anders Svenningsson, M., PhD. Reduced inflammation in relapsing-remitting multiple sclerosis after therapy switch to rituximab. *American Academy of Neurology* (2016).

133. Xu, H., Williams, M.S. & Spain, L.M. Patterns of expression, membrane localization, and effects of ectopic expression suggest a function for MS4a4B, a CD20 homolog in Th1 T cells. *Blood* **107**, 2400-2408 (2006).

134. Xu, H. *et al.* MS4a4B, a CD20 homologue in T cells, inhibits T cell propagation by modulation of cell cycle. *PLoS One* **5**, e13780 (2010).

135. Chen, Q., Yuan, S., Sun, H. & Peng, L. CD3(+)CD20(+) T cells and their roles in human diseases. *Hum Immunol* **80**, 191-194 (2019).

136. Dopfer, E.P., Minguet, S. & Schamel, W.W. A new vampire saga: the molecular mechanism of T cell trogocytosis. *Immunity* **35**, 151-153 (2011).

137. Wiendl, H. Fast track to becoming a regulatoryT cell- trogocytosis ofimmune-tolerogenic HLA-G. *blood* (2007).

138. Jing-Feng Huang, Y.Y., Homero Sepulveda, Weixing Shi, Inkyu Hwang, Per A. Peterson, Michael R. Jackson, Jonathan Sprent, Zeling Cai. TCR-Mediated Internalization of Peptide-MHC Complexes Acquired by T Cells. *SCIENCE* (1999).

139. Wetzel, S.A., McKeithan, T.W. & Parker, D.C. Peptide-specific intercellular transfer of MHC class II to CD4+ T cells directly from the immunological synapse upon cellular dissociation. *J Immunol* **174**, 80-89 (2005).

140. Polyak, M.J., Li, H., Shariat, N. & Deans, J.P. CD20 homo-oligomers physically associate with the B cell antigen receptor. Dissociation upon receptor engagement and recruitment of phosphoproteins and calmodulin-binding proteins. *J Biol Chem* **283**, 18545-18552 (2008).

141. Claire Leveille, R.A.-D.a.W.M. CD20 is physically and functionally coupled to MHC class II and CD40 on human B cell lines. *Eur. J. Immunol.* (1999).

142. Nissimov, N. *et al.* B cells reappear less mature and more activated after their anti-CD20-mediated depletion in multiple sclerosis. *Proc Natl Acad Sci U S A* (2020).

143. Tsang, J.Y., Chai, J.G. & Lechler, R. Antigen presentation by mouse CD4+ T cells involving acquired MHC class II:peptide complexes: another mechanism to limit clonal expansion? *Blood* **101**, 2704-2710 (2003).

144. Avraham Ben-Nun, W.S., Sara A. Leeman , Lauren E. Cohn , Cornelis Murre , Allan Duby , J. G. Seidman, and Laurie H. Glimcher. An Ia-Positive Mouse T-Cell Clone Is Functional in presenting antigen to ohter T cells. *Immungenetics* (1985).